CONTACT METAMORPHISM OF THE HEATHCOTE GREENSTONE AT MOUNT WILLIAM AND MOUNT CAMEL, CENTRAL VICTORIA.

by

A.L. WATCHMAN

Thesis submitted as a requirement for admission to the degree of Master of Science, Australian National University.

February, 1977

This thesis is my own original piece of work,

except where acknowledgements are made.

Signed 

A.L. WATCHMAN

ABSTRACT

The effects of contact metamorphism are studied at Mount William and Mount Camel in central Victoria. Actinolite-cummingtonite hornfels and metadolerite result from contact metamorphism of Alpine-type ultramafic extrusives and dolerite respectively. Aboriginal axe stones quarried in actinolite-cummingtonite hornfels at Mount William and Mount Camel are distinguished by geochemistry and petrography. The concentrations of Fe_2O_3, MgO, and Y are greater whereas TiO_2, Al_2O_3, CaO, Na_2O and P_2O_5 are lower in rocks from Mount William than at Mount Camel. Samples from these locations are readily distinguished by using Ti-Zr-Y and Ti-Zr diagrams. Actinolite-cummingtonite hornfelses at Mount William are petrographically different from those at Mount Camel, being strongly recrystallised, green-black and not green-brown, and lack diopside, amphibole pseudomorphs and tuffaceous texture.

Metadolerite at Mount William is olivine normative, shows classical tholeiitic mineralogical and geochemical fractionation trends and is relatively unaffected by isochemical contact metamorphism. Dehydration, recrystallisation and growth of hornblende are caused by thermal effects on emplacement of the Cobaw Granite.

Compositions of actinolite, cummingtonite and hornblende are affected by bulk chemistry and temperature, the effect of the host rock being less in the highest grade parts of the aureole. The contact aureole in greenstone is zoned with respect to amphibole and plagioclase compositions. Within 80 metres of the granitic contact hornblende increases in Al^{iv}, Al^{vi}, Ti, Fe, Mn, Na and K whereas Mg, Ca and Mg/Mg+Fe decrease with progressive metamorphism. Plagioclase becomes more calcic as the granite is approached.

ACKNOWLEDGEMENTS

I acknowledge the assistance given to me by many people during the two years (part-time) which I spent on this thesis. Dr. I. McBryde of the Department of Prehistory and Anthropology provided initial encouragement and gave support as the work progressed. Dr. R.A. Eggleton supervised the project and criticised an early draft of the thesis. The analytical results were obtained under the guidance of Dr. B.W. Chappell with the help of Mr. R.S. Freeman and Mr. Z.L. Wasik. Professor A.J.R. White of the Geology Department, La Trobe University, kindly invited presentation of a seminar on the work and I thank him and his staff for their helpful comments. Mr. A. Crawford stimulated discussion at the start of the project. Dr. J.A. McDonald assisted with identification of opaque minerals and Mr. J.H. Pennington helped with x-ray diffraction techniques. Mr. K. Massey and Miss E. Rees prepared thin and polished sections. Mr E.H. Pedersen and Mr. N. Ware of the Research School of Earth Sciences, A.N.U., provided facilities for sample preparation and use of the electron microprobe. Miss B. Ross gave instructions in drafting maps and diagrams. Mr K.J. Johnson kindly read and criticised a draft of this thesis. The help freely given by all these people is greatly appreciated.

TABLE OF CONTENTS

LIST OF FIGURES

LIST OF TABLES

LIST OF PLATES

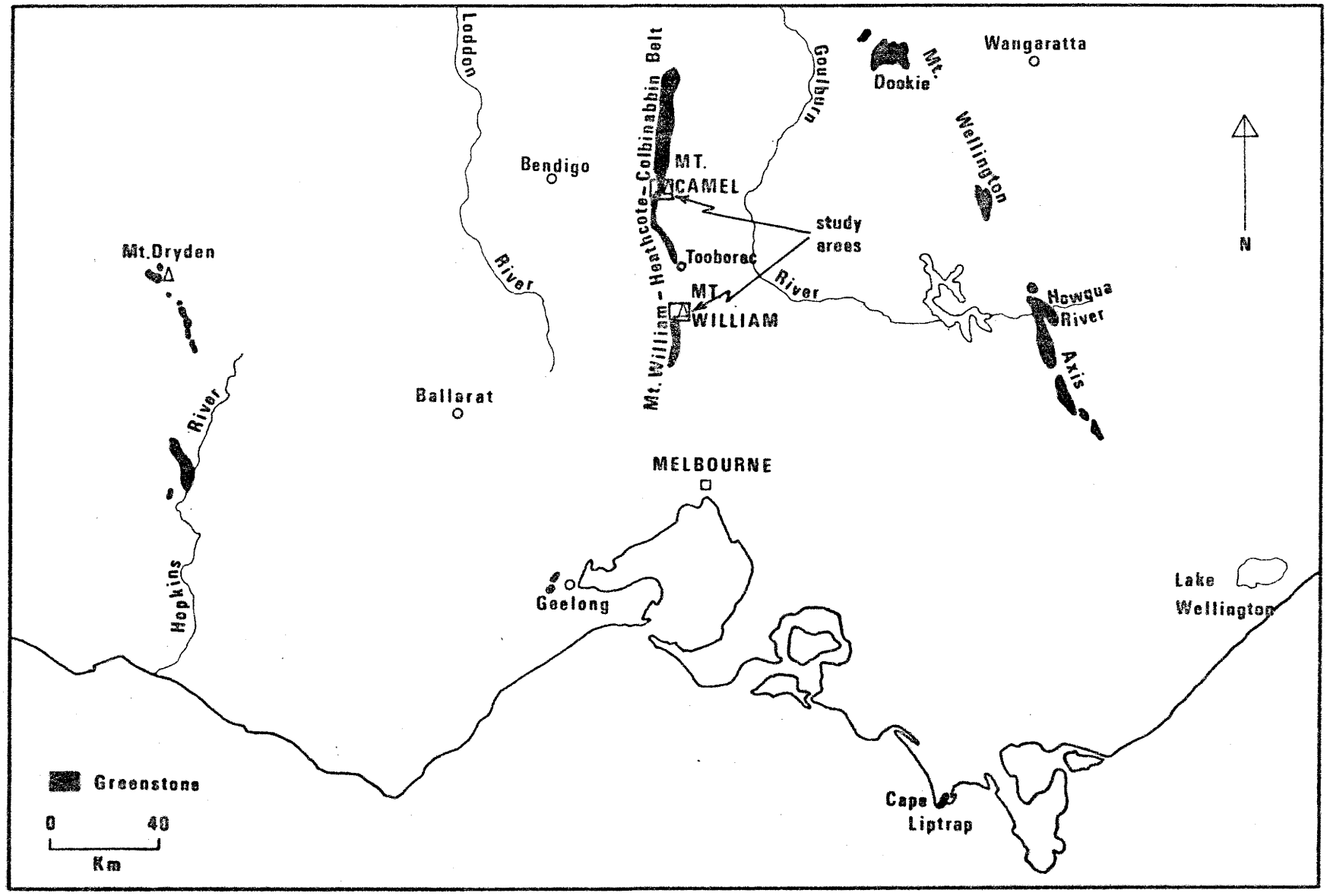

1. Areas of Cambrian greenstone

INTRODUCTION

The Heathcote Greenstone is the basal unit of Cambrian rocks which form the Heathcote Axis (Thomas, 1939), a narrow, thrust-faulted, sub-meridional inlier marking the junction of Ordovician and Silurian sediments of central Victoria (Williams, 1964). The rocks are submarine lavas and tuffs with subordinate chert lenses (Gregory, 1903; Skeats, 1908; Thomas, 1939, 1959). The original rocks of calc-alkaline and ultramafic types reached up to the greenschist facies of regional metamorphism (Thomas et al, 1976), presumably after undergoing submarine weathering and burial metamorphism. Thomas & Singleton (1956) and Stewart (1966), believed that the rocks belong to the spilite-keratophyre association. In any case the rocks studied were altered by various processes prior to contact metamorphism by Devonian granitic plutons.

Detailed petrographic studies of rocks from the Heathcote Greenstone were made by Gregory (1903), Skeats (1908), Singleton (1949) and Thomas & Singleton (1956). The geology and geochemistry of rocks from along the Heathcote Axis were discussed in theses by Nicholls (1965), Hamlyn (1971) and Green (1972). However, no detailed studies have been made on contact metamorphism of greenstone from this region. Stewart (1966) briefly described contact metamorphism of Silurian and Ordovician pelites in the aureole around the Cobaw Granite, a large pluton which also caused thermal metamorphism of greenstone.

The present study was undertaken following another project, the aim of which was to establish exchange patterns of Aboriginal axe stones in Victoria by determining the petrology of axes and their sources (McBryde & Watchman, 1976). In the course of this undertaking it proved difficult to precisely distinguish between rock types derived from Aboriginal axe stone

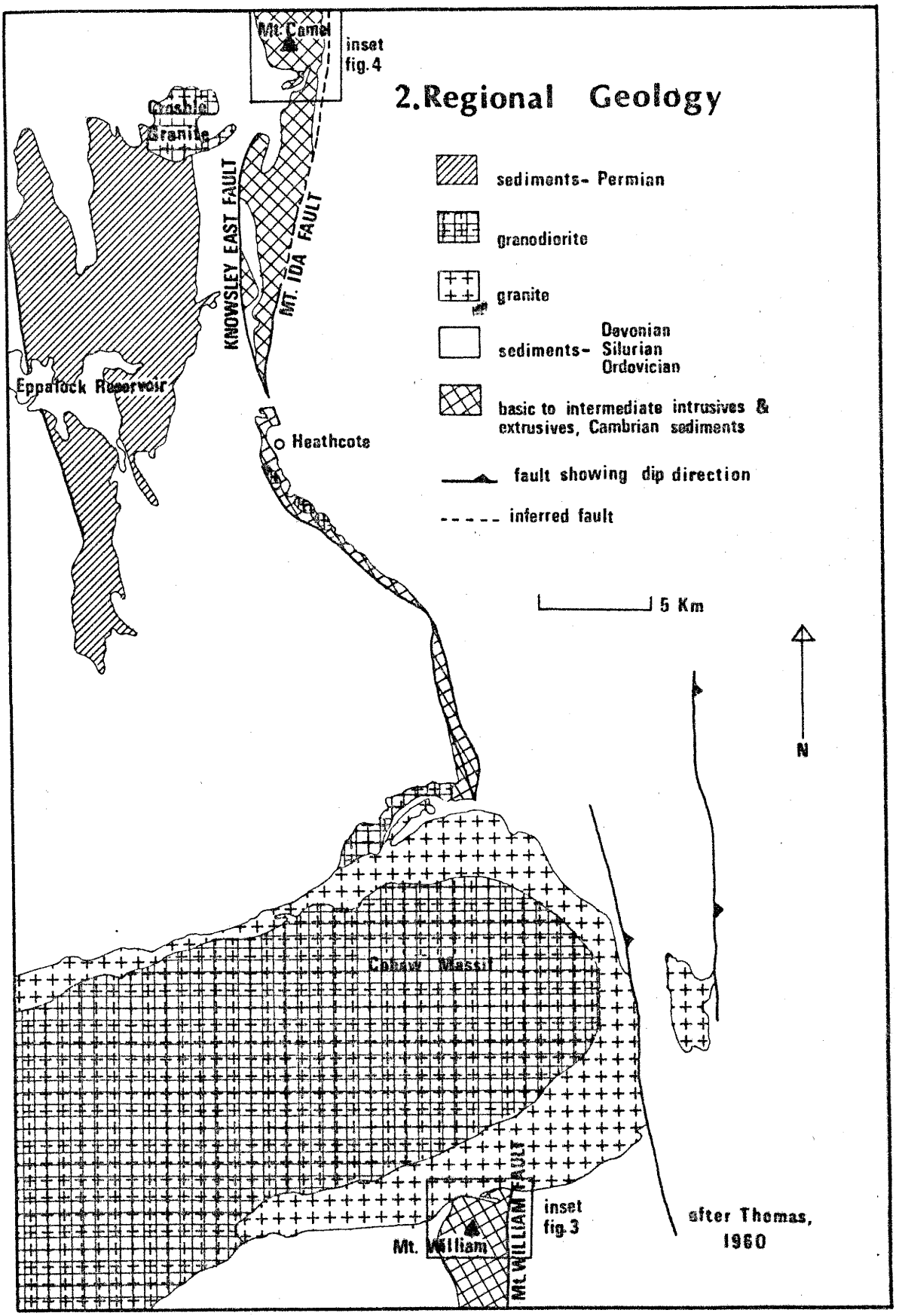
2.Regional Geology
Mt. Camel
inset fig. 4
Granite
KNOWSLEY EAST FAULT
MT. IDA FAULT
Eppalock Reservoir
Heathcote
sediments- Permian
granodiorite
granite
sediments- Devonian Silurian Ordovician
basic to intermediate intrusives & extrusives, Cambrian sediments
fault showing dip direction
inferred fault
5 Km
N
Cobaw Massif
Mt. William
MT WILLIAM FAULT
inset fig. 3
after Thomas, 1960

quarried at Mount William and Mount Camel. Petrographic and selected trace element geochemical studies are used to characterise most greenstone axes derived from these sources (Watchman & Freeman, 1977). The purpose of this thesis is to examine the mineralogical and geochemical variations in rocks from the two areas and to understand their genesis so that source discriminations of axes may be more precisely determined.

LOCATION AND REGIONAL GEOLOGY

The two areas of interest, Mount William and Mount Camel, are 60km and 110km north of Melbourne respectively (Fig. 1). They lie along the Heathcote Axis, a narrow sinuous ridge less than 5km wide which extends for over 100km except where it is broken by the Cobaw and Crosbie granites.

Outcrop is sparse, generally found as isolated exposures of rocks resistant to weathering.

The Heathcote Axis (Mount William-Heathcote-Colbinabbin Greenstone Belt) and the Mount Wellington Axis are major structural trends which controlled sedimentation and igneous activity until the Middle Palaeozoic (Thomas, 1939, 1959). West of the Heathcote Axis a thick sequence of Cambrian-Ordovician marine sediments were deposited after early Cambrian volcanism (Brown et al, 1968). Ordovician and Silurian sediments were deposited in the Melbourne Trough, between the Heathcote and Mount Wellington Axes. After folding, and during the Middle Devonian, acidic rocks were intruded and extruded as part of the Tabberabberan Orogeny. The Cobaw and Crosbie granitic masses were emplaced at that time.

Along the eastern margin of the Heathcote Axis high-angle reverse faults separate Cambrian and Silurian rocks. Near Mount William the Cambrian sequence is conformably overlain by Ordovician sediments. West of Mount Camel, Cambrian rocks are faulted against Lower Ordovician sediments.

Oversby (1971), Crook (1974), Packham & Leitch (1974), Solomon & Griffiths (1974), Crook & Felton (1975) and Rutland (1976) interpreted the geology of the Tasman Geosyncline in several ways using different models. Discussions and appraisals of these various theories are not the subject of this thesis. However, petrological and geochemical evidence presented

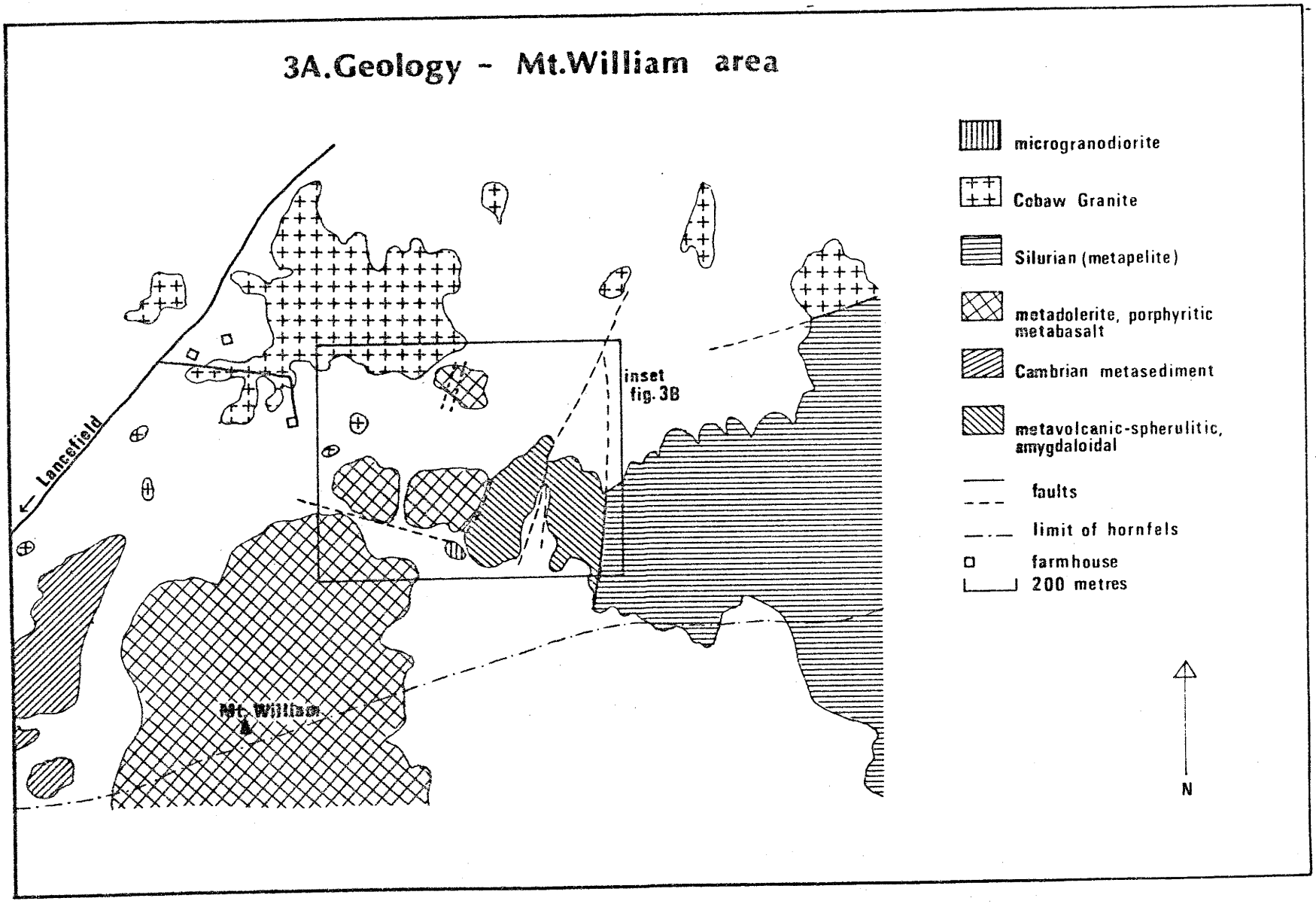
3A.Geology - Mt.William area
micrograndiorite
Cobaw Granite
Silurian (metapelite)
metadolerite, porphyritic metabasalt
Cambrian metasediment
metavolcanic-spherulitic, amygdaloidal
faults
limit of hornfels
farmhouse
200 metres
N
inset fig. 3B
← Lancefield
Mt. William

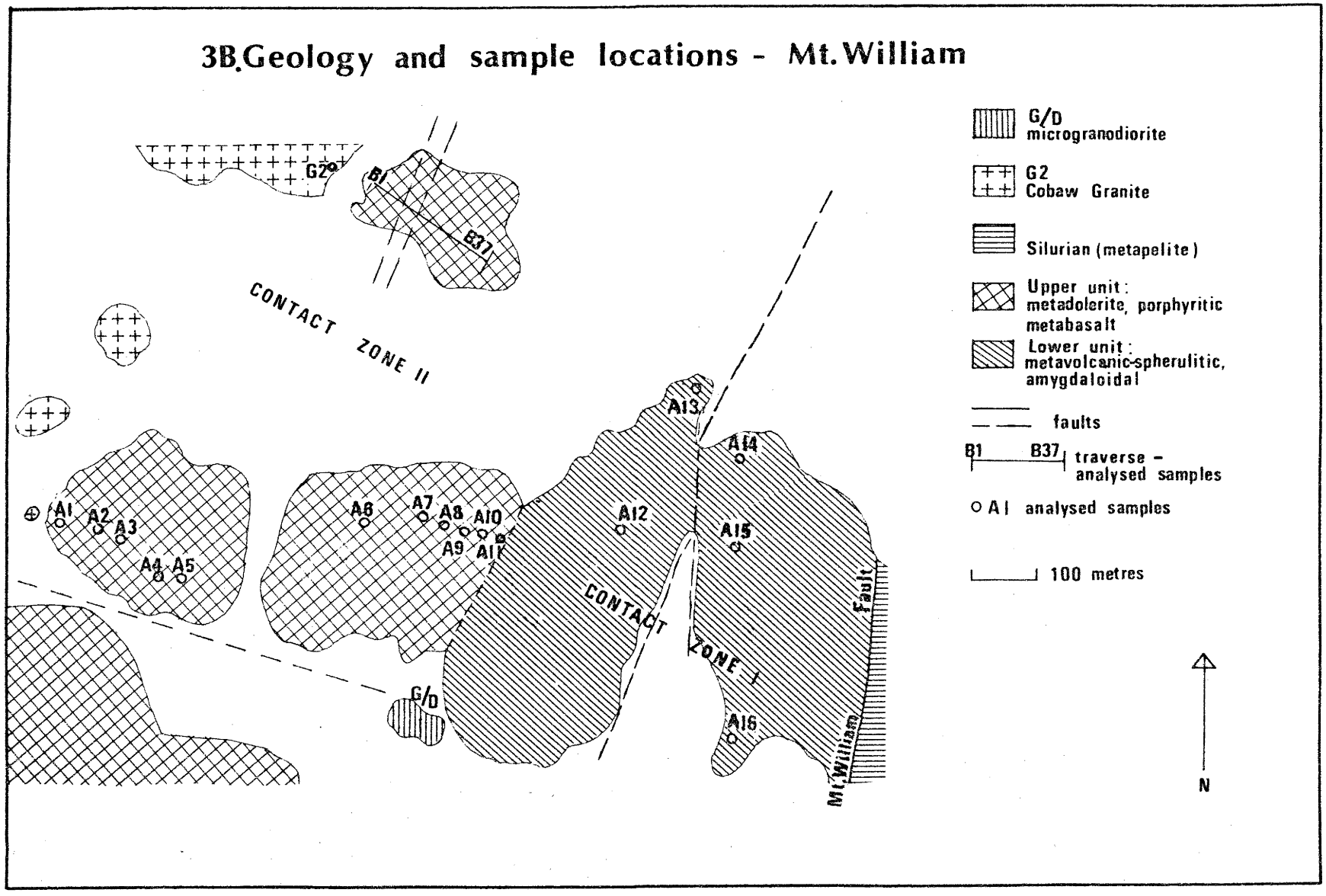
3B.Geology and sample locations - Mt.William
G2
B1
B37
CONTACT ZONE II
A1
A2
A3
A4
A5
A6
A7
A8
A9
A10
A11
A12
A13
A14
A15
A16
G/D
CONTACT ZONE I
Mt.William Fault
G/D microgranodiorite
G2 Cobaw Granite
Silurian (metapelite)
Upper unit: metadolerite, porphyritic metabasalt
Lower unit: metavolcanic-spherulitic, amygdaloidal
faults
B1 B37 traverse - analysed samples
A1 analysed samples
100 metres
N

herein will contribute towards a greater understanding of the geology of the Tasman Geosyncline, and the orogenic events that affected the Geosyncline.

Detailed mapping by Thomas (1956, 1960), outlined the main stratigraphic units of the greenstone belt. The basal unit of the Cambrian stratigraphy is the Heathcote Greenstone, 1500m thick and composed of lava, ash, tuff and agglomerate. It is associated with intrusive bodies of basic and intermediate composition (Singleton, 1949). Chert lenses are interbedded within the volcanics. The base of the Cambrian is not exposed and amygdaloidal and spherulitic lava flows occur in the lower parts of the Heathcote Greenstone.

Ground traverses, petrographic and geochemical studies as part of this thesis allow subdivision of the Heathcote Greenstone into Lower and Upper Units at Mount William. Rocks of the Lower Unit are altered ?volcanics and chert, and in the Upper Unit, metadolerite. Similar division is not possible at Mount Camel because dolerite intrusives are subordinate to the volcanics.

Stratigraphically above the Heathcote Greenstone is an interbedded succession of black shales, 150m thick, containing dendroids and trilobites. Near Mount William the shale is called the Mount William Group and at Mount Camel it is known as the Knowsley East Formation.

Above the black shale is a sequence of unfossiliferous shale and mudstone, the Goldie Shale. It passes gradationally up into Lower Ordovician sediments at Mount William but is faulted against Ordovician pelites in the Mount Camel area.

Figures 3A and 3B illustrate the geology and sample locations near Mount William and Figure 4 shows the geology in the vicinity of Mount Camel. The Cambrian stratigraphy in the two areas is shown in Figures 5 and 6.

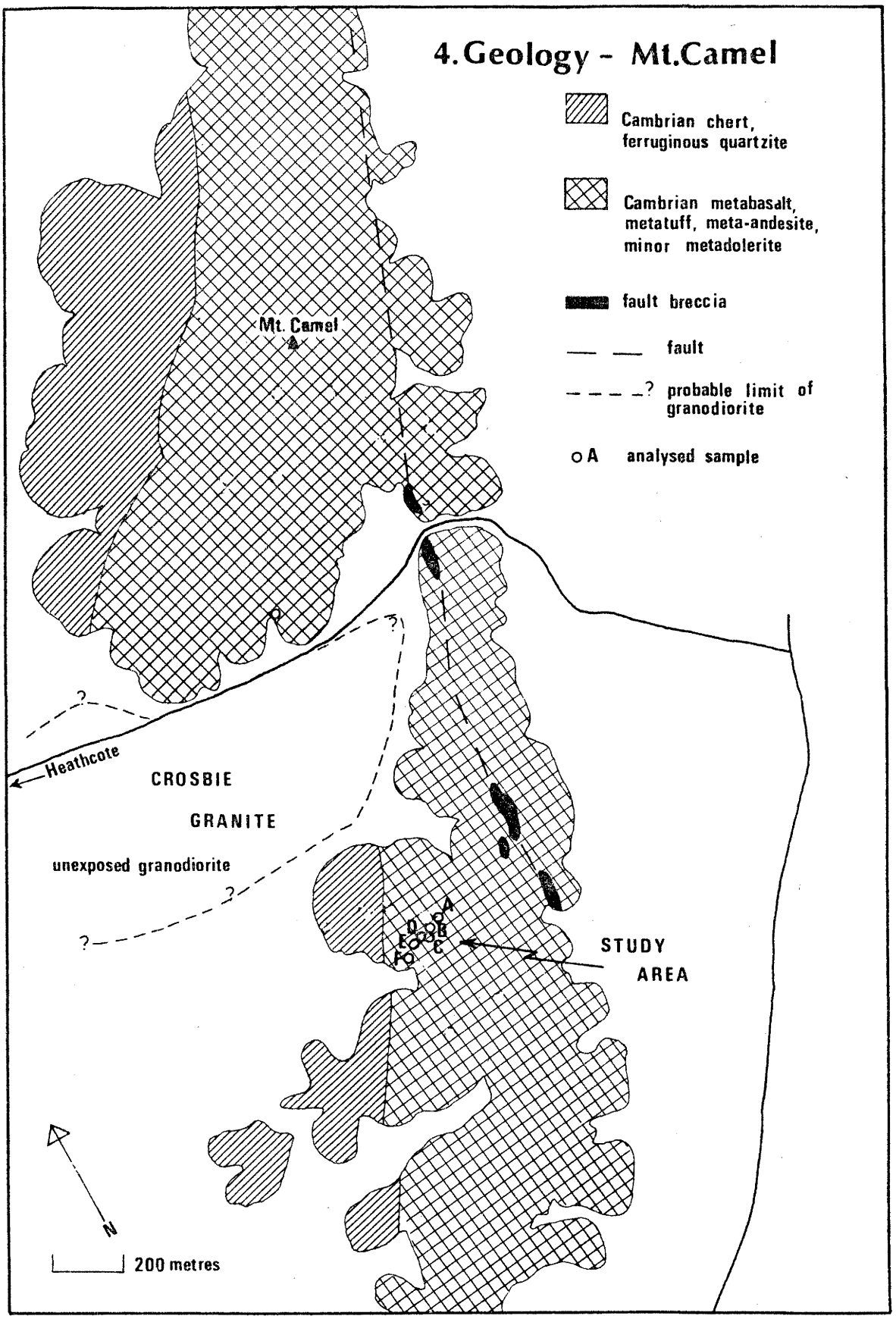
4. Geology - Mt. Camel
Cambrian chert, ferruginous quartzite
Cambrian metabasalt, metatuff, meta-andesite, minor metadolerite
fault breccia
fault
probable limit of granodiorite
A analysed sample
Mt. Camel
Heathcote
CROSBIE
GRANITE
unexposed granodiorite
STUDY AREA
N
200 metres

5. Cambrian stratigraphy – Mt. William

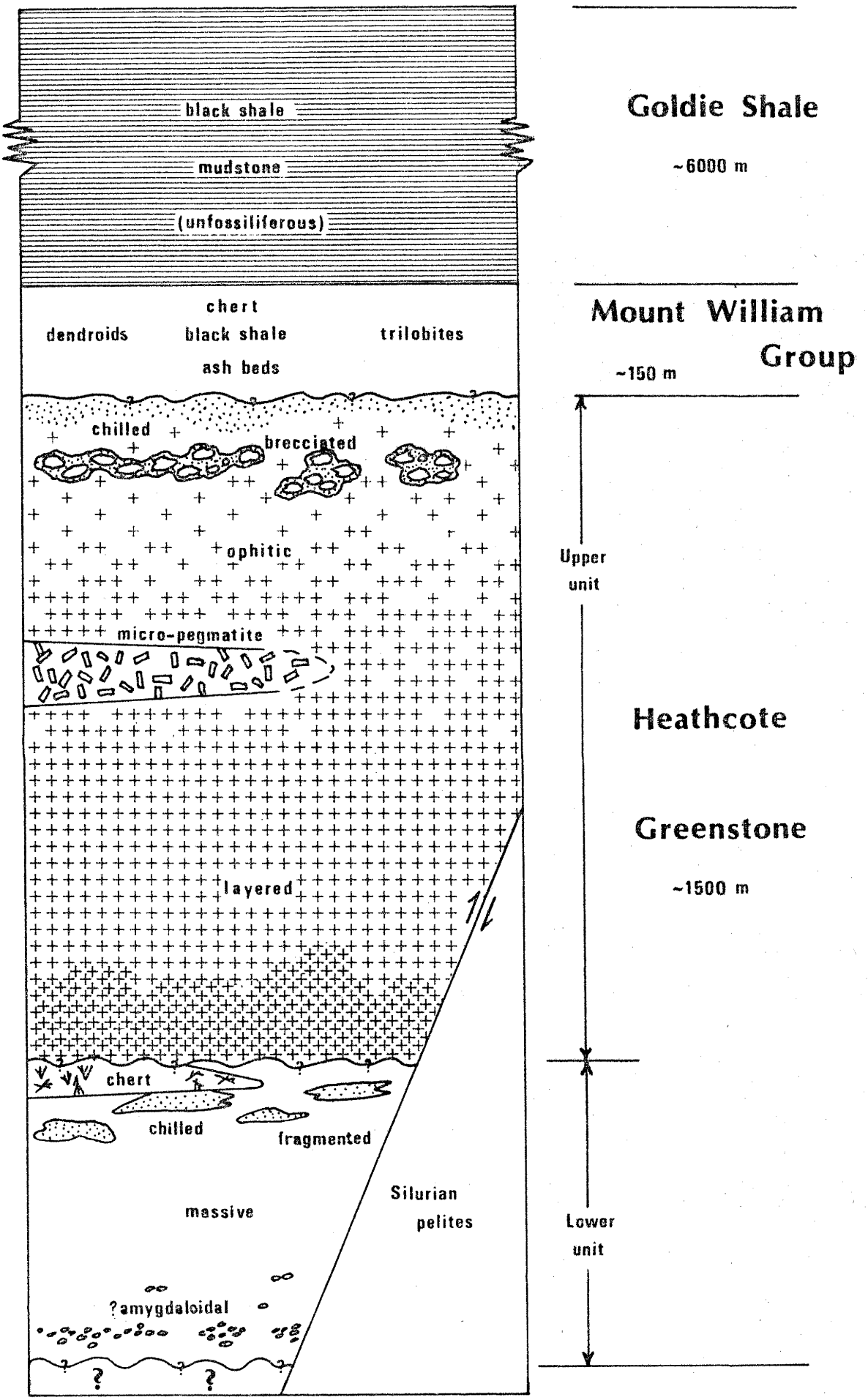

6. Cambrian stratigraphy - Mt. Camel

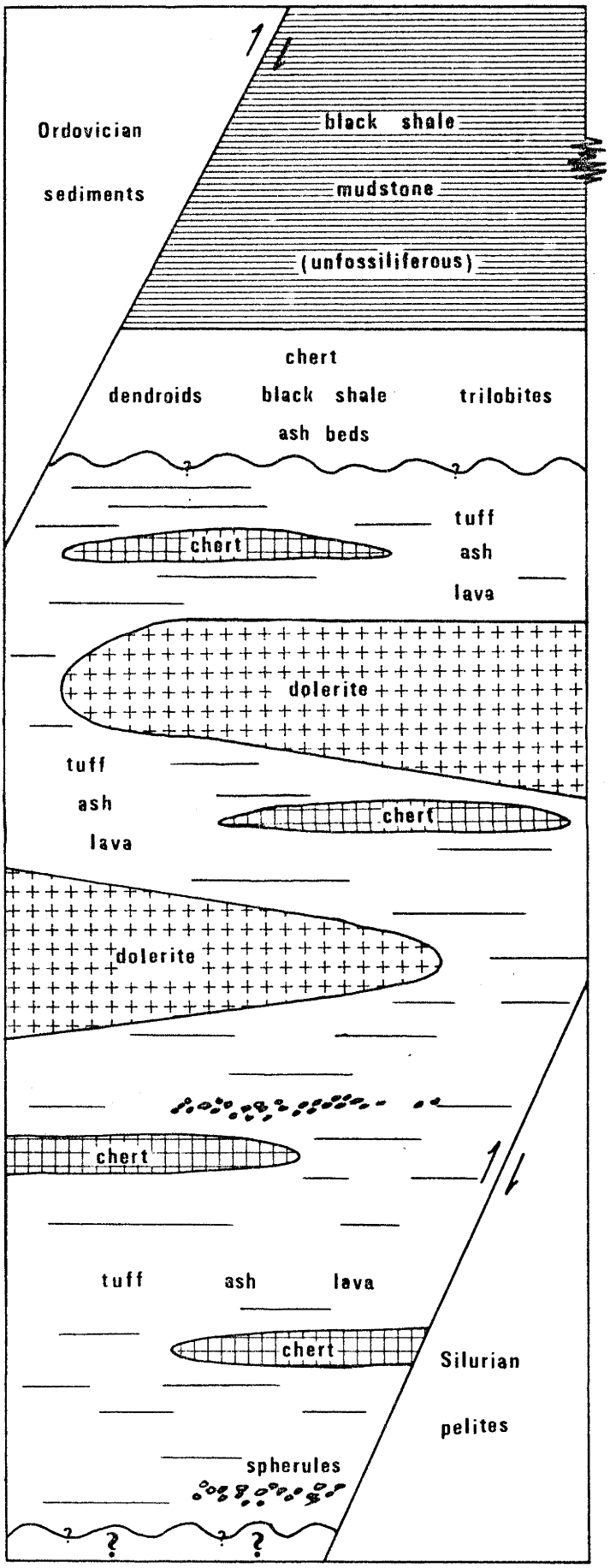

Goldie Shale

~6000 m

Knowsley East Formation

~150 m

Heathcote

Greenstone

~1500 m

NATURE OF THE GRANITIC PLUTONS

The Heathcote Greenstone was affected by contact metamorphism near Mount William and Mount Camel by the Cobaw and Crosbie Granites respectively (Fig. 2). A comprehensive study of the Cobaw Granite was made by Stewart (1966), and because the Crosbie Granite is poorly exposed it has not been studied in detail.

Stewart (1966) classified the granitic rocks in central Victoria as 'high-level plutons' using Read's Granite Series (Read, 1949), and 'Epizonal plutons' according to Buddington's scheme (Buddington, 1959). On the basis of mineralogy and geochemistry, Chappell & White (1974) subdivided granitoids in the Lachlan Mobile Zone into I- and S-types depending upon whether granitic magma was derived from igneous or sedimentary source material. Assuming a similar petrogenetic model and classification scheme to theirs, convenient labels may be placed on the Victorian granitoids.

On a regional scale the Cobaw and Crosbie granite plutons are discordant bodies to the main structural trends, for they are emplaced across the general strike of Cambrian, Ordovician and Silurian sediments. The Cobaw Granite has an outcrop area of approximately 190 sq km whereas the Crosbie Granite covers 40 sq km. Petrographic descriptions of rocks from both granitic bodies are given in Appendix 1.

The Devonian Cobaw Granite consists of four main intrusions which are in order of emplacement, hypersthene porphyrite (G1), granite (G2), granodiorite (G3) and (G4), a porphyritic granodiorite (Singleton, 1949; Stewart, 1966; McLaughlin & Tattam, 1976). The granite (G2) is of particular interest to this study as it lies adjacent to greenstone. It is coarse-grained, composed of perthite, quartz, biotite and minor plagioclase

and may be classified as an S-type granite because it contains scattered xenoliths of sedimentary origin. It encloses hornblendic granodiorite (G3) which is probably an I-type granite because igneous xenoliths are common. However, until detailed geochemical studies are done on these rocks the classifications used above must be regarded as tenuous.

Stewart (1966) proposed that stoping was the emplacement mechanism of the composite Cobaw Granite. However, if the tenuous I- and S-type labels placed on rocks of the pluton are substantiated, this poses an interesting genetic problem. Distribution of rocks of I- and S-types within the massif suggests a mechanism other than stoping but a likely model cannot be stated until further work is carried out.

The contact between the Cobaw Granite and country rocks near Mount William was not found. Though the granite is neither sheared nor foliated at the margins of the pluton several xenoliths are elongate parallel to the contact. This suggests that the partly assimilated xenoliths were aligned with their long axes parallel to the flow direction in the granitic magma.

A narrow granodiorite dyke was emplaced, apparently along a fault, into greenstone 800m northeast of Mount William. Movement along the fault, intrusion of the dyke, or both, displaced the general trend of the greenstone by about 30^{o} (Fig. 3A). Emplacement of the granodiorite dyke caused local variation to the main influence of thermal metamorphism in which the temperature gradient predictably decreases with distance from the intrusive contact (Jaeger, 1957, 1959).

Stewart (1971), determined K-Ar ages of 359m yr and 358m yr for the granite (G2) and granodiorite (G3) respectively. Although the Cobaw Granite is composed of several intrusions it cooled essentially as a single mass (Stewart, 1971).

On emplacement of the granite (G2), contact metamorphism affected all the surrounding country rocks resulting in a ridge of resistant hornfels ranging from 1km to 2km in width. The metamorphic mineral assemblages and their distributions in Ordovician and Silurian metasediments indicate a zoned aureole, with an inner zone of biotite and cordierite hornfels of the hornblende hornfels facies, and an outer zone of sericite hornfels of the albite-epidote hornfels facies (Stewart, 1966).

Contacts between the Crosbie Granite and country rocks were not observed. The granite is leucocratic in outcrop, containing quartz, orthoclase, plagioclase and muscovite. Lack of fresh samples does not permit easy classification of I- or S-types and also prevents reliable age dating.

Mapping by Thomas (1956, 1960) and several traverses as part of this study reveal a hornfels zone less than 1km wide around the Crosbie Granite. The nature of contact metamorphism of the country rocks by the Crosbie Granite is difficult to ascertain because continuous outcrop is absent. Thomas et al (1976, p21), reported that the Crosbie Granite caused some biotite to develop in altered dolerite.

SUMMARY

1. The Cobaw and Crosbie granitic plutons are high-level discordant intrusions.
2. The Cobaw Granite has an outcrop area five times that of the Crosbie Granite and, unless the surface exposure of the latter is not representative of its size, the Cobaw Granite cooled over a much longer period.
3. At Mount William the metamorphic aureole is zoned in pelites and up to 2km wide whereas near Mount Camel contact hornfels extends for less than 1km into country rocks.
4. Contact metamorphism was essentially thermal at Mount William and metasomatic (Ca, ?Na) at Mount Camel.

PLATE 1

1.1 Southeast view from the Cobaw Granite (G2) towards the start of traverse B. The location of sample A12, on the ridge in the background, is also shown.

1.2 Southerly view from the margin of the Cobaw Granite showing the locations of samples along traverse A.

CONTACT METAMORPHISM

Mount William and Mount Camel

Volcanics of the lower unit at Mount William and near Mount Camel were regionally metamorphosed to the greenschist facies (Thomas et al, 1976). At Mount William dolerite intruded the metavolcanics after regional metamorphism but before contact metamorphism.

Intrusion of the Cobaw Granite had an essentially thermal effect on the country rocks as there is an absence of replacement veins and exotic minerals typical of metasomatism. Nicholls (1965) regards calcium metasomatism as an important factor in the alteration of rocks in the Mount Camel area but he is not explicit as to the source of the calcium. Development of biotite in altered dolerite near Mount Camel (Thomas et al, 1976) suggests mobility of potassium.

Mount William Area

Not only is it possible to subdivide the greenstone at Mount William into Lower and Upper stratigraphic Units based on relict textures and minerals, but also these units conveniently fit two metamorphic zones because of their metamorphic mineral assemblages. Zone 1 is characterised by actinolite-cummingtonite and occurs between 600m and 1500m from the intrusive contact. Zone 2 contains a hornblende-calcic plagioclase assemblage and lies within 600m of the Cobaw Granite. Rocks outside the aureole are regionally metamorphosed volcanics containing greenschist facies minerals actinolite, chlorite and carbonate. Petrographic descriptions of the rock types in these zones are set out in Appendix 1 and a summary of the mineral assemblage in each zone is given in Table 1.

TABLE 1. Mineral assemblages in metamorphic zones at Mount William.

MINERAL	REGIONAL ZONE	CONTACT ZONE 1	CONTACT ZONE 2
plagioclase	albite	albite	anorthite
amphibole	actinolite	actinolite cummingtonite	hornblende
pyroxene	--	--	augite (relict igneous)
	chlorite	(chlorite)	--
	epidote	(epidote)	(epidote)
	stilpnomelane	--	--
other	quartz	quartz	--
	(sphene)	sphene	sphene
	calcite	(calcite)	--
	magnetite	magnetite	ilmenite

Dash = absent, parentheses = rare amounts.

CONTACT ZONE 1

The location of this zone is illustrated in Figure 3B and the mineral assemblage (Table 1) fits the albite-epidote hornfels facies of contact metamorphism, suggesting a temperature of about 400°C in the outer part of the aureole (Winkler, 1965, Table 4). Actinolite and cummingtonite are the main minerals, making up to 95% of most rocks. Spheroids of granular albite, quartz and carbonate are common and either represent altered amygdales or accretions resulting from local remobilisation of Na, Ca, Al and Si. Nicholls (1965) regarded the pale spheroids as replacement textures. The nature of mineral replacement is significant for any understanding of the history of alteration of these rocks.

Silicification seems likely considering the high SiO_2 content of the rocks, up to 55.84 weight per cent (Table 2). However, selective deposition

TABLE 2

Compositional range of amphiboles and rocks in Zone 1, Mount William.

	ZONE 1								
WT%	INNER			CENTRE			OUTER		
ELEMENT	ROCK	ACT	CUMM	ROCK	ACT	CUMM	ROCK	ACT	CUMM
SiO_2	54.47	55.45	55.77	55.84	54.71	56.92	51.20	50.13	49.94
TiO_2	.03	-	-	.03	-	-	.01	-	-
Al_2O_3	3.26	2.94	1.78	3.08	3.41	1.08	1.29	7.52	4.40
FeO	12.45	6.60	15.39	11.77	7.36	13.56	10.98	7.84	12.33
MnO	.18	-	.19	.17	-	-	.24	.34	.38
MgO	22.85	21.00	24.12	23.75	20.36	26.13	24.12	17.96	23.53
CaO	3.92	11.19	.60	2.29	11.03	.51	5.00	9.12	2.26
Na_2O	.19	.15	-	.20	.25	-	.22	-	-
K_2O	.07	-	-	.02	-	-	.01	-	-
Cr_2O_3	-	.82	.24	-	.85	-	-	.10	.37
TOTAL	97.42	98.15	98.10	97.15	97.98	98.20	93.07	93.02	93.20
	NUMBER OF IONS ON BASIS OF 23(0)								
Si		7.69	7.79		7.63	7.86		7.34	7.35
Al^{iv}		.31	.21		.37	.14		.66	.65
Al^{vi}		.16	.08		.20	.04		.64	.12
Ti		-	-		-	-		-	-
Fe		.77	1.80		.86	1.57		.96	1.52
Mn		-	.03		-	-		.04	.05
Mg		4.34	5.02		4.23	5.38		3.92	5.16
Ca		1.66	.09		1.65	.08		1.43	.36
Na		.03	-		.07	-		-	-
K		-	-		-	-		-	-
Cr		.08	.03		.09	-		.01	.04
TOTAL		15.05	15.05		15.08	15.05		15.00	15.24
$\frac{Mg}{Mg+Fe}$	.879	.880	.782	.862	.864	.977	.919	.841	.814
Ca	8.3	22.1	1.2	4.8	22.1	0.8	11.8	20.6	4.5
Mg	80.5	68.5	77.3	82.1	67.3	80.8	81.0	66.8	77.8
Fe	11.1	9.4	21.5	13.1	10.6	18.3	7.1	12.6	17.8

ACT = actinolite CUMM = cummingtonite

of silica in spheroids requires a unique mechanism. Addition of SiO_2 during burial metamorphism followed by preferential growth of amphibole under regional metamorphic conditions may lead to quartz and albite occuping the smallest possible volume, hence the spheroidal shape.

Mobility of calcium under partial pressure of CO_2 explains the presence of carbonate. Local stresses caused by development of amphibole, confining pressure and presence of voids may control concentration of this mineral in spheroidal structures. A similar mechanism is needed for concentrating albite in granular mosaic aggregates. Mobilisation of Na and Al during submarine weathering and burial metamorphism is suggested by their low concentrations, and indicates that they were lost from the original rocks during alteration.

To understand the nature of the alteration processes and effects of contact metamorphism a study was made of changes in amphibole chemistry across the zone. The general structural formula of amphiboles is $W_{0-1}X_2Y_5Z_8O_{22}(OH)_2$ (Ernst, 1968) and calculation of this formula, on the basis of 23 oxygens (anhydrous), follows Papike et al (1969). Distinction is made between tremolite and actinolite on the basis that most actinolites have Mg/Mg+Fe between 0.75 and 0.85 (Hietanen, 1974), and tremolites greater values than 0.90 (Stout, 1972). Cummingtonite is used to describe amphiboles containing 5 Mg ions and less than 1 Ca ion in their structural formula.

The range of amphibole compositions across Zone 1 is illustrated in Figure 7. The ratio of major element content (in weight per cent) between amphibole and rock (X_{amph}/X_{rock}) is plotted against distance from the Cobaw Granite. This ratio indicates changes in amphibole composition with bulk chemistry and increasing temperature.

7. Ratio between Amphibole composition and bulk chemistry - variation with distance from the Cobaw Granite

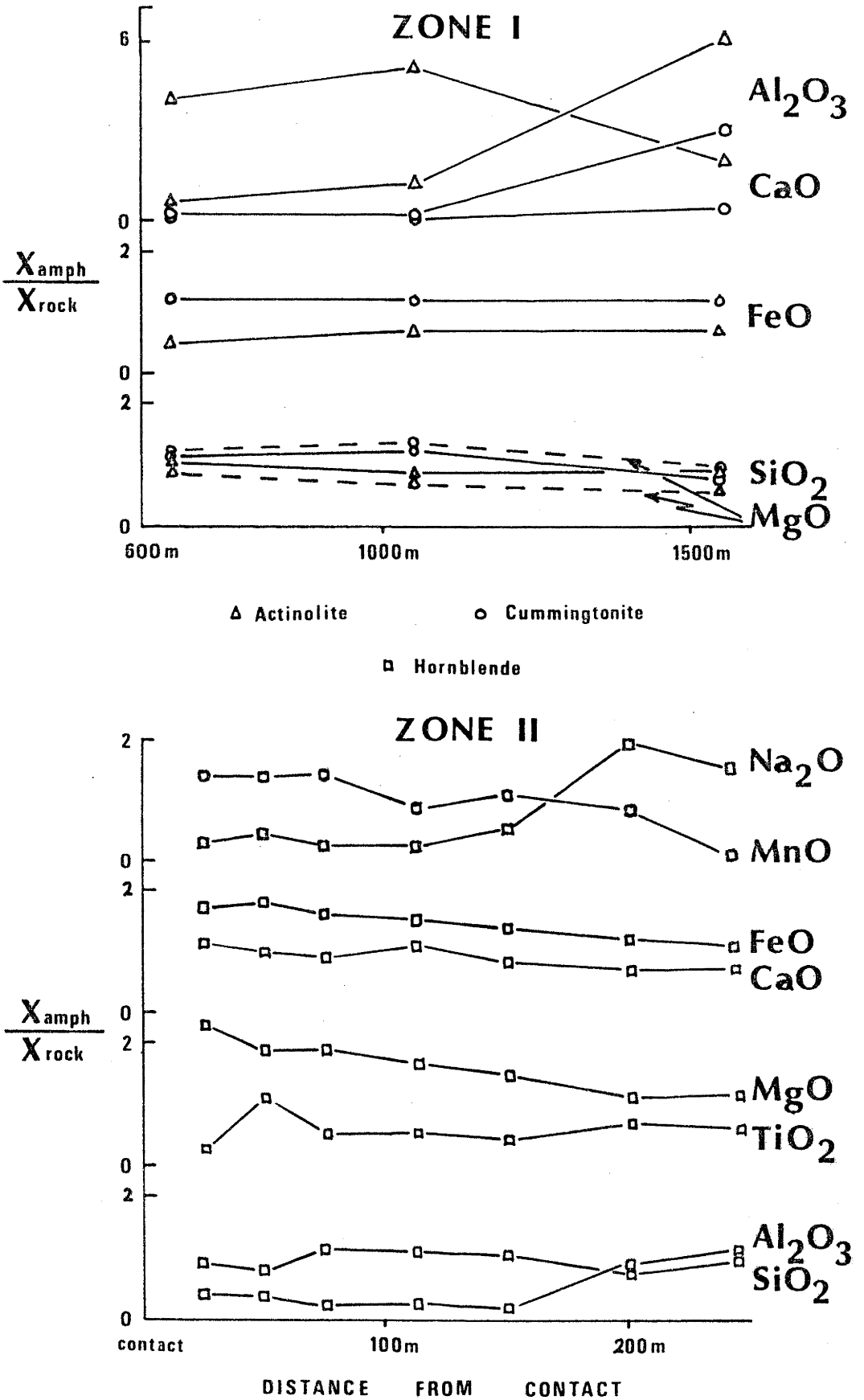

Aluminium decreases in actinolite and cummingtonite whereas calcium increases in tremolite and decreases in cummingtonite as the granite is approached. Silicon increases in both amphiboles but magnesium only increases in actinolite. FeO is relatively constant and sodium, titanium, manganese and chromium very low or absent. These trends must be rationalised in conjunction with structural formulae of the amphiboles (Table 2) and major element variation of the rocks (Figure 8).

The highest aluminium content of amphiboles occurs in the outermost part of the aureole even though the rocks contain little Al_2O_3 (1.29 wt %). In this case silicon is lower than in other parts of the zone suggesting that the availability of SiO_2 to amphiboles from the rocks affects the relative proportions of Si and (tetrahedral) Al in the Z-sites.

Though the content of CaO in the rocks decreases as the intrusive contact is approached the amount of calcium increases in the X-sites, suggesting that acceptance of this element into the actinolite structure increases with progressive metamorphism. The low calcium content of cummingtonite is not significant in controlling the composition of this amphibole.

Magnesium is the most abundant element in both amphiboles as it accounts for over 80% of the total number of ions in the Y-sites. For the sum of cations ($Fe+Mg+Al^{vi}$) in the Y-sites to equal 5.00 there is an excess of Mg. The surplus of magnesium from the Y-sites can be added with the insufficient amount of calcium to fill the X-sites. The relative availability of calcium and magnesium is most important in controlling the composition of actinolite and cummingtonite. As the content of iron is much lower than magnesium the relative abundance of iron in the rocks contributes less to the composition of amphibole than variation in magnesium.

PLATE 2

2.1 View from the Cobaw Granite to the east along the start of traverse A. Note the sparse and rubble strewn exposures.

2.2 Northerly view from traverse A towards traverse B and the Cobaw Granite.

The *mg* values (Mg/Mg+Fe) of the rocks (Table 2), decrease across the zone toward the granite. England (1972) recognised a similar decrease with increasing grade of regionally metamorphosed basic rocks. In contact metamorphosed terrains Compton (1958), recorded a decrease in the *mg* values for rocks and amphiboles whereas Green (1964), found an increase in Mg/Mg+Fe for both rocks and amphiboles with increasing metamorphism. Binns (1965) and Cahill (1968) determined increases in the *mg* value for amphiboles with increasing temperature in contact aureoles.

A parallel trend of decreasing *mg* values is found between rocks and cummingtonite with increasing temperature across Zone 1. However, actinolite increases in Mg/Mg+Fe as the Cobaw Granite is approached. Similar relations between rocks and cummingtonite conform to the opinion expressed by Hietanen (1974), that the *mg* value of amphiboles is dependent on bulk chemistry and degree of oxidation of the host rocks. Bulk chemical variations toward the Cobaw Granite do not account for the *mg* trend of actinolite, suggesting that the composition of actinolite must be influenced by progressively higher temperatures. Therefore the compositions of actinolite and cummingtonite are dependent on bulk chemistry as well as temperature.

CONTACT ZONE 2

Zone 2 extends out from the margin of the Cobaw Granite for 600 metres (Fig. 3B). The rocks in this zone belong to the Upper Unit and change in texture from relict doleritic to noticeably granular and hornfelsic with progressive metamorphism. Table 1 lists the mineral assemblage in the rocks belonging to the hornblende-hornfels facies and which reached a temperature of less than 600°C (Winkler, 1965).

Plagioclase changes from euhedral laths to anhedral and granoblastic as the granite contact is approached. Augite is rimmed by blades and prisms

of hornblende which successively change from bluish-green through brown-green to green-brown toward the Cobaw Granite. Skeletal ilmenite develops poikiloblastic intergrowths of colourless sphene and relict iron-titanium oxide. Red-brown sphene forms small fields around clusters of iron oxide granules. Detailed petrographic descriptions are given in Appendix 1.

Plagioclase compositions range from An_{97-98} to An_{67-72} as the granite contact is approached. These compositions were determined by electron microprobe and must be regarded as representing analyses of metamorphic rather than igneous minerals. The high anorthite component of plagioclase in rocks from the outermost part of the zone is not easily reconciled with the common feldspar compositions of dolerite (An_{50-60}); early formed crystals may reach An_{70-90} (Williams et al, 1954). Plagioclase commonly becomes more calcic with progressive metamorphism (Compton, 1958; Engel, Engel & Havens, 1964; Binns, 1965; Loomis, 1966; Liou et al, 1974), however exact PT-conditions have not been determined for the start of this process. High grades of metamorphism are probably needed before plagioclase is significantly enriched in anorthite molecule. As the rocks in Zone 2 contain large amounts of CaO, between 11.07 and 15.13 weight per cent, the high activity of calcium during metamorphism would enhance conversion to anorthite-rich plagioclase.

Petrographic and mineralogical studies reveal the colour change of hornblendes noted above, which reflects compositional variations in the mineral attributed to differences in bulk chemistry. The trend from bluish green to brown with increasing temperature is usually found in regionally metamorphosed areas (Shido, 1958; Shido & Miyashiro, 1959; Engel, Engel & Havens, 1964; England, 1972). A similar colour range to that shown by hornblendes from Zone 2 at Mount William was found by Binns (1965) during a study of basic hornfelses in the New England region. In other contact

metamorphic terrains opposite trends are observed (Cahill, 1968; Stindl, 1971). Changes in colour of hornblende is attributed to the titanium content (Liou et al, 1974) but the oxidation state of iron and to a lesser extent, manganese content may also be important factors.

In rocks close to the Cobaw Granite, where the TiO_2 content of the rocks is high (Appendix 2), blades of hornblende contain parallel streaks of sphene. Similar textures were observed by Binns (1965) in hornblendes from New England. He thought that excess titanium from clinopyroxene could not be accepted by the replacing amphibole and exsolved from the metamorphic mineral as platelets and rods. These features are neither found in prismatic hornblende nor in amphibole rims around pyroxene cores, suggesting that exsolution of sphene must be crystallographically controlled.

Epidote is a minor constituent of this zone. It is limited in occurrence to several small areas, affected by deformation and probable local hydrothermal fluids. For the above reasons, in constructing reactions to explain metamorphic processes in Zone 2, epidote is neglected.

Sphene is present throughout the zone, being abundant close to the Cobaw Granite where TiO_2 is high (Appendix 2). In the outer parts of Zone 2, sphene rims small iron oxide grains whereas nearer the granite it encloses dust-like clusters of opaque minerals and forms poikiloblastic intergrowths with relict skeletal ilmenite. The high activity of calcium together with the readily available titanium from ilmenite account for the stability of sphene under the PT-conditions of this zone.

The main metamorphic effects are recrystallisation, compositional changes of minerals and growth of hornblende.

Two reactions are constructed to illustrate metamorphic changes in the outer and inner parts of Zone 2. Electron probe microanalyses for

sphene, ilmenite, pyroxene, amphibole and (metamorphic) plagioclase are listed in Appendix 2. In drawing up the reactions isochemical metamorphism was assumed, in order to derive the primary plagioclase composition.

Metamorphic reaction in the outer part of contact Zone 2;

$4Ca_{.87}(Mg_{.86}Fe_{.22}Al_{.02})(Al_{.05}Si_{1.95})O_6$ clinopyroxene

+

$3(Na_{.14}Ca_{.86})Al_{1.88}(Al_{.12}Si_{1.88})O_8$ plagioclase

+

$2Fe_{.54}Ti_{.46}O_3$ ilmenite

+

H_2O

yields

$Ca_{1.96}(Mg_{3.17}Fe_{1.33}Na_{.37}Al_{.58})(Al_{1.27}Si_{6.73})O_{22}(OH)_2$ hornblende

+

$2(Na_{.02}Ca_{.98})Al_{1.99}(Al_{.01}Si_{1.99})O_8$ plagioclase

+

$3Ca_{.75}Fe_{.21}Ti_{.31}Al_{.05}Si_{.91}O_5$ sphene

Compositional balance is obtained in this reaction by formulating the initial plagioclase composition so that the necessary Na, Ca, Al and Si is available. The main metamorphic effect is one of hydration with water supplied by the granite. The reaction is acceptable because volume calculations, based on data from Robie et al (1966), suggest a 1% decrease in volume.

Metamorphic reaction in the inner part of contact Zone 2;

$5Ca_{.94}(Mg_{.65}Fe_{.39}Al_{.01})(Al_{.04}Si_{1.97})O_6$ clinopyroxene

+

$(Na_{.76}Ca_{.24})Al(Al_{1.97}Si_{1.95})O_8$ plagioclase

+

$2Fe_{.52}Ti_{.45}O_3$ ilmenite

+

H_2O

yields

$Ca_{1.98}(Mg_{2.31}Fe_{2.25}Na_{.37}Al_{.34})(Al_{1.23}Si_{6.77})O_{22}(OH)_2$ hornblende

+

$(Na_{.39}Ca_{.54})Al_{1.03}(Si_{.38}Al_{.62})Si_2O_8$ plagioclase

+

$3Ca_{.50}Ti_{.30}Fe_{.35}Mg_{.31}Si_{.66}O_5$ sphene

The reaction is balanced by devising a composition for primary plagioclase which supplies the appropriate amount of elements. A check on volume changes shows an increase of approximately 8%. Substantial recrystallisation and loss of primary igneous textures explain the volume change. The greater volume change in rocks close to the granite compared with those farther away is expected because metamorphism is more advanced near the Cobaw Granite. In volume for volume replacement orthopyroxene or some other 'low-volume' mineral needs to crystallise, but because minerals of this kind do not occur recrystallisation results in a volume increase.

The compositional changes in hornblende across Zone 2 (Table 3) are illustrated in Figure 7. The ratio X_{amph}/X_{rock} plotted against distance from the Cobaw Granite is used to identify relative influences of bulk chemistry and increasing temperature. The ratio X_{amph}/X_{rock} decreases for Na_2O and Al_2O_3, increases for MnO, FeO, CaO, TiO_2 and MgO, whereas SiO_2 remains relatively constant. If the amphibole composition is solely dependent on bulk chemistry then the ratio should be constant, however, most elements do not conform to this relation suggesting that the nature of metamorphism controls amphibole chemistry.

TABLE 3

Contact Zone 2 - Hornblende.

WT%	B1	B7	B12	B15	B20	B27	B31	B36
SiO_2	45.01	43.97	48.53	49.70	47.75	47.71	47.01	46.87
TiO_2	.99	1.87	.42	.50	.60	.44	.59	.32
Al_2O_3	10.04	9.92	6.98	7.00	9.31	11.49	9.51	10.96
FeO	19.47	19.21	18.76	14.73	12.14	12.88	11.84	11.11
MnO	.40	.40	.24	.12	.14	.16	.14	-
MgO	10.18	10.00	11.99	13.60	14.00	12.72	14.75	14.82
CaO	11.67	11.82	11.75	12.79	12.67	12.32	12.22	12.79
Na_2O	2.11	1.82	1.19	1.18	1.59	2.15	1.65	1.32
K_2O	.39	.43	.12	.23	.18	.12	.20	.07
Cr_2O_3	.10	-	-	.16	.13	-	.12	.22
TOTAL	100.36	99.44	99.08	100.01	98.52	97.25	98.04	98.48
NUMBER OF IONS ON BASIS OF 23(O)								
Si	6.64	6.56	7.09	7.13	6.89	6.55	6.82	6.73
Al^{iv}	1.36	1.44	.91	.87	1.11	1.45	1.18	1.27
Al^{vi}	.38	.30	.18	.32	.47	.50	.44	.58
Ti	.11	.21	.04	.05	.07	.09	.06	.04
Fe	2.40	2.39	2.29	1.77	1.47	1.81	1.44	1.33
Mn	.05	.05	.03	.02	.02	.02	.02	-
Mg	2.24	2.22	2.61	2.90	3.01	2.72	3.19	3.17
Ca	1.84	1.89	1.84	1.97	1.96	1.90	1.90	1.97
Na	.60	.52	.33	.33	.45	.63	.46	.37
K	.07	.09	.02	.03	.03	.05	.04	.01
Cr	.01	-	-	.02	.02	.02	.01	.03
TOTAL	15.71	15.67	15.44	15.40	15.48	15.72	15.55	15.49
$\frac{Mg}{Mg+Fe}$	.546	.544	.595	.679	.726	.660	.741	.754
Ca	27.5	28.1	26.1	27.9	28.5	28.1	27.1	28.3
Mg	39.6	39.1	43.9	48.9	51.9	47.5	54.0	54.1
Fe	32.9	32.8	29.9	23.1	19.6	24.5	18.9	17.6

Total iron as FeO, analyses by probe.

The Na content of amphibole increases from the outer part of Zone 2 toward the granite (Table 3). The sodium content of rocks increases as the granite is approached, implying that progressive metamorphism and bulk chemistry govern the amount of Na in the A-site. That is, the tendency to fill the A-site in hornblende increases as the temperature increases. This contrasts with the analytical results from two other contact metamorphic areas. In a study of the Bidwell Bar region of California, Compton (1958) found increases in sodium content for amphiboles and host rocks with increasing temperature. On the other hand, Green (1964) determined that sodium decreased in amphiboles whereas the bulk chemistry showed an increase in Na_2O as the temperature increased. These contrasts in the behaviour of sodium in hornblende during contact metamorphism indicate that PT-conditions and bulk chemistry govern the amount of sodium in amphiboles.

Manganese increases slightly in amphiboles and rocks as the Cobaw Granite is approached. The pronounced rise in the X_{amph}/X_{rock} ratio with metamorphism indicates that hornblende accepts manganese more readily at higher temperature, and the increase is at a greater rate than the increase in MnO in the rocks. In contrast, Green (1964), found a parallel trend of decreasing manganese in amphiboles and host rocks with progressive metamorphism. Clearly the bulk chemistry is an important influence on the manganese content of hornblende.

Increasing content of iron in amphiboles and host rocks results in a gradual increase in the X_{amph}/X_{rock} ratio. Iron increases at a greater rate in amphiboles than in the rocks, a trend which is attributed to higher temperature. On the other hand, Green (1964) and Compton (1958) measured decreases in the iron content of amphiboles and host rocks. The amount of FeO in hornblende is strongly dependent on the bulk chemistry of the host rocks, and when iron is abundant hornblende readily accepts more of it at higher temperatures.

TABLE 4

BULK CHEMISTRY - ZONE 2

WT%	B1	B7	B12	B20	B27	B31	B36
SiO_2	49.66	49.17	49.08	49.03	49.01	48.05	47.86
TiO_2	1.15	1.06	.89	.79	.69	.56	.53
Al_2O_3	16.61	17.02	16.65	15.76	14.16	10.48	10.15
Fe_2O_3	1.80	2.29	1.82	1.57	2.00	2.49	2.06
FeO	8.58	8.10	8.23	6.85	6.86	7.15	7.33
MnO	.19	.19	.18	.18	.17	.19	.17
MgO	5.50	5.86	6.67	8.70	10.20	13.56	14.23
CaO	11.59	11.90	12.71	12.37	13.50	14.58	14.62
Na_2O	3.15	2.96	2.26	2.27	1.90	.82	.87
K_2O	.17	.18	.11	.08	.08	.07	.06
P_2O_5	.09	.09	.08	.07	.06	.04	.04
S	.01	.02	.05	.02	.02	.05	.04
H_2O+	1.04	1.06	1.16	1.29	1.31	1.57	1.84
H_2O-	.06	.08	.06	.04	.05	.06	.06
CO_2	-	.01	.09	.07	.06	.08	.12
SUBTOTAL	99.60	99.99	100.04	100.09	100.07	99.75	99.98
O = S	-	.01	.02	.01	.01	.02	.02
TOTAL	99.60	99.98	100.02	100.08	100.06	99.73	99.96
$\frac{Mg}{Mg+Fe}$	.533	.562	.589	.695	.727	.771	.776
Ca	45.2	46.0	46.0	44.3	44.1	41.3	40.4
Mg	21.4	22.7	24.2	31.2	33.4	38.4	39.3
Fe	33.4	31.3	29.8	24.5	22.5	20.3	20.3

Calcium and magnesium share similar trends; decreasing in the rocks and hornblende but increasing in X_{amph}/X_{rock} with increasing temperature. The change in bulk chemistry is therefore greater than the variation of these elements in hornblende across the zone. CaO and MgO are also temperature dependent as smaller amounts are accepted into hornblende at higher temperature.

Titanium increases slightly in hornblende and bulk chemistry across the zone and the X_{amph}/X_{rock} ratio is relatively constant. The belief (Liou et al, 1974) that colour change in hornblende is caused by its TiO_2 content is supported because of the large increase of Ti in hornblende near the granite. Bluish green and brown-green hornblende contain approximately equal amounts of Ti whereas green-brown hornblende contains significantly more of this element.

Even though the Al_2O_3 content of the rocks increases toward the Cobaw Granite the aluminium content of hornblende is relatively constant, a relation which must surely be temperature dependent. Similar amounts of aluminium are accepted into hornblende at high and low temperatures.

Silicon is relatively constant in its X_{amph}/X_{rock} ratio across Zone 2. As the rocks increase in SiO_2 toward the granite a similar trend is found for the silicon content of hornblende. The composition of hornblende, with respect to silicon, depends on the bulk chemistry of the rocks.

Possible explanations of major element changes across Zone 2 are discussed in a later section.

PLATE 3

3.1 View from sample location A looking across the alluvial flat which covers the Crosbie Granite, toward Mount Camel (centre) and Mount Pleasant (right).

3.2 The small area near Mount Camel from which samples D, E and F were collected. Note the lack of continuous rock exposure over a wide area.

CONTACT METAMORPHISM - Mount Camel

Contact metamorphic zones are not recognised around the Crosbie Granite, and petrographic studies of rocks collected from the Mount Camel area reveal different intensities of recrystallisation over a few metres. Descriptions of rocks from near Mount Camel are given in Appendix 1. The mineral assemblage is plagioclase, actinolite, cummingtonite, diopside and minor amounts of chlorite, epidote, quartz, sphene, calcite and magnetite. The rocks essentially belong the albite-epidote hornfels facies of contact metamorphism (Winkler, 1965).

Plagioclase (An_{56}) is anhedral and granoblastic whereas the amphiboles are acicular, sheath-like and commonly pseudomorph ?clinopyroxene. Diopside forms large plates (marginally altered to amphibole) and are of primary igneous origin. Epidote, quartz and calcite are abundant as veins. Spheroids of quartz, carbonate and plagioclase are common in some rocks and either represent altered amygdales or accretions resulting from local remobilisation. Similar textures are observed in rocks of the Lower Unit at Mount William and are attributed to migration of Na, Ca, Al and Si during submarine weathering, burial metamorphism and contact metamorphism.

The amphiboles, actinolite and cummingtonite have compositional ranges as set out in Table 5. In actinolite Ca, Mg, Fe, Al and Si occur in variable amounts. Low calcium contents are associated with high magnesium as excess Mg in the Y-sites is needed to fill X-sites. Iron reaches its highest value in actinolite in which the X-sites are filled by calcium. There is only slight variation in the amount of Si and Al in the tetrahedral sites. Minor amounts of Cr and Ti are also incorporated in actinolite.

A difference of 1.17 weight per cent in SiO_2 between rock samples D and E accounts for a gain of 0.23 Si ions per formula unit in actinolite.

TABLE 5

Compositions of amphiboles and rocks - Mount Camel.

	ROCK		ACTINOLITE		CUMMINGTONITE	
WT%	D	E	D	E	D	D
SiO_2	50.12	51.29	54.67	60.69	56.40	56.44
TiO_2	.22	.19	.22	-	-	-
Al_2O_3	9.28	8.51	3.59	1.54	.34	.94
Fe_2O_3	2.14	2.35	-	-	-	-
FeO	6.61	6.06	8.46	11.99	15.89	14.07
MnO	.18	.19	-	-	.14	.19
MgO	14.37	13.32	20.03	18.78	23.10	22.83
CaO	14.54	15.29	10.38	14.38	1.30	3.49
Na_2O	.59	.54	-	-	-	-
K_2O	.07	.09	-	-	-	-
P_2O_5	.03	.03	-	-	-	-
Cr_2O_3	-	-	.54	.14	-	.14
loss	1.92	2.27	-	-	-	-
TOTAL	100.07	100.13	98.89	107.51	97.17	98.11
			NUMBER OF IONS ON BASIS OF 23(0)			
Si			7.63	7.86	7.98	7.90
Al^{iv}			.37	.14	.02	.10
Al^{vi}			.22	.09	.04	.06
Ti			.02	-	-	-
Fe			.99	1.30	1.88	1.65
Mn			-	-	.02	.02
Mg			4.17	3.62	4.87	4.76
Ca			1.55	1.99	.19	.52
Na			-	-	-	-
K			-	-	-	-
Cr			.06	.01	-	.02
TOTAL			15.02	15.02	14.99	15.02
$\frac{Mg}{Mg+Fe}$	.834	.834	.845	.782	.769	.788
Ca	33.9	36.7	21.0	26.7	2.5	6.8
Mg	55.1	52.8	66.8	57.4	74.9	73.5
Fe	11.0	10.5	12.2	16.0	22.5	19.7

Decreasing the amount of Al_2O_3 in the rocks causes a decrease in the number of Al ions in the structural formulae for the two amphiboles. Cummingtonite is more dependent than actinolite on bulk chemistry for its iron content. This feature is probably due to oxidation state of iron, but as there is no way to correctly estimate Fe^{3+} from microprobe analyses the cause of this phenomenon remains unsolved.

There is a consistent relation between MgO in the rocks and decreasing Mg ions per formula unit in actinolite. Also, increasing CaO in the bulk chemistry corresponds to an increase in Ca ions per formula unit.

Cummingtonite in sample D contains low amounts of aluminium, variable iron, and up to 0.52 cations of calcium in its structural formula. No cummingtonite was found in sample E and diopside commonly occurs. Presence of clinopyroxene and absence of magnesium-rich amphibole is attributed to the high calcium content of the rocks (15.29wt%). High activity of calcium controls the composition of minerals formed in greenstone near Mount Camel.

SUMMARY

1. Mineral assemblages allow subdivision of the Heathcote Greenstone at Mount William into two metamorphic zones:

   ZONE 1 - Actinolite-cummingtonite hornfels.

   ZONE 2 - Hornblende-calcic plagioclase hornfels.

2. Zone 1 reached the albite-epidote hornfels facies and Zone 2 the hornblende hornfels facies of contact metamorphism.

3. Similar zones cannot be constructed in the Mount Camel area because of a lack of continuous outcrop.

4. Compositional changes in amphiboles and plagioclase indicate their variation with progressive metamorphism and bulk chemistry.

BULK CHEMICAL VARIATIONS

Mount William - CONTACT ZONE 1

Major element analyses of rocks from Zone 1 are listed in Appendix 2 and illustrated in Figure 8. From the outer parts of the aureole toward the Cobaw Granite the major element contents of the rocks change. There is an increase in SiO_2, TiO_2, Al_2O_3, FeO and P_2O_5, a decrease in MnO and MgO, and relatively constant values for K_2O, Na_2O, CaO, and Fe_2O_3.

Contributions to these trends are either from original bulk chemical differences, results of progressive metamorphism, or a combination of both factors. Appraisal of the parts played by each factor cannot be correctly assessed because extensive recrystallisation of all rocks in the zone, and of the Lower Unit generally, prevents comparison with geochemical trends of unaltered rocks. Therefore little can be said of element behaviour during contact metamorphism of rocks in Zone 1.

The absolute values of elements in the rocks pose an interesting genetic problem; to determine the nature of the original rocks from which the actinolite-cummingtonite hornfels developed. Possible parental rocks are indicated by comparing analyses of rocks from Zone 1 with average compositions of some igneous rocks (Nockolds, 1954). Though the silicon content of rocks in Zone 1 suggests andesitic affinity, the low concentrations of TiO_2 and Al_2O_3, together with magnesium and calcium indicate ultramafic parental rocks. Clearly the pristine magma type of rocks in Zone 1 is not easily determined.

In an earlier discussion, on contact metamorphism, it was stated that because minor amounts of plagioclase, carbonate and quartz occur as spheroids Si, Na, Al, and Ca were mobile during alteration processes. Low

8. Major element variation with distance from the Cobaw Granite

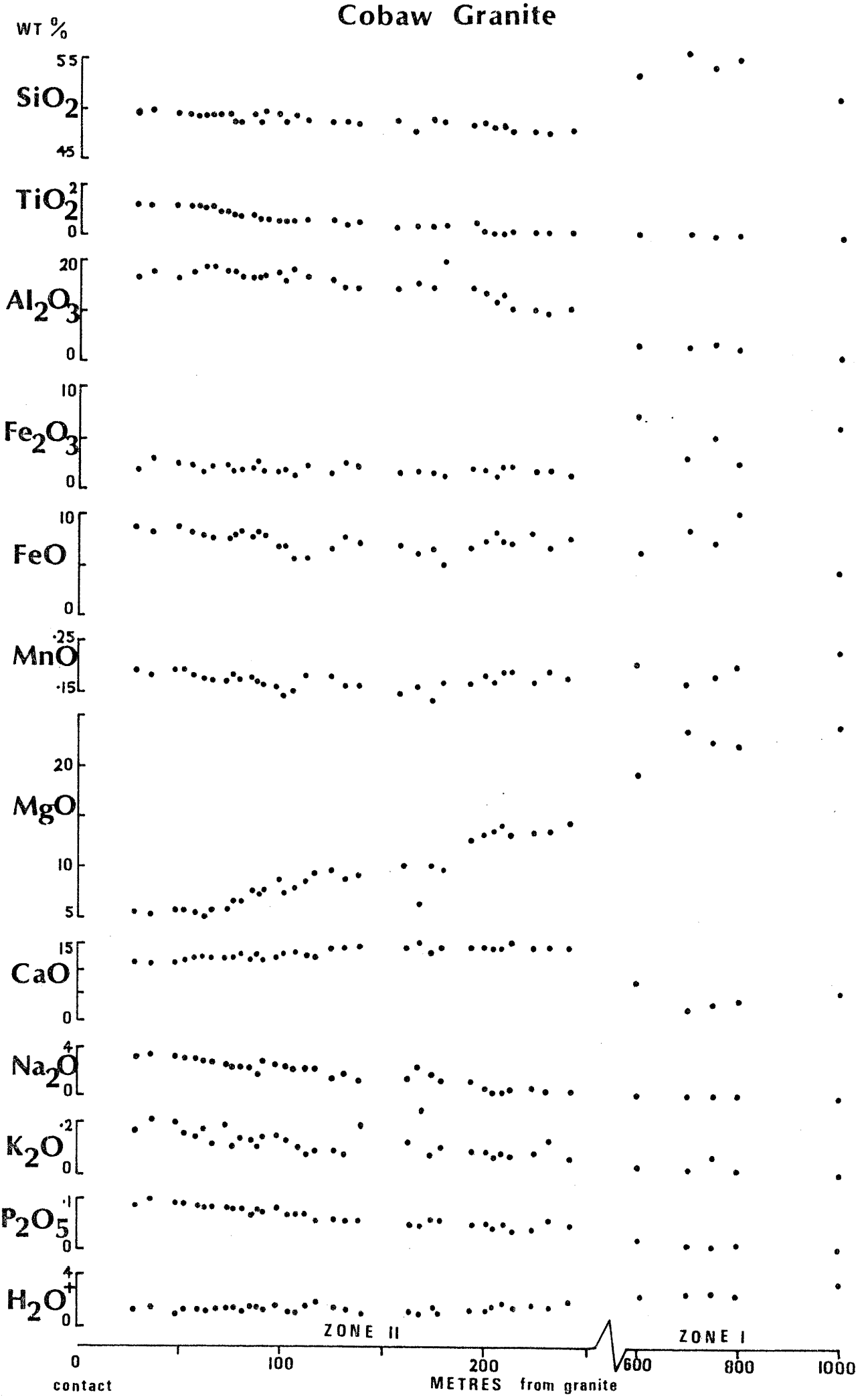

concentrations of Na_2O, K_2O, CaO, and Al_2O_3 together with high SiO_2 in rocks of Zone 1 is evidence for loss of alkalies and calcium and a gain in silicon. Though aluminium was mobile during alteration, the rocks probably retained their original Al_2O_3 content (Table 6.). Melson & Van Andel (1966), Cann (1969, 1970), Hart (1970), and Pearce (1974) mentioned that loss of aluminium occurs during greenschist facies metamorphism of basaltic rocks. Aluminium was lost initially from rocks in Zone 1 and added later during silicification and albitisation.

TABLE 6

Mobility of major elements and genesis of actinolite-cummingtonite hornfels at Mount William (Zone 1) and Mount Camel.

ELEMENT	MT. WILLIAM ZONE	MOBILITY	OLIVINE PYROXENITE	MOBILITY	MT. CAMEL
SiO_2	54.03	gain	49.2	gain	52.47
TiO_2	0.03	immobile	0.2	immobile	0.19
Al_2O_3	2.61	gain	2.4	gain	7.62
Fe_2O_3	4.88	gain	2.0	gain	2.27
FeO	7.48	gain	6.8	gain	6.93
MnO	0.20	immobile	0.2	immobile	0.20
MgO	22.42	gain	19.1	loss	14.64
CaO	4.74	loss	18.9	loss	12.82
Na_2O	0.21	?gain	0.2	gain	0.50
K_2O	0.03	loss	0.1	unchanged	0.10
H_2O	2.64	gain	0.6	gain	1.89
TOTAL	99.28		99.7		99.63

Olivine Pyroxenite (Ruckmick & Noble, 1969).

Table 6 summarises the mobility of major elements and the genesis by which alteration of olivine pyroxenite, or a rock of similar composition, results in analyses typical of actinolite-cummingtonite hornfels.

The relative mobility of major elements expected in submarine weathering and greenschist facies metamorphism is taken from published data (Melson & Van Andel, 1966; Cann, 1969; Hart, 1970; Pearce, 1974). Alteration of olivine pyroxenite, or rocks of similar composition, requires addition of SiO_2, MgO, total Fe and H_2O with loss of CaO and K_2O. The parent rocks from which the actinolite-cummingtonite hornfels developed are therefore thought to be ultramafics, compositionally similar to olivine pyroxenite.

Comparison of published analyses (Dawson, 1967; Goles, 1967) with trace element contents of samples from Zone 1 (Appendix 2) indicates ultramafic rather than basic or intermediate affinity. However, the strontium content in rocks of Zone 1 range between 50ppm and 400ppm, values which are high for ultramafic rocks. Faure & Hurley (1963) report a Sr content in pyroxenite of 49ppm compared with 6ppm in Alpine-type intrusions (Stueber & Murthy, 1966). Strontium is known to be mobile during albitisation and extreme weathering (Pearce & Cann, 1973). In some weathered submarine basalts Sr was found to be almost twice as abundant in the altered parts compared to the fresh rock (Philpotts et al, 1969). Therefore the mobility of Sr during submarine weathering, burial metamorphism and contact metamorphism isused to explain the variation of this element in rocks from Zone 1.

In a later discussion comparisons are made between analyses of rocks from Zone 1 at Mount William and similar rock types in Victoria and elsewhere.

9. Ca-Mg-Fe diagrams for greenstones and minerals

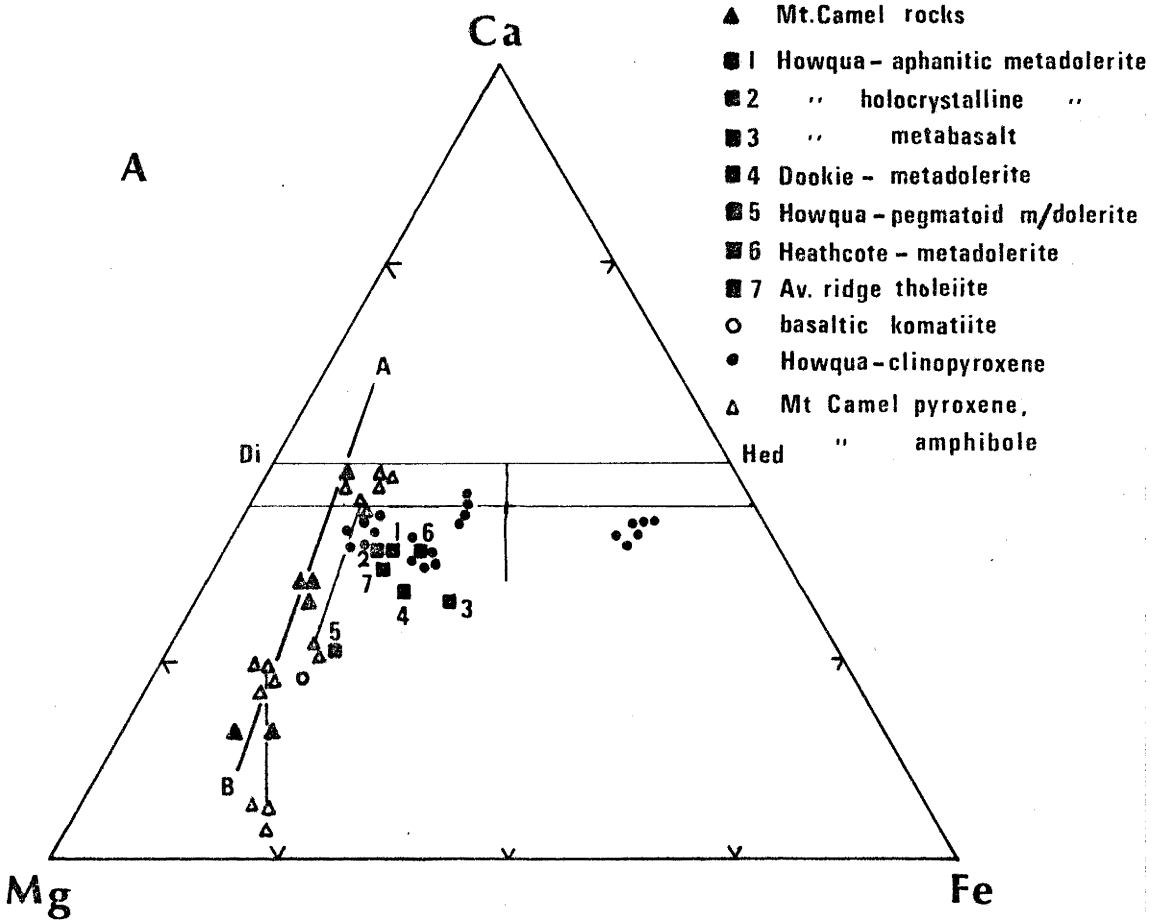

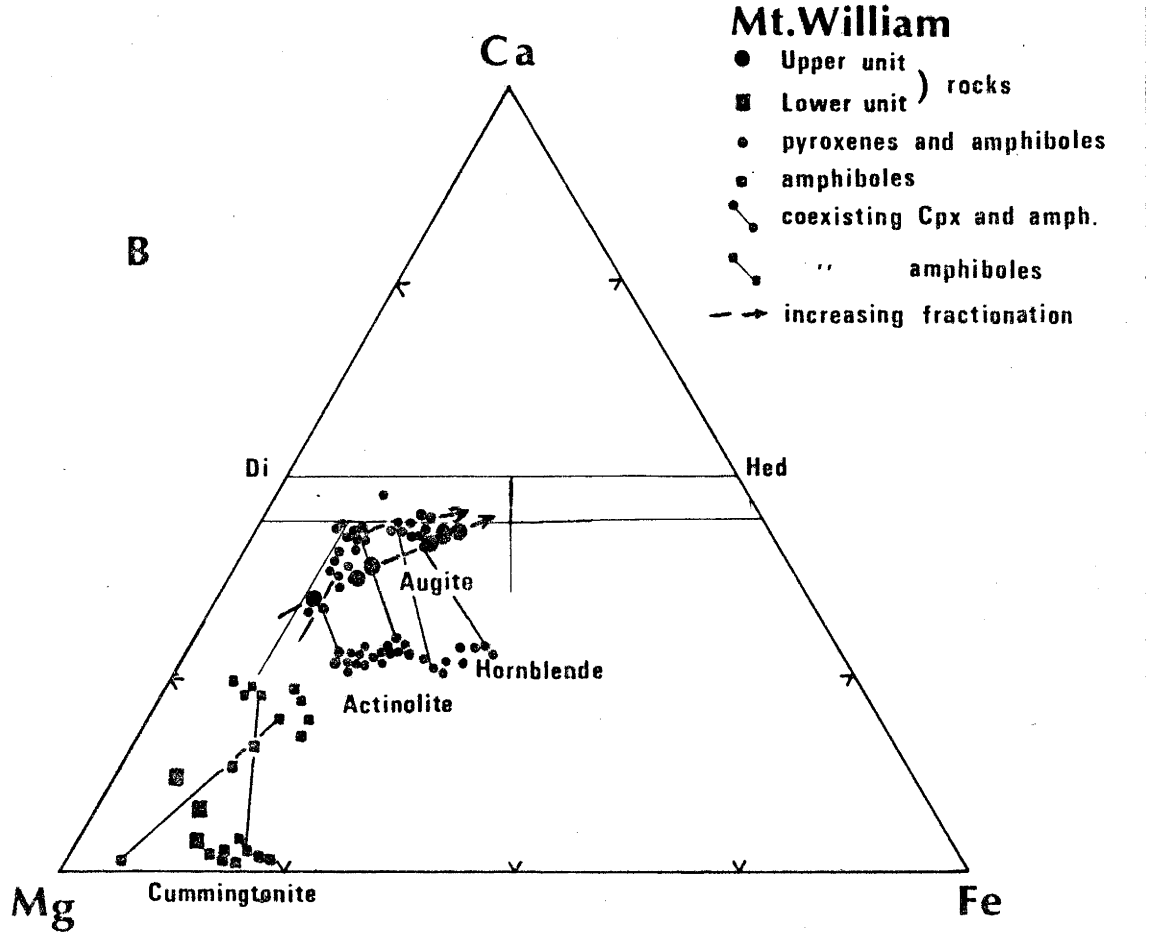

9. Ca-Mg-Fe diagrams for greenstones and minerals

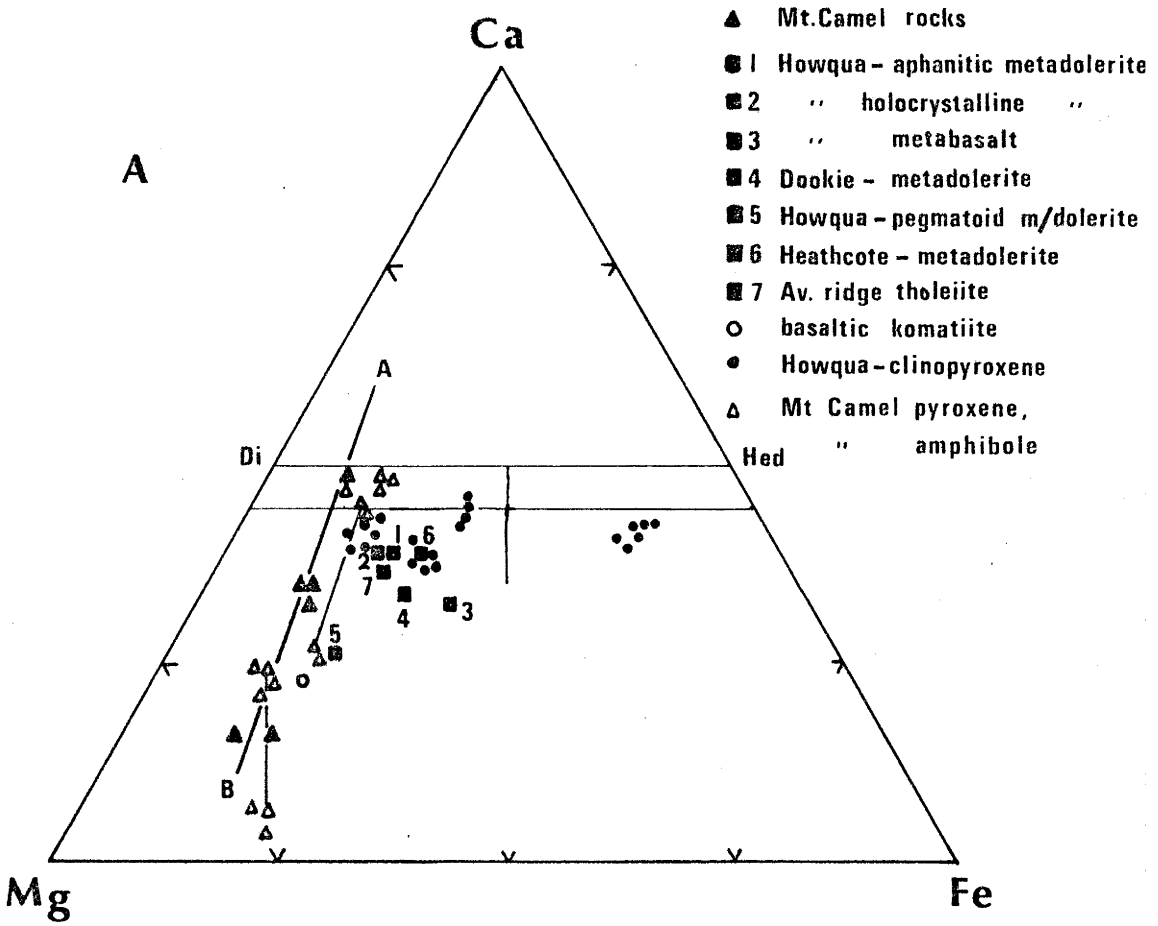

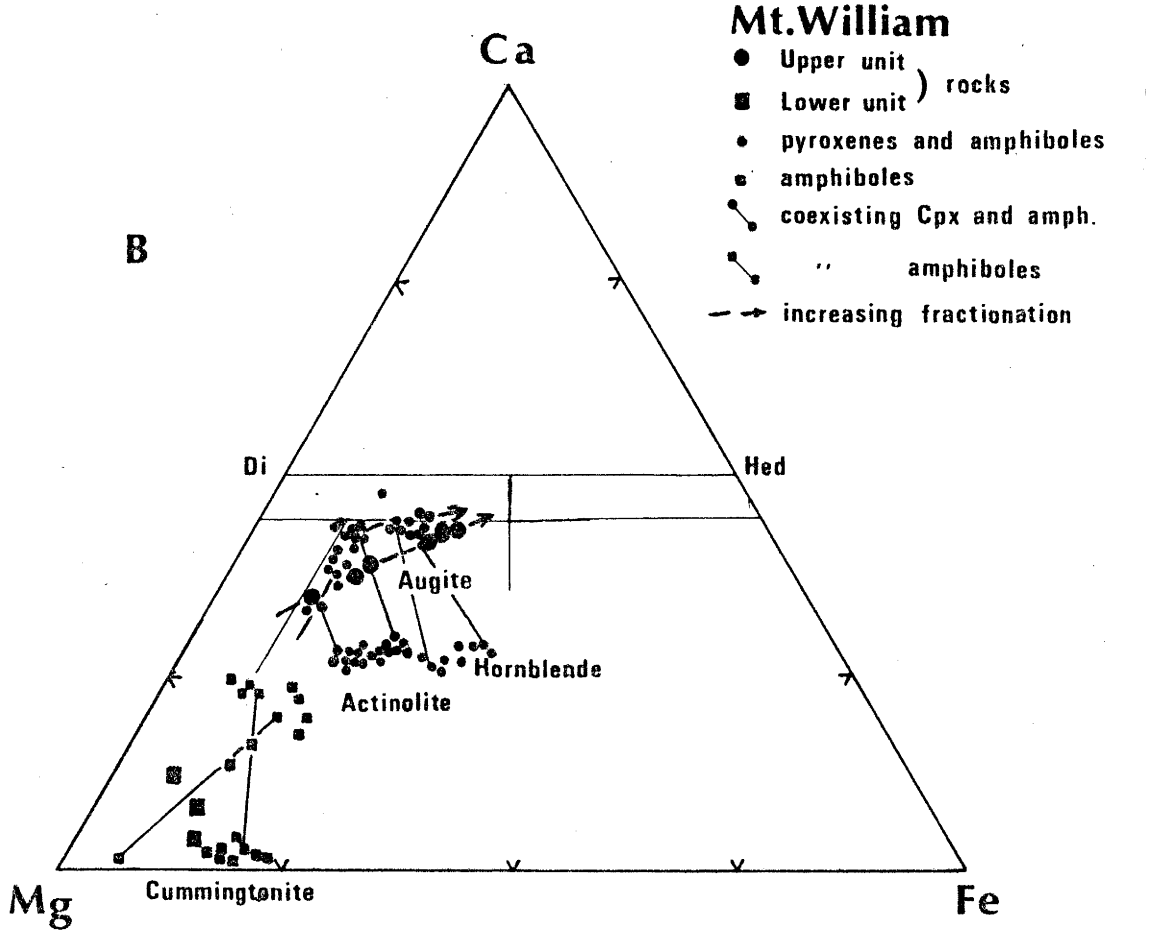

Trace element contents of Mount Camel rocks are similar to each other and compare favourably with analyses of ultramafic rocks. Ruddidium, strontium and zirconium are lower in rocks from Mount Camel than Mount William (Zone 1), however the overlapping ranges in concentration of trace elements do not permit precise discrimination between the two areas, evidence for similar genetic origin.

The Mount William and Mount Camel rocks are derived from genetically related parents, not necessarily identical in composition. Although stratigraphically equivalent, fractionation, contamination, and magma inhomogeneities probably resulted in slightly different compositions for the initial rocks at Mount William and Mount Camel.

DISCUSSION

Similarity between rocks from Mount William (Zone 1) and Mount Camel is the fundamental problem in discrimination between axe stones derived from these locations. It was pointed out in preceding sections that rocks from both areas contain similar mineral assemblages and almost identical major and trace element chemistry. The exceptional difference between rocks from the two localities is calcium metasomatism at Mount Camel and isochemical contact metamorphism at Mount William.

Evidence of calcium metasomatism is obvious in the field and from petrographic and geochemical studies. Isochemical contact metamorphism was presumed in constructing reactions to explain metamorphic changes in metadolerite from Zone 2 at Mount William. In the following part of this chapter, major and trace elements are used to establish isochemical contact metamorphism in the aureole around the Cobaw Granite.

The chemistry of rocks in Zone 1 at Mount William is regarded as representing their composition after burial and regional metamorphism, but

prior to contact metamorphism. That is, they remained relatively unaltered by contact metamorphism. They are better suited than the Mount Camel rocks for studies on the genesis of greenstone in the Heathcote Axis. Comparative studies of major and trace elements show ultramafic affinity for rocks of Zone 1. Using published major element mobilities, alteration of parent rocks with compositions similar to olivine pyroxenite, results in compositions approximately equal to rocks from Mount William and Mount Camel. The analysis of olivine pyroxenite from the Union Bay Ultramafic Complex (Ruckmick & Noble, 1969), is only an approximation to a possible original rock chemistry. Possible affinities of the Mount William and Mount Camel parent rock types are komatiite, mid-ocean ridge tholeiite, and Alpine-type ultramafic because these share similar features to the Victorian greenstones.

Interlayered mafic and ultramafic rocks comprising the komatiite assemblage have been recorded in Archaean rocks from South Africa (Viljoen & Viljoen, 1969), Western Australia (Nesbitt, 1971; Hallberg & Williams, 1972; Williams & Hallberg, 1973) and Canada (Naldrett & Mason, 1968; Brooks & Hart, 1972; Pyke et al, 1973). Komatiites as described by Viljoen & Viljoen (1969) are magmas containing MgO>9%, CaO/Al_2O_3>1%, K_2O<0.9% and TiO_2<0.9% (Brooks & Hart, 1974). However, most samples of komatiite analysed are altered, generally serpentinised, metamorphosed or metasomatised so that the existence of primary komatiite magma is subject to debate (Brooks & Hart, 1972; McIver & Lenthall, 1973; Green et al, 1975; Anhauser, 1976). For example, Cawthorn & Strong (1974) argued that komatiites do not constitute a distinctive isolated new class of magma, but fit into a continuous spectrum of rocks approaching oceanic tholeiites with chemical characteristics imposed by limiting PT-conditions. Viljoen & Viljoen (1969) showed that Ca and to a lesser extent Si, Al, Na, and K were preferentially lost during serpentinisation of ultramafic komatiites of South Africa. The

10. Differentiation trends

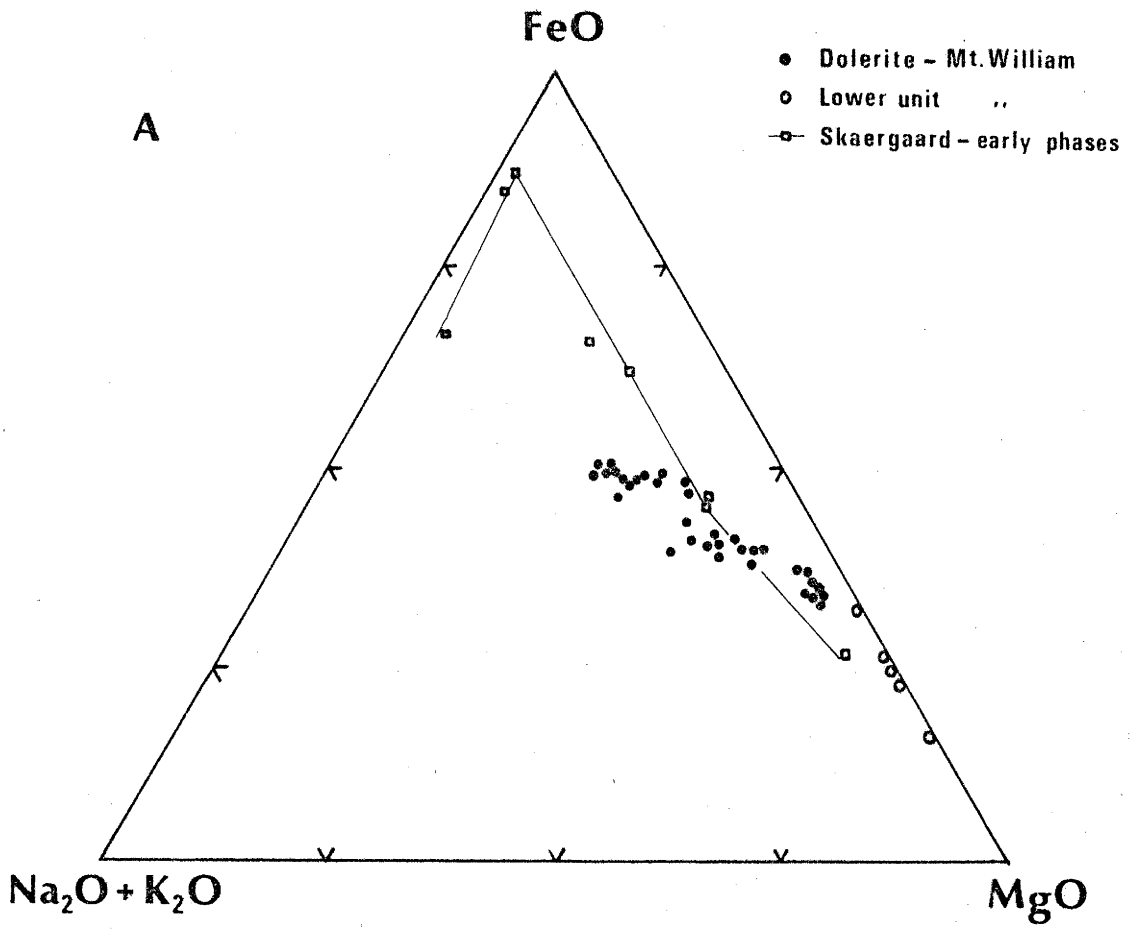

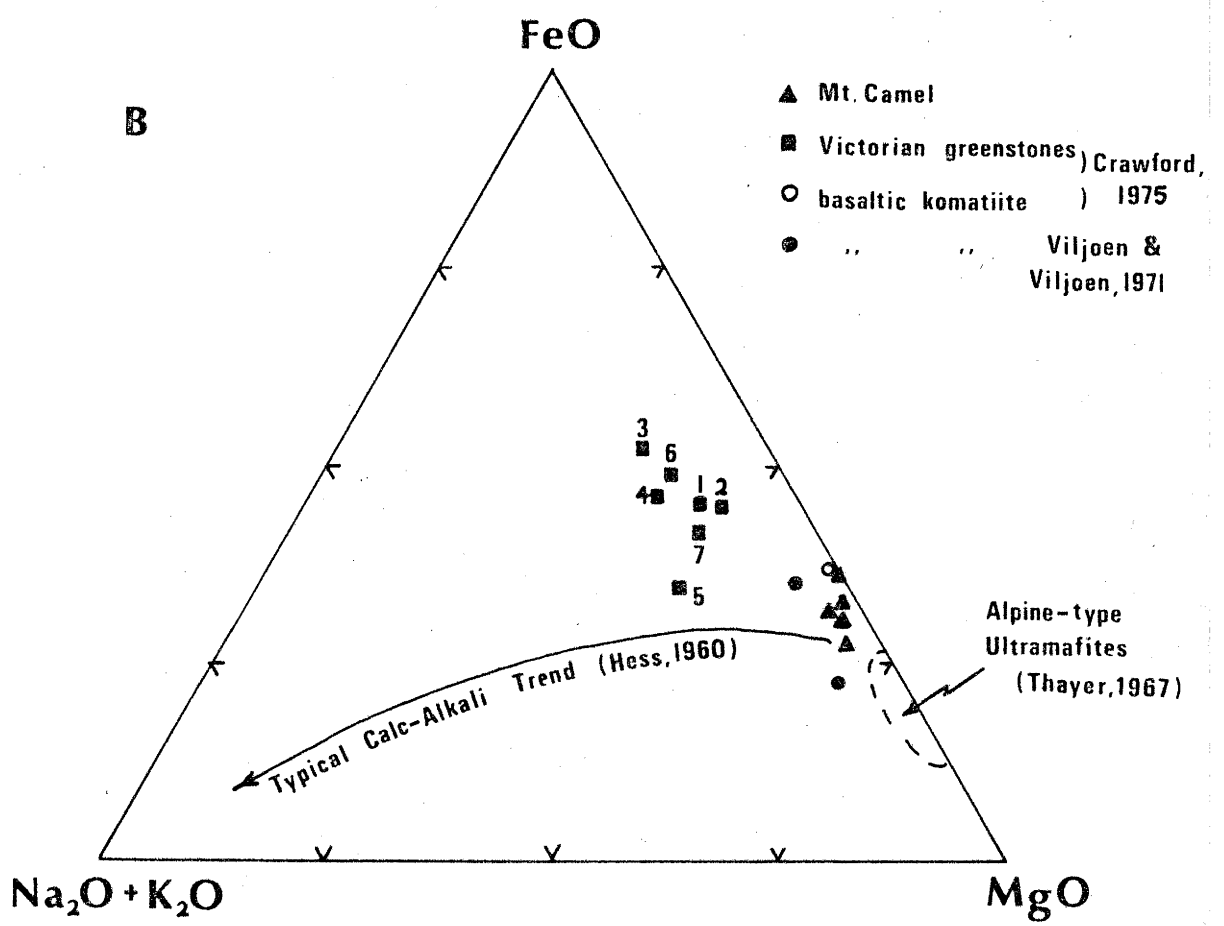

mobility of these elements, in so called 'primary' komatiites, makes interpretations of analyses of such rocks suspect. It should also be pointed out that corresponding element mobilities are found in rocks from Mount William and Mount Camel.

In Figures 10A and 10B, greenstone from Mount William (Zones 1, 2) and Mount Camel are compared with other Victorian greenstones (Crawford, 1975), basaltic komatiite (Viljoen & Viljoen, 1971), average mid-ocean ridge tholeiite (Crawford, 1975) and Alpine-type ultramafites (Thayer, 1967). The Mount William actinolite-cummingtonite hornfels plot near Alpine-type ultramafites whereas the Mount Camel rocks lie adjacent to basaltic komatiite. However, with the exception of three samples (A and C - Mount Camel; A14 - Mount William) which have low CaO/Al_2O_3 ratios, rocks from both areas generally fit Brooks & Hart (1974) geochemical definition of komatiite.

Figure 11B, a plot of $MgO-CaO-Al_2O_3$, illustrates compositions and fractionation trends of rocks from Mount William and Mount Camel compared with Archaean ultramafic assemblages (Naldrett & Mason, 1968; Viljoen & Viljoen, 1969; Wilson et al, 1965; Nesbitt, 1971). The trend for Mount William rocks (Zone 1) parallels that for Barberton, South Africa, whereas the Mount Camel rocks are significantly different, being enriched in calcium.

Slightly different initial bulk chemistry and fractional crystallisation paths account for the difference between Archaean ultramafics and rocks from Mount William (Zone 1). Bulk chemical differences probably result from different degrees of partial melting of the mantle and the PT-conditions of the tectonic environment govern the crystallisation trend. Mantle inhomogeneity may contribute to initial bulk chemical differences between parent rocks at Mount William and Mount Camel.

11. Covariance of K and Rb in greenstone

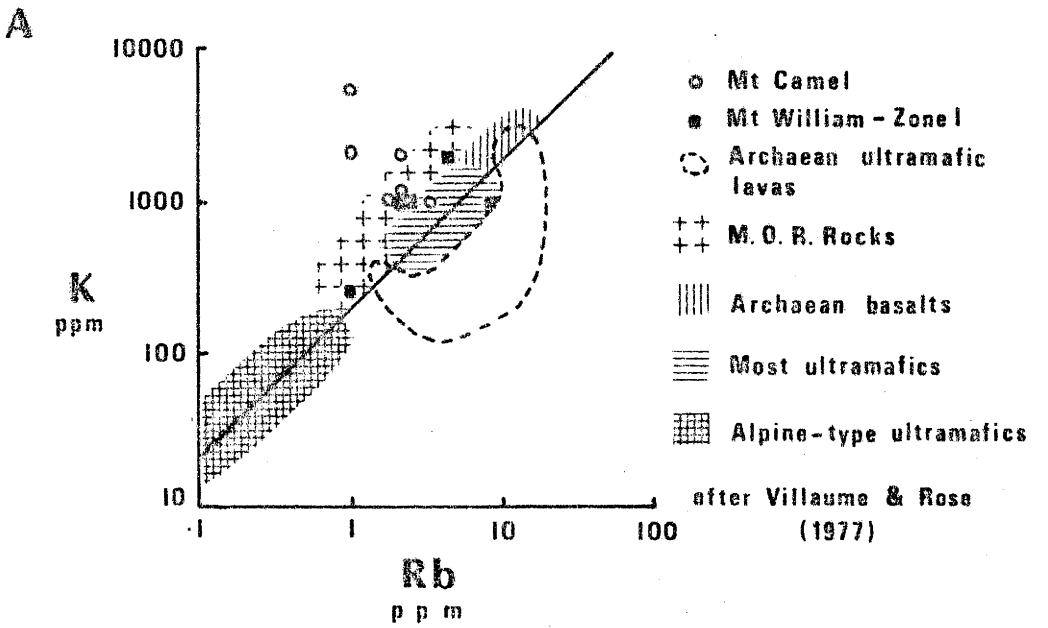

Compositions and fractionation trends

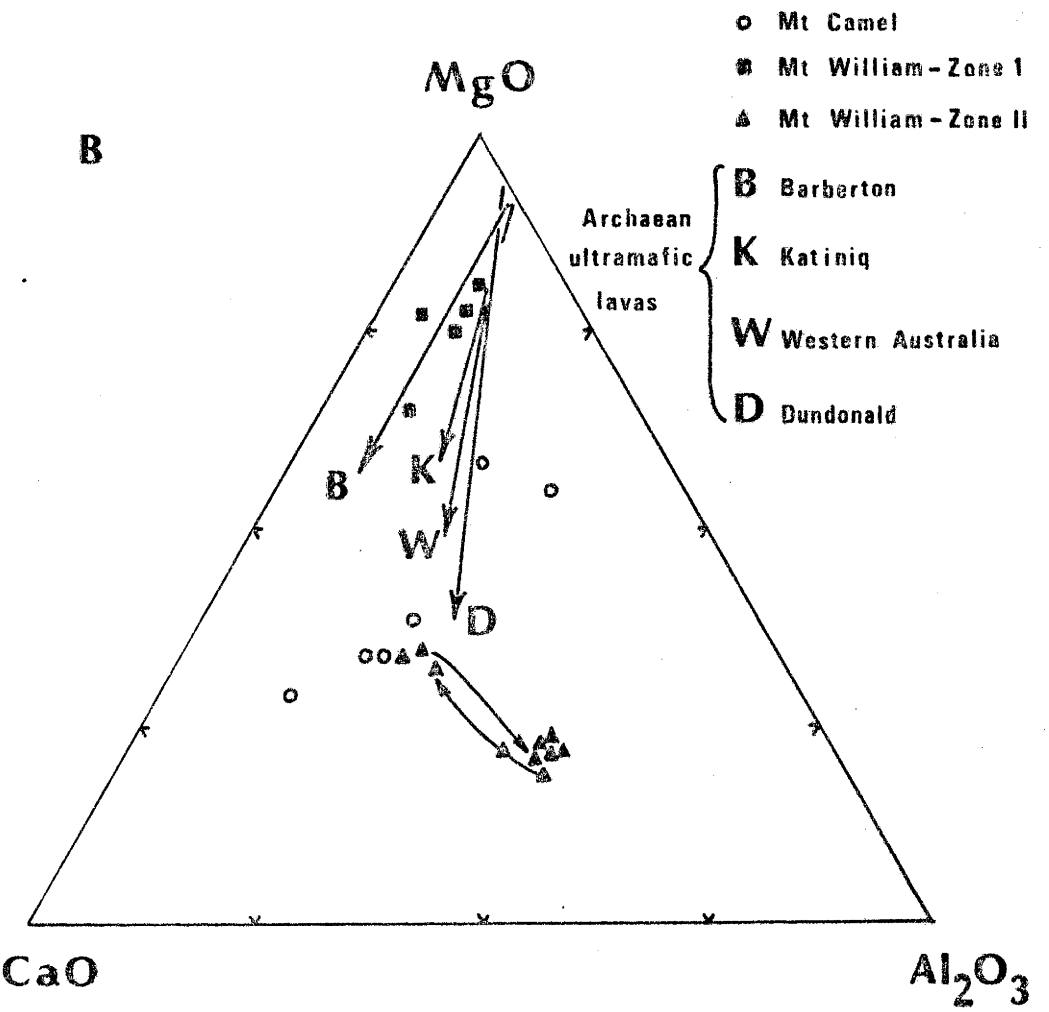

The significant conclusion from the statements above is that magnesium-rich 'komatiite-type' magmas typical of Archaean volcanism found in several continents continued to form, rise through the crust and flow onto the surface until the Early Cambrian. This is contrary to the ideas expressed by most workers who have studied komatiites and other magnesium-rich volcanics. It would seem (Anhaeusser, 1976), that the relatively thin Archaean crust, together with large degrees of partial melting in the mantle (Nesbitt & Sun, 1976) are necessary pre-requisites for generation of Mg-rich magmas. It is beyond the realms of this thesis to postulate similar environments and processes for evolution of Alpine-type ultramafic lavas of the Heathcote Axis.

Similarity between mid-ocean ridge tholeiites and rocks from Mount William (Zone 1) and Mount Camel is illustrated in a plot of potassium against rubidium (Fig. 11A), used by Villaume & Rose (1977) to compare Archaean ultramafic lavas from Canada and South Africa with several broad classes of igneous rocks. The covariance relation between K and Rb leads to an erroneous conclusion because of element mobility during alteration. Addition of potassium (Table 6) with a consequent increase of Rb during alteration of rocks with Alpine-type affinity is a plausible explanation of the present concentration of these elements in rocks from Mount William and Mount Camel.

Alpine-type ultramafics, as defined by Benson (1926), although variable in their associations have characteristic features (Thayer, 1967). Goles (1967) described trace element contents in ultramafic rocks and Gulacar & Delaloye (1976) presented partial analyses of Alpine-type ultramafic rocks. Analyses of Mount William (Zone 1) and Mount Camel greenstones closely fit partial analyses of fresh to slightly serpentinised websterite (Gulacar & Delaloye, 1976).

Therefore, geochemical evidence and the inferred alteration of metavolcanics of the Heathcote Greenstone at Mount William and Mount Camel leads to the conclusion that the parent rocks of actinolite-cummingtonite hornfels belonged to an Alpine-type ultramafic affinity.

Mount William - CONTACT ZONE 2

Rocks from this zone belong to the Upper Unit of the Heathcote Greenstone at Mount William and their bulk chemical analyses are listed in Appendix 2. Petrographically distinct parts of metadolerite which comprise the zone are described in Appendix 1.

There are at least two possible explanations for the geochemical trends found in metadolerite at Mount William. Firstly, bulk chemical variations in metadolerite are caused by the mobility and migration of elements during contact metamorphism by the Cobaw Granite. Secondly, the geochemical trends for major and trace elements result from fractional crystallisation in the original dolerite, which is relatively unaffected by contact metamorphism.

In the first case the trends must be studied with distance from the margins of the Cobaw Granite (Fig. 8, 14, 15) and in the second, by noting the variation from bottom to top through the metadolerite (Fig. 12). In a directional sense, upwards through the metadolerite is equivalent to approaching the Cobaw Granite. Both interpretations are based on the same geochemical trends, decrease in MgO and CaO, increase in SiO_2, TiO_2, Al_2O_3, FeO, Na_2O, K_2O, and P_2O_5, with Fe_2O_3 and MnO being relatively constant as the granite is approached. These trends are rationalised by comparison of element behaviour in other contact metamorphic areas and in fractionated intrusions. Major element chemistry is looked at prior to trace elements.

MAJOR ELEMENTS

SiO_2

The silica content of metadolerite increases by 1.46 weight per cent across the zone toward the granite. In low-grade metamorphic rocks Cann

12.Geochemical and Mineralogical variations in the Mt.William metadolerite

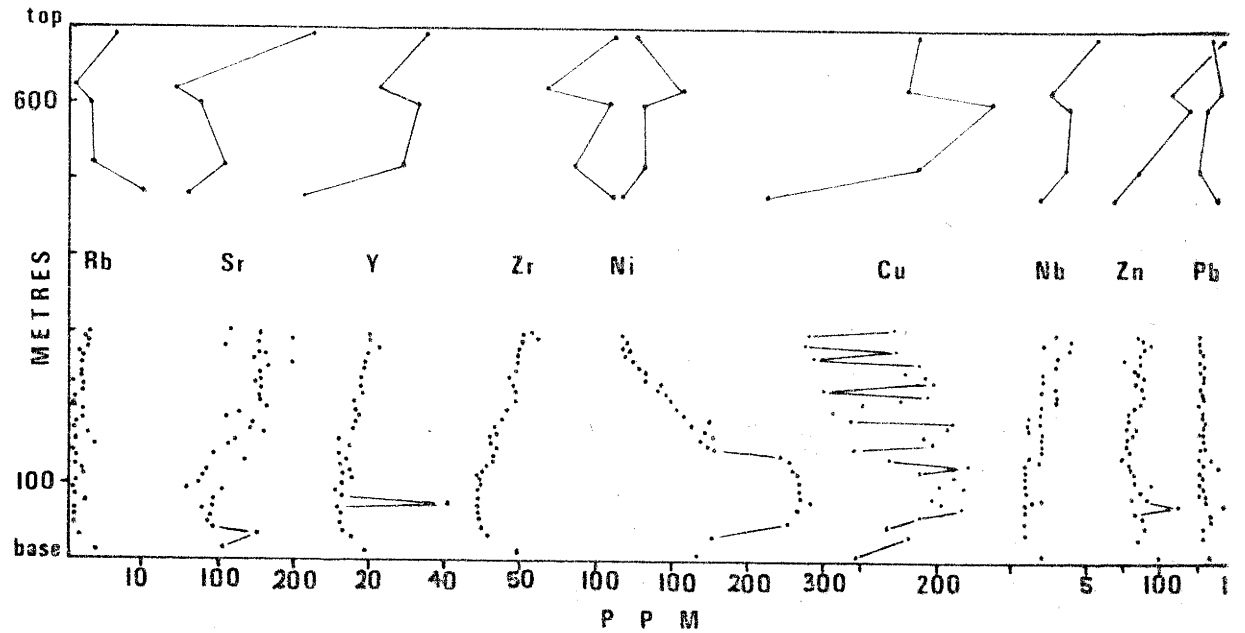

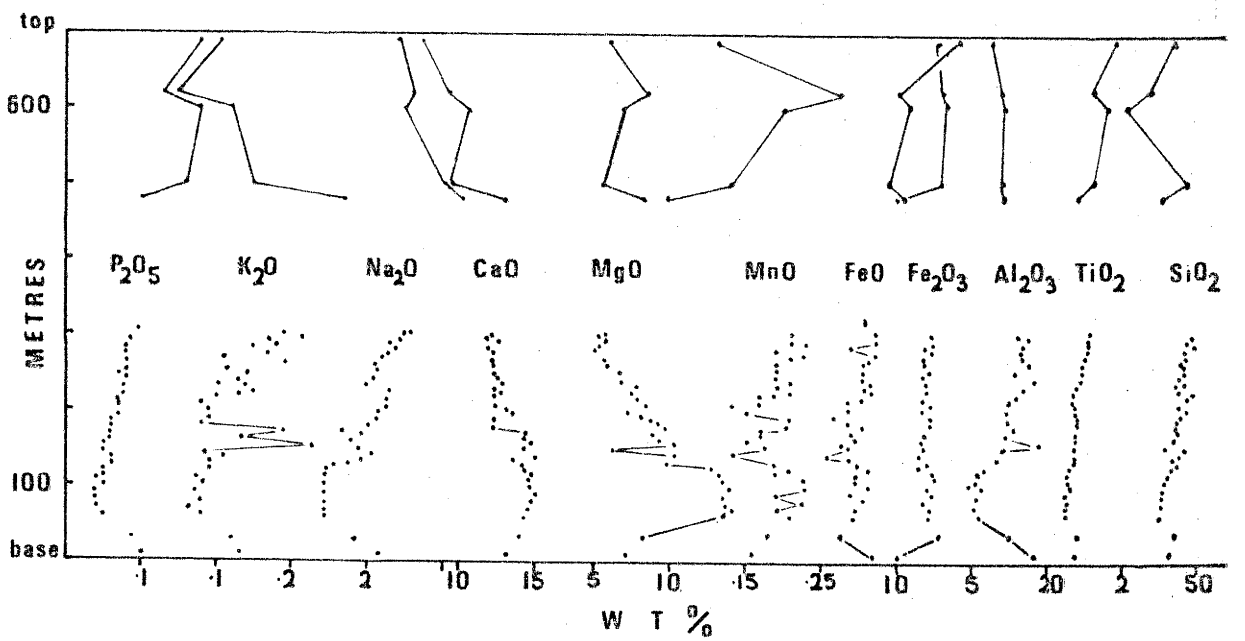

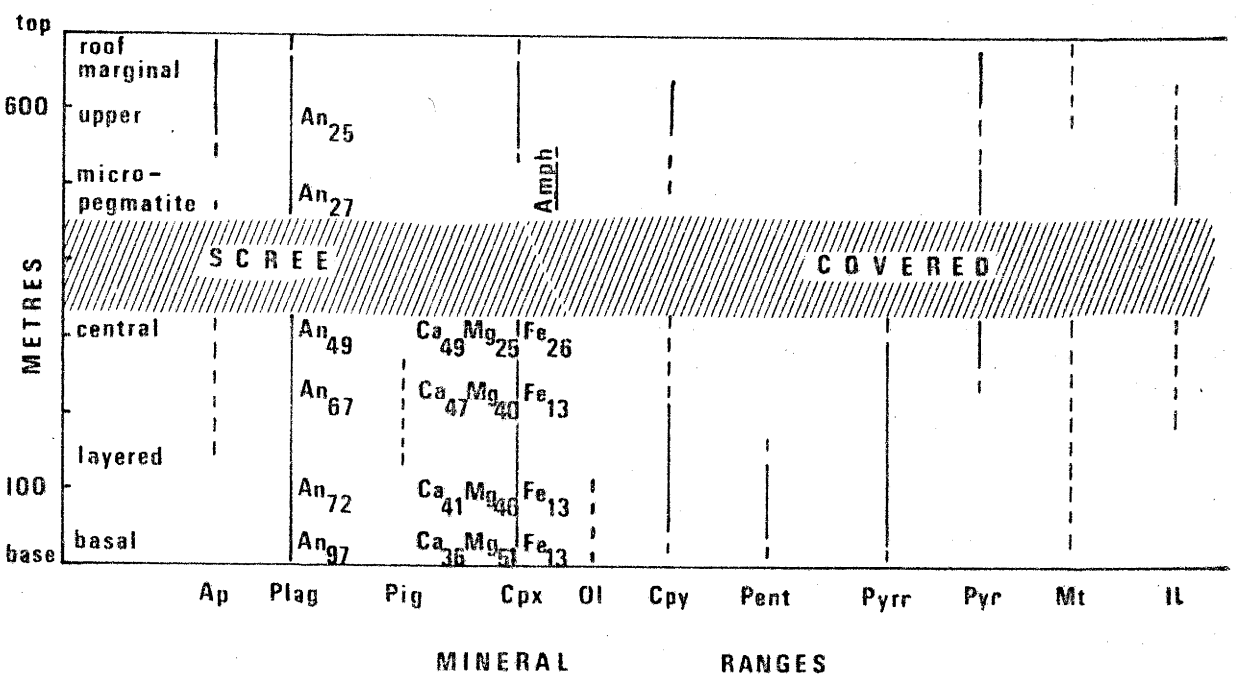

(1969) recorded an increase in SiO_2 of up to 3.1 weight per cent, whereas Vallance (1974) noted a decrease. Contact metamorphism results in a gain of silica for greenstones (Engel & Engel, 1961) and in pelitic hornfelses (Aparicio & Bellido, 1976; Joyce, 1970). Migration of silica towards the metadolerite is favoured because of the chemical gradient between the Cobaw Granite and greenstone.

Fractional crystallisation of basic magmas generally results in enrichment of silica in the final phases of cooling (Wager & Mitchell, 1951; Walker, 1969). Both interpretations can be used to explain the behaviour of SiO_2.

$\underline{TiO_2}$

Titanium increases by 1.33 weight per cent as the granite is approached (Fig. 8). Cann (1970) and Pearce (1974) regard TiO_2 as immobile during metamorphism up to the amphibolite facies. Metasomatic addition of titanium is recorded by Hietanen (1962) from Idaho, but metasomatic metamorphism is untenable at Mount William because of an unfavourable chemical gradient and lack of evidence of metasomatism. TiO_2 increases during fractionation of tholeiitic magmas (Wager & Mitchell, 1951; Walker, 1969). The gradual increase in titanium across the metadolerite is unrelated to metasomatism or metamorphism and reflects relict igneous crystallisation of ilmenite.

$\underline{Al_2O_3}$

There are conflicting reports of the behaviour of aluminium during progressive metamorphism (Engel & Engel, 1961; Smith, 1968; Cann, 1969; Vallance, 1974). From field observations and petrographic studies the metadolerite becomes more felsic towards the top, the increase in modal plagioclase accounting for the gain in aluminium. The composition of the

feldspar also changes from calcic to sodic with an increase in felsic nature of the rocks, a trend which reflects igneous fractionation rather than metamorphism. The large increase in aluminium (7.89 wt%) across the metadolerite is caused by continued fractionation of plagioclase from a magma and not from metamorphism.

FeO and Fe_2O_3

Cann (1969), Chernysheva (1971) and Vallance (1974) found that the ratio Fe_2O_3/FeO decreases with progressive metamorphism. Rationalisation of the trends for iron in Figure 8 is difficult using metasomatic processes because of the relative increases in Fe_2O_3 (1.0 wt%) and FeO (6.13 wt%). The large increase in ferrous iron suggests iron enrichment during fractional crystallisation of dolerite.

MnO

The manganese content of metadolerite increases progressively towards the Cobaw Granite. Manganese is considered very mobile during secondary alteration processes and migrates readily (Engel & Engel, 1961). It is also known to be preferentially enriched in the final phases of solidification of basaltic magmas (Wager & Mitchell, 1951; Gunn, 1966). Immobility of MnO in the metadolerite at Mount William strongly suggests isochemical contact metamorphism because relict igneous geochemical trends are preserved.

MgO

Magnesium shows the most significant variation across the hornfels zone. A decrease of 17 weight per cent over 800 metres must be exceptional for contact metamorphic terrains. Migration of large amounts of magnesium should result in cordierite, orthopyroxene or other magnesium rich minerals. In the absence of magnesium-rich metasomatic minerals evidence for metasomatism and element migration during metamorphism is lacking. The

variation of magnesium is easily explained by fractional crystallisation of magma, magnesium depletion by precipitation of olivine and clinopyroxene in early stages and iron enrichment in later stages of cooling (Wager & Mitchell, 1951; Walker, 1969).

CaO

Conflicting behavioural trends are known for calcium during progressive metamorphism (Engel & Engel, 1961; Hietanen, 1962; Cann, 1970; Hallberg, 1972; Vallance, 1974; Aparicio & Bellido, 1976). In the metadolerite at Mount William, the calcium content decreases by approximately half from the basal parts to the top. Absence of carbonate and epidote veins are evidence of calcium immobility during contact metamorphism. For most of the cooling history of dolerite crystallisation of augite (Appendix 1) results in gradual depletion of Ca and Mg from magmatic liquid. Consequently the final fractions to solidify are depleted in calcium and magnesium. The trend for calcium clearly fits fractional crystallisation of a single magma without introduction of another magmatic fluid.

Na_2O

Contradictory evidence exists for the behaviour of sodium during low-grade metamorphism (Engel & Engel, 1961; Cann, 1969; Vallance, 1974).

Analyses of plagioclase (Appendix 2) shows that feldspars become richer in albite upwards through the metadolerite. In an earlier discussion on contact metamorphism it was determined that the composition of plagioclase which crystallised during metamorphism is more calcic than the initial igneous feldspar. Amphibole analyses (Appendix 2) contain low concentrations of sodium, so that the increase of Na_2O in the bulk chemistry reflects slight sodium enrichment, additional evidence for fractional crystallisation.

K_2O

In low-grade metamorphic terrains increasing and decreasing trends are recorded for potassium (Pitcher & Sinha, 1958; Oki, 1961; Loomis, 1966) with progressive metamorphism. Metasomatic addition of potassium was found by Verbeck & Schreiner (1967) in a contact aureole, copious amounts of biotite being characteristic. No biotite is present in the metadolerite at Mount William.

Potassium increases across the metadolerite reaching a maximum (0.27 wt%) in micropegmatite. As the maximum value for K_2O occurs in micropegmatite, associated with high sodium, and not adjacent to the Cobaw Granite the geochemistry of potassium is related to fractionation of magma.

High alkali content of rocks in and above the micropegmatite signifies alkali enrichment during late stages of cooling. The onset of precipitation of minerals rich in alkalies is associated with reaction between magmatic liquid and water as evidenced by crystallisation of amphibole.

P_2O_5

Phosphorous increases slightly (0.12 wt%) across the metadolerite towards the Cobaw Granite. Hietanen (1962) found that phosphorous increased by metasomatic rather than metamorphic processes. Cann (1969) and Vallance (1974) determined that P_2O_5 is immobile under low-grade regional metamorphic and local hydrothermal conditions. Minor amounts of phosphorous are therefore not expected to migrate, especially not over 800 metres.

In fractionation of tholeiitic magma the amount of phosphorous is related to precipitation of apatite. P_2O_5 is preferentially enriched in the liquid phase during early stages of crystallisation (Wager & Mitchell, 1951), so that until apatite crystallises the phosphorous content of

residual liquids increases progressively. Gradual increase in phosphorous (Fig. 8, 14) is clearly indicative of fractionation.

H_2O+

In rocks adjacent to the margins of the Cobaw Granite, presence of hornblende indicates hydrous conditions of contact metamorphism. Formation of hornblende from reaction between clinopyroxene and plagioclase necessitates addition of water. Gradual loss of combined water as the Cobaw Granite is approached (Fig. 8) indicates progressive dehydration of rocks directly related to increase in temperature during contact metamorphism. Complete dehydration should result in orthopyroxene, but as specimens from this mineral group are absent the metadolerite was only partially dehydrated, suggesting that pyroxene-hornfels facies was not attained. Partial dehydration may compensate for the increase in volume calculated for reaction between the minerals.

Fractional crystallisation of 'wet' tholeiitic magma leads to precipitation of hydrous minerals, usually as a pegmatitic phase, approximately two-thirds above the base of the intrusion (Hess, 1960; Wager & Brown, 1967). Amphibole, quartz and feldspar are the main pegmatitic minerals, commonly deuterically altered. The occurrence of micropegmatite in the upper parts of metadolerite at Mount William strongly indicates fractionation of magma.

Geochemical trends for rocks from across the metadolerite at Mount William are parallel to major element variations determined for tholeiitic intrusions (McDougall, 1962; Gunn, 1966; Wager & Brown, 1967; Walker, 1969). Enrichment of iron and incompatible elements are characteristic of fractionation of tholeiitic magma, and preservation of these geochemical features in metadolerite at Mount William, indicate isochemical contact metamorphism of fractionated tholeiitic dolerite.

Calculation of CIPW normative compositions for samples across the metadolerite results in most rocks being olivine normative and others nepheline normative (Fig. 13B). Nepheline normative rocks suggest either undersaturation of doleritic liquid during fractionation or element migration (alkalies, aluminium and silica) during weathering. Undersaturated minerals are not found in the metadolerite and weathering is proposed as the reason for several samples yielding nepheline in their norms.

The basal parts and roof margins have widely different normative compositions, reflecting Ca and Mg depletion and Fe enrichment during fractional crystallisation. Normative amounts of albite, anorthite, ilmenite, and apatite increase whereas normative diopside, hypersthene and olivine decrease upwards through the metadolerite (Fig. 13A). This trend of increasing felsic and decreasing mafic constituents is parallel to that in differentiation of basaltic magmas. These are normative mineral variations and so cannot be used to state explicitly the processes of fractional crystallisation. As a generalisation however, the normative mineral variation reflects crystallisation of olivine and pyroxene in early stages and feldspars near the end of cooling.

In Figures 10A and 10B, metadolerite from Mount William is compared with early fractionated phases of the Skaergaard intrusion, the fractionation trend for calc-alkali rocks (Hess, 1960), and with metadolerite and metavolcanics from several areas of greenstone in Victoria. The purpose for this comparison is to determine the fractionation trend which is most like that for the Mount William metadolerite. Two features are obvious from these diagrams. Firstly, the fractionation trend in metadolerite at Mount William parallels typical tholeiitic fractionation and secondly, metabasalt and metadolerite from other Cambrian greenstone areas in Victoria (Crawford, 1975) suggest tholeiitic differentiation. The implication from

13. Variation in Normative Mineral Composition

A. Metadolerite – Mt. William

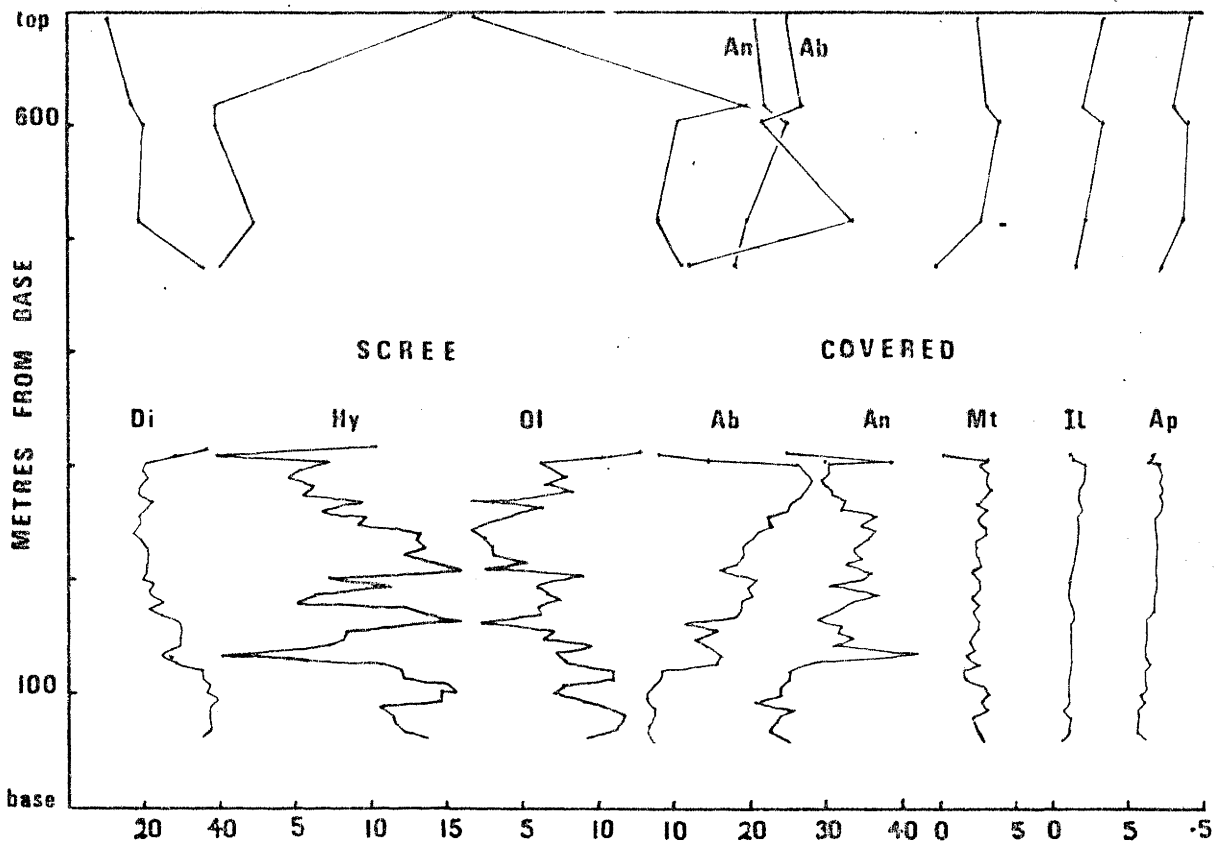

B. Greenstones

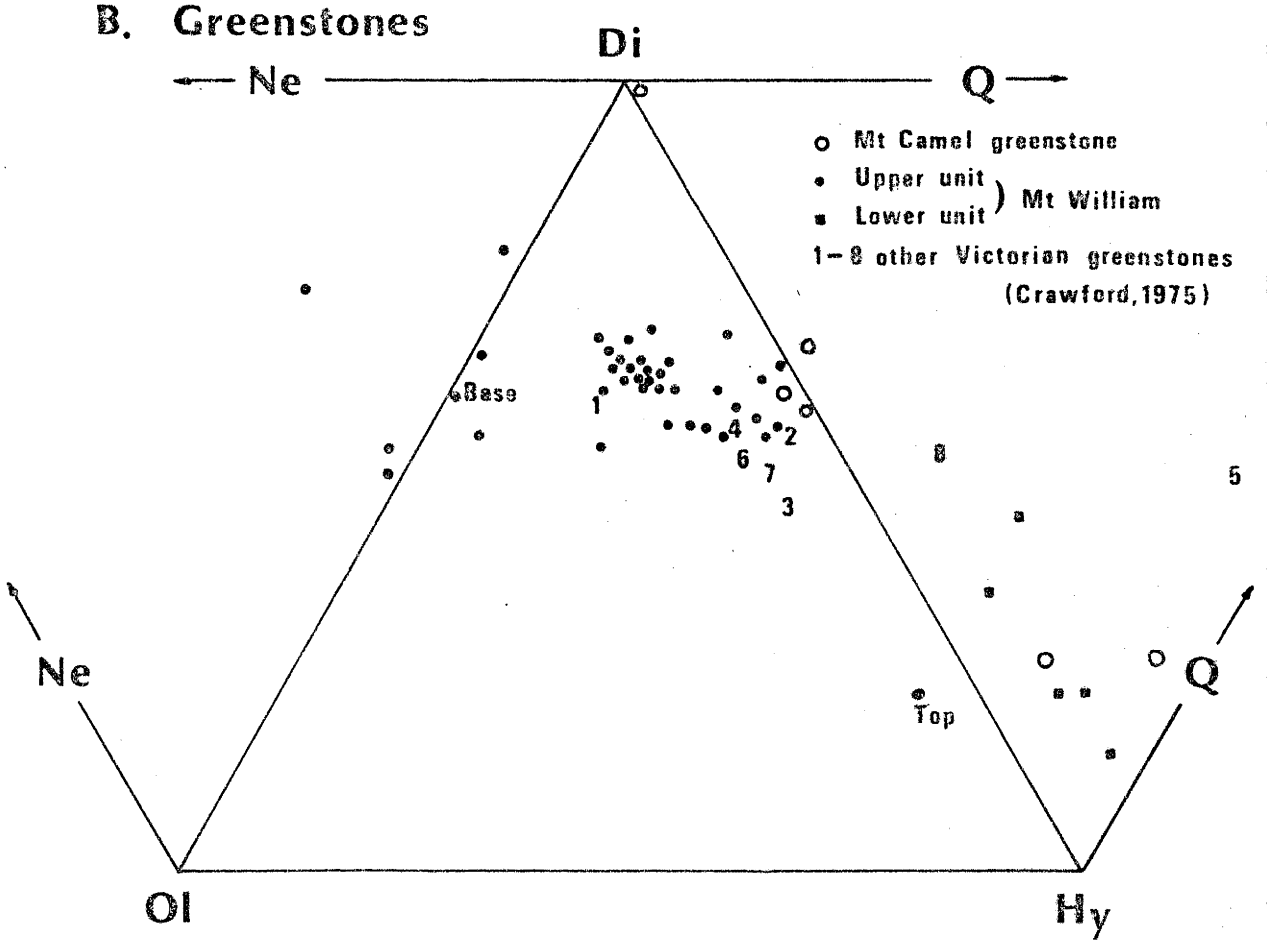

these observations is geochemical affinity between greenstones in several widely separated areas of Victoria, evidence of similar genesis for ?Cambrian metadolerites.

TRACE ELEMENTS

Trace element contents across the metadolerite are illustrated in Figures 12, 14, 15 and tabled in Appendix 2. Variation of trace elements are discussed in terms of their mobility during metamorphism and fractionation of magma.

Rb

There is a progressive increase in rubidium across the metadolerite, the maximum (10ppm) being found in micropegmatite. In the basal parts of the zone rubidium is low and variable, but near the Cobaw Granite rocks contain uniform values of Rb (Fig. 14) suggesting control by contact metamorphism. Mobility of rubidium during low-grade metamorphism is well known (Cann, 1970; Pearce, 1974), however, migration of Rb during metamorphism could not account for gradually increasing concentrations which reach a maximum in the micropegmatite. The increase in rubidium across the metadolerite closely follows that of potassium and agrees with classical trends found by Wager & Mitchell (1951), theoretical considerations (Goldschmidt, 1954; Ringwood, 1955; McIntire, 1963) and observations made by Rivalenti (1974).

Sr

Although having wide variation in concentration across the metadolerite (Fig. 14), strontium increases towards the Cobaw Granite. Aparicio & Bellido (1976) determined an increase in Sr with progressive metamorphism in pelitic hornfelses. Sr and Ca share similar ionic radii and electronegativities, consequently strontium commonly substitutes for

14. Variation of trace elements with distance from the Cobaw Granite - Zone 2

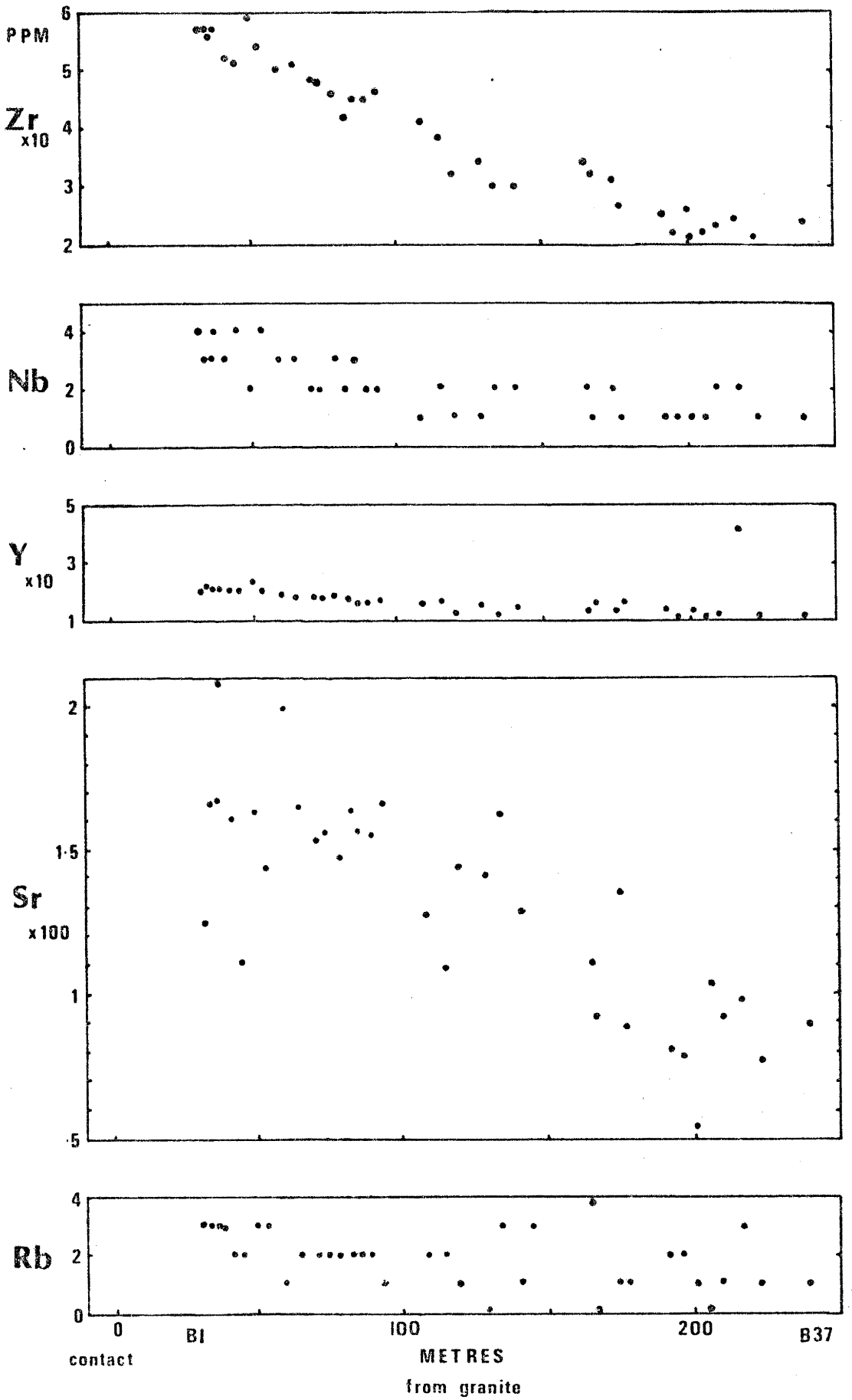

calcium in plagioclase. As calcium decreases toward the Cobaw Granite and strontium increases the latter must be increasingly substituting for calcium.

The wide variation in concentration of Sr is attributed to a large range in modal plagioclase (c.f. Wager & Mitchell, 1951), and the mobility of strontium during post-intrusive alteration processes may also contribute to the scatter of points in Figure 14. The trend observed does not conform to theoretical considerations of McIntire (1963), that during the course of crystallisation of a magma Sr should increase initially and then decrease. Variation in the concentration of Sr in the metadolerite at Mount William is parallel with its distribution in Antarctic tholeiites. Gunn (1966), found that in tholeiitic sills of Antarctica the behaviour of strontium was parallel to that of sodium rather than calcium. Similarly, in a study of the Palisades sill Walker (1969), established that Sr mainly followed alkalies (Na + K) in early fractionated phases and only K during late stages. It is clear from Figure 12 that strontium does not substitute for calcium but follows the alkalies during fractional crystallisation.

Y

Yttrium increases progressively across the width of the metadolerite from bottom to top (10-36ppm) and is very low in the micropegmatite (1ppm). Wager & Mitchell (1951), Flower (1973) and Thompson (1973) showed that Y is preferentially concentrated in late fractionated phases, in particular, by replacing Ca in apatite and late-formed pyroxene. The absence of apatite and clinopyroxene in micropegmatite means that there are only a few favourable sites for location of yttrium. Above the micropegmatite the concentration of Y continues to increase (Fig. 12). The micropegmatite represents a change in the nature of crystallisation because of its different geochemistry and mineralogy. The crystallisation history of

dolerite, the parent rock type of metadolerite of Zone 2 at Mount William, is discussed later.

Cann (1970) and Pearce (1974) recognised that Y is immobile during low-grade metamorphism and thus could be used to indicate parental magma types for metavolcanic rocks. In contact metamorphic aueroles, yttrium was found to increase with progressive metamorphism (Hietanen, 1962; Joyce, 1970) and is related to the occurrence of xenotime. The relative immobility of Y, its regular variation across the metadolerite and the lack of xenotime strongly suggests that the geochemical trend for yttrium is due to fractional crystallisation.

Pb

Values for lead are relatively constant across the metadolerite and the trend is inconclusive evidence for either metamorphism or fractionation.

Zr

In contact metamorphosed pelites and greenstones zirconium shows variable behaviour (Pitcher & Sinha, 1958; Hietanen, 1962; Aparicio & Bellido, 1976). Generally, Zr is regarded as an immobile element during weathering and low-grade metamorphism (Cann, 1970; Pearce, 1974) and it should reflect pre-alteration concentrations.

With fractionation of tholeiitic magmas Zr is concentrated in late stages (Wager & Mitchell, 1951; Walker, 1973; Thompson, 1973). In Figure 12, zirconium increases from 22ppm near the base up to 114ppm at the top of the metadolerite and progressive increase in Zr across the metadolerite conforms to its preferential enrichment in successive residual liquids.

Nb

Cann (1970) found that niobium was little affected by secondary alteration processes and is regarded as immobile. There is an increase in

15. Trace element variation from the Cobaw Granite in metadolerite – Mt. William

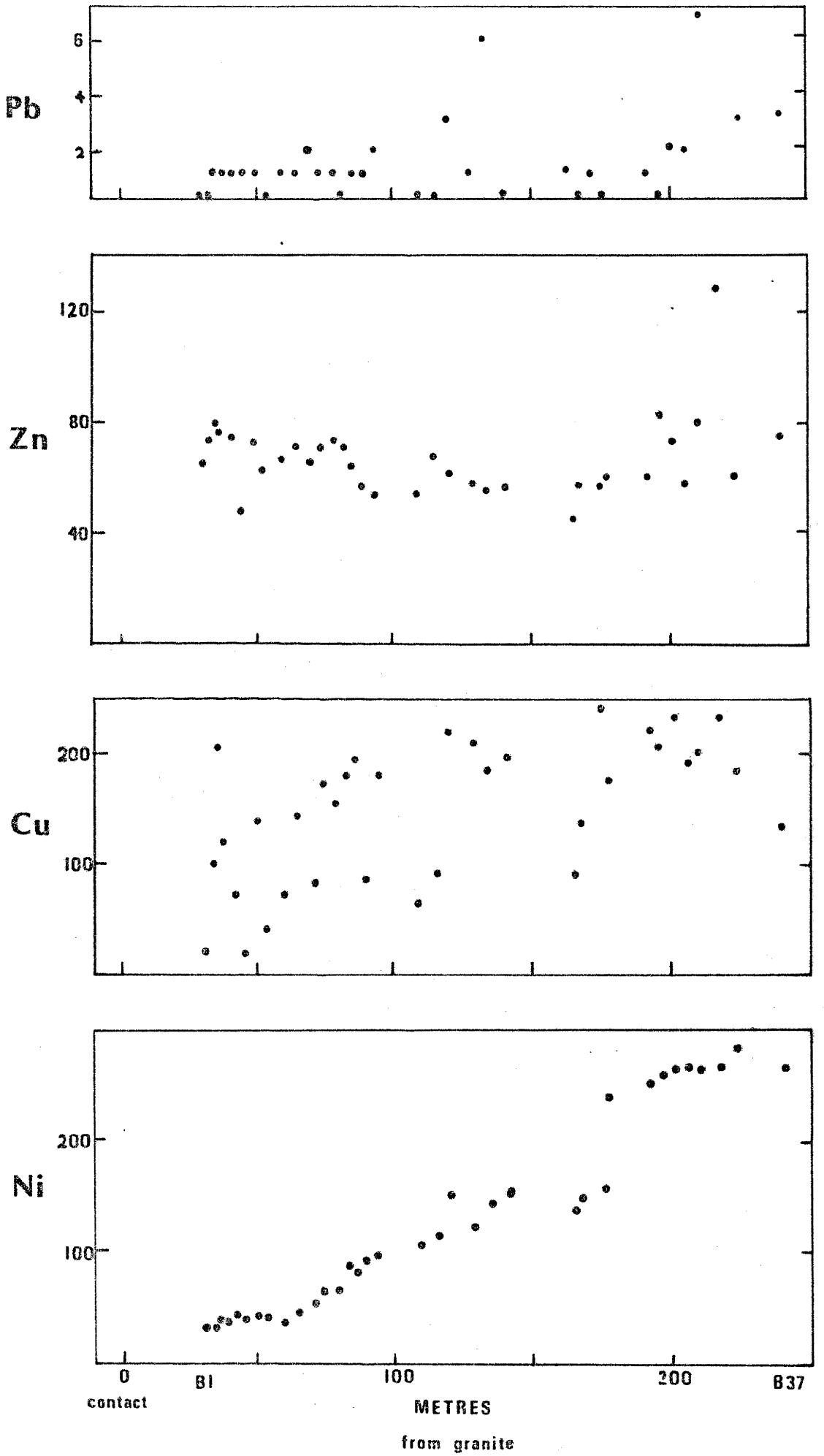

Nb from bottom to top through the metadolerite, a trend which agrees with an observation by Flower (1973) that it appears to follow other large-ion elements such as Rb, Sr, Y and Zr. The trend reflects fractional crystallisation.

Ni

The nickel content decreases from 280ppm near the base to 15ppm in micropegmatite and up to 50ppm at the top of the metadolerite. A parallel trend was found for magnesium (Fig. 12), the correlation between magnesium and nickel is well known (Vogt, 1923; Wager & Mitchell, 1951). Various amounts of Ni can be contained within oxide, sulphide and silicate phases (McDougall & Lovering, 1963; Greenland & Lovering, 1966). In the basal parts of metadolerite at Mount William oxides are negligible and chalcopyrite and pyrrhotite common. Pentlandite forms exsolution 'flames' in pyrrhotite and accounts for the rocks in the lower parts of the sill being enriched in nickel. As the modal percentage of sulphides decrease up through the metadolerite there is an associated decrease in nickel.

In pelitic hornfelses the amount of Ni decreases with progressive metamorphism (Shaw, 1954, 1956; Hietanen, 1962; Aparicio & Bellido, 1976). Metamorphism or metasomatism seem doubtful causes for the observed trend of Ni in metadolerite because the granite, itself depleted in this element, is unlikely to enrich the country rocks in nickel.

The ratios Ni/Fe and Ni/Mg decrease with fractionation which suggests (c.f. Greenland & Lovering, 1966) that fractionation of Ni proceeded independently to that of Mg.

Cu

The trend for copper is obscure because of the scatter of points (Fig. 15), although a general variation is obvious in Figure 12. Copper

decreases upwards through the metadolerite from 200ppm near the base to less than 100ppm in the central parts. Thompson (1973) showed that Cu varied greatly in concentration without any obvious correlation with mineral phases or differentiation. However, Wager & Mitchell (1951), McDougall & Lovering (1963), and Walker (1969) found that copper increased successively with fractionation. It seems from geochemistry and abundances of sulphides that copper is related to fugacity of sulphur and to activity of iron. The amount of chalcopyrite which crystallised from the magma is dependent upon changes in the availability of iron, copper and sulphur, elements whose abundances at a given time during crystallisation depend on the nature of fractionation.

In Figure 15 the scatter of copper values gives no indication as to the effects of contact metamorphism, except that the apparent random distribution of Cu may be caused by mobility during weathering.

Zn

Flower (1973), described the behaviour of zinc during fractionation of magmas as unpredictable, commonly bearing little relation to the general geochemical trend. Near the basal part of the metadolerite values of Zn are variable, averaging about 80ppm and probably reflecting the amount in sulphides. In the upper portion of the sill the content of zinc increases sharply, sympathetically with copper. During crystallisation, Zn preferentially remains in the liquid phase (Wager & Mitchell, 1951) so that the last phases to crystallise are enriched in Zn.

DISCUSSION

The low levels of Sr, Y, Ni, Cu, Nb and Zn in the micropegmatite are accounted for by lack of suitable minerals into which these elements are

capable of being accommodated. Rubidium and zirconium are enriched in the micropegmatite, most likely being incorporated into plagioclase and amphibole respectively.

The micropegmatite, by comparison with several zoned intrusions (Wyllie, 1967, Chpt. 3, 4), cannot be interpreted as representing final cooling of the last liquid fraction because iron enrichment continues across the width of the sill. Not only is iron enriched in rocks above the micropegmatite but also other major and trace elements continue their earlier fractionation trends.

Geochemical trends for major and trace elements across the metadolerite are explained by fractionation of a tholeiitic magma, similar to classical geochemical variations found in the Skaergaard, Palisades sill, and sills in Tasmania and Antarctica.

COMPOSITIONAL VARIATION OF MINERALS

Amphiboles

There are three compositional groups of amphiboles in greenstone from Mount William and Mount Camel (Fig. 9 - tie lines connect analyses in the same specimen). At Mount William (Zone 1) and Mount Camel the rocks contain actinolite and cummingtonite, whereas metadolerite (Zone 2 - Mount William) has hornblende. Various diagrams (Fig. 9, 16-20), are used to show compositional variation in amphiboles.

Actinolite and hornblende, although found in rocks with different bulk chemistry, form a continuous spectrum of composition (Fig. 9, 16C, 17B, 18B). The major compositional control of calciferous and sub-calciferous amphiboles is rock composition (Leake, 1965, 1968, 1971; Hietanen, 1971; England, 1972), and it is clear from Figures 9, 17A and 18A that bulk chemistry controls the composition of amphiboles from Mount William and Mount Camel.

An indication of the influence bulk chemistry has on amphibole chemistry is shown in a plot of $Mg/Mg+Fe_{amph}$ against $Mg/Mg+Fe_{rock}$ (Fig. 17A). The almost linear relation suggests direct dependence of Mg and Fe between amphiboles and their host rocks. A linear relation points to an absence of Mg-Fe compositional variance in the 'total' system (Sen, 1970), but as the covariance is not exactly 1:1, small quantities of iron, occurring as magnetite and ilmenite, are not associated with amphiboles. This evidence means that equilibrium conditions were not attained.

The *mg* values for clinopyroxene share a parallel relation with hornblende when plotted against $Mg/Mg+Fe_{rock}$ (Fig. 17A), indicating direct exchange of elements between the two minerals. Covariance between the *mg*

16. Comparison between Amphiboles

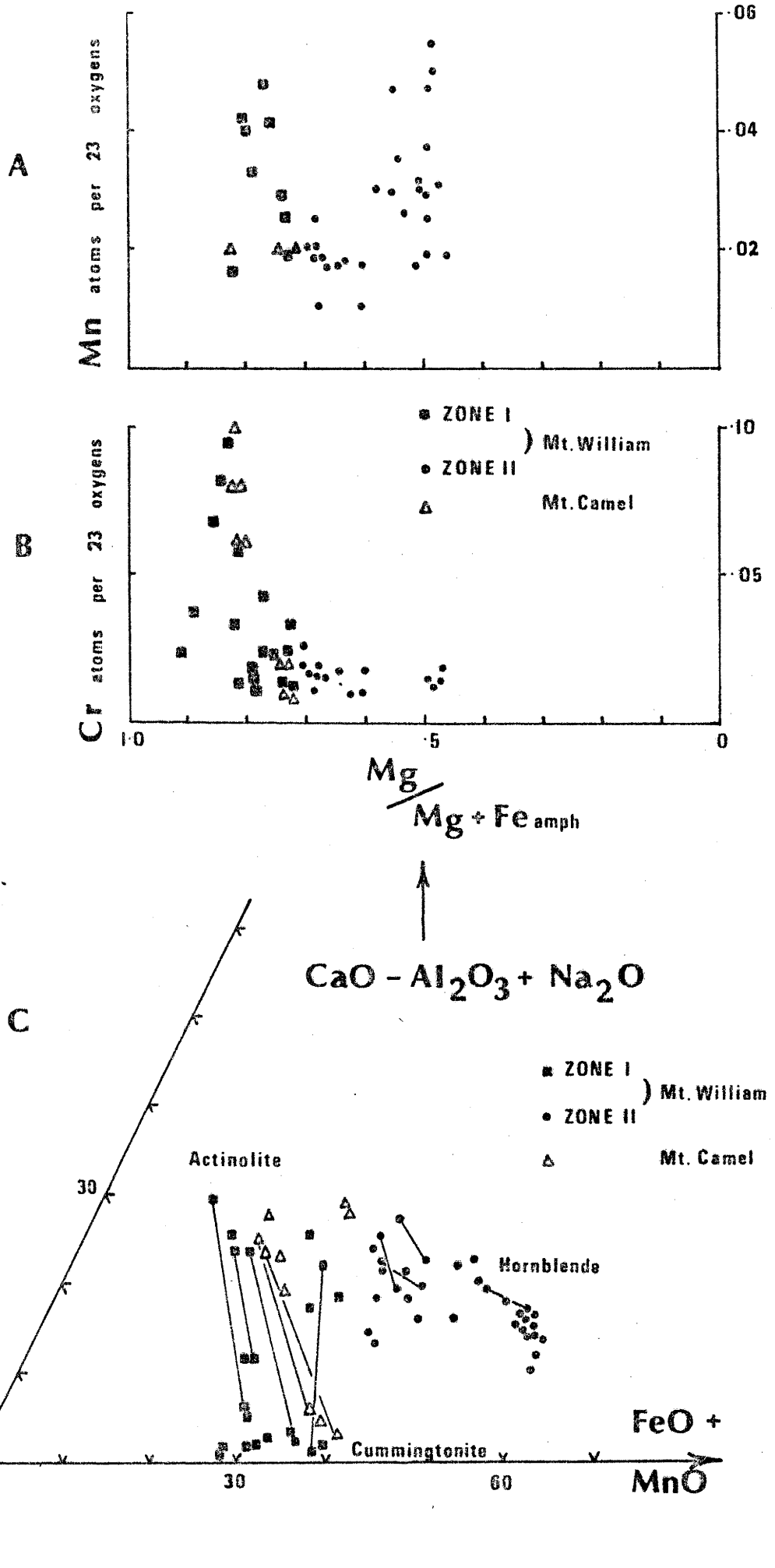

values of pyroxene and amphibole denotes lack of introduction of components from external sources and signifies equilibrium reactions during isochemical contact metamorphism.

An immiscibility gap between actinolite and hornblende is not evident from the analyses (Appendix 2) and diagrams used to illustrate their compositions (Figs. 9, 16C, 18B). Though continuity of composition is the predominant feature, variability in Mn and Cr indicates genetic differences between actinolite and hornblende (Fig. 13).

Hornblende from metadolerite (Zone 2 - Mount William) is characterised by low *mg* values, and Cr decreases and Mn increases with progressively lower *mg* values. This contrasts with actinolites from Mount William (Zone 1) and Mount Camel which have higher *mg* values, and Cr and Mn decrease variably with decreasing $Mg/Mg+Fe_{amph}$.

Similar amounts of chromium and manganese in actinolites from Mount William and Mount Camel do not permit discrimination between rocks from these locations. However the high chromium content in actinolite implies Cr-rich parental minerals (and rocks) from which they formed, additional information supporting ultramafic parent rock affinity.

In general, analyses of actinolite and cummingtonite from Mount William and Mount Camel are so similar that their compositions cannot be used to source axe stones. Ultramafic parent rocks in both areas, initially of similar bulk chemistry, formed actinolite-cummingtonite hornfelses by almost identical alteration and metamorphic processes.

Hornblende, in metadolerite at Mount William, should reflect compositional variations of pyroxene and plagioclase (bulk chemistry) provided isochemical metamorphism took place. Compositional changes in

17. Variation of $Mg/Mg+Fe$ between rocks and minerals

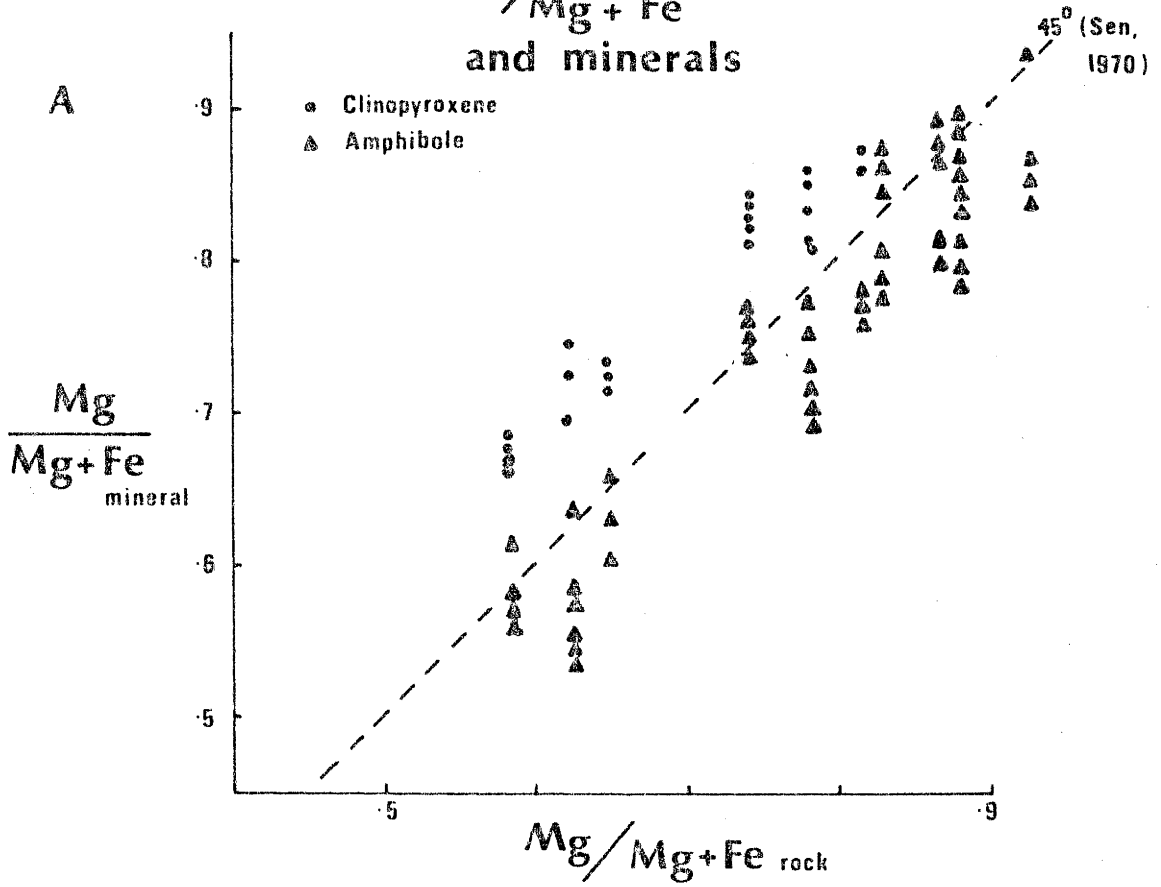

B Content of alkalies and Al^{IV} in amphiboles

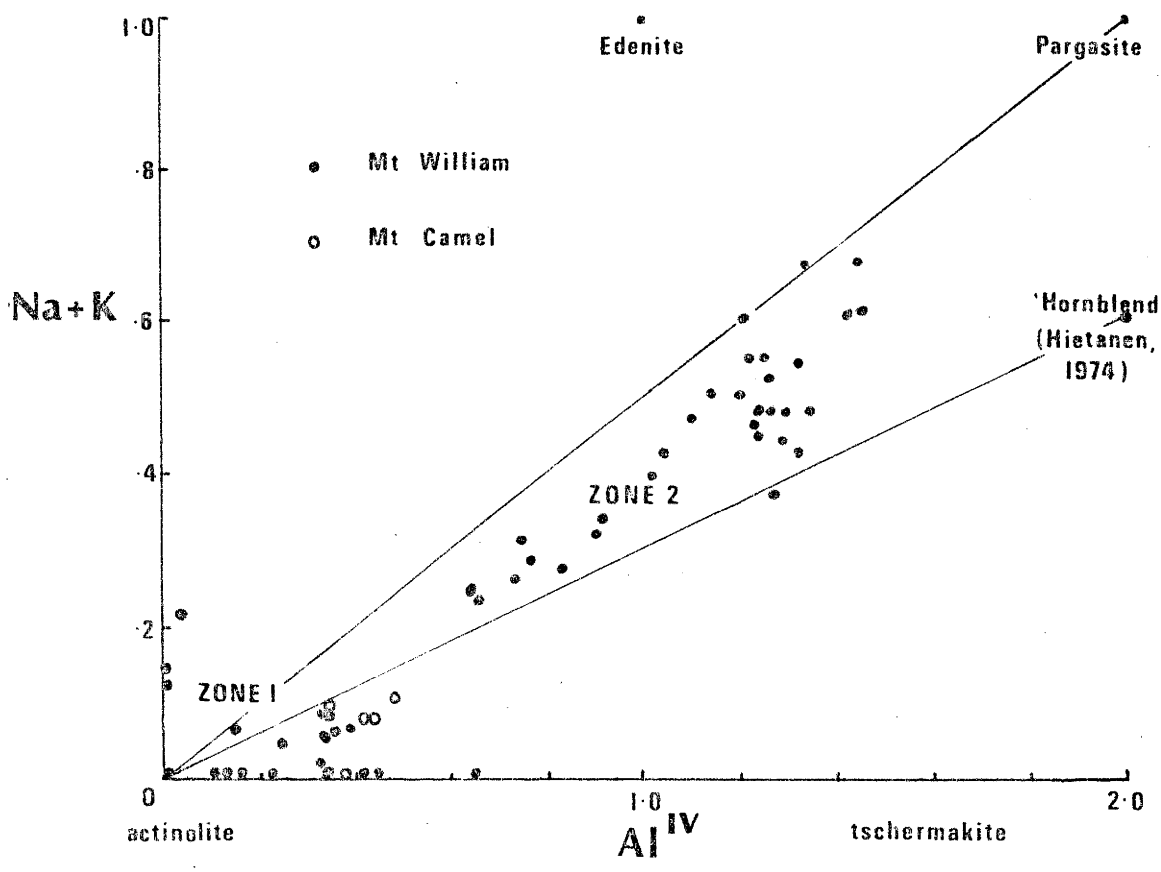

hornblende are investigated by examining the variation in the content of alkalies within the A-site. From a study of the major element variation in the rocks across the metadolerite there is a progressive increase in sodium and potassium with fractionation. A plot of total alkalies against tetrahedral Al (per formula unit) in Figure 17B shows that hornblendes from the metadolerite lie along a line between tremolite and pargasite. The total alkali content of hornblende decreases with decreasing Al^{iv} and the ratio is constant at 1:2. This ratio contrasts with 1:3 found by Hietanen (1974) for amphiboles in a contact aureole, and reflects the lower alkali content of the rocks studied by her.

The range in alkali contents of amphiboles is shown by two samples, 30 metres and 100 metres away from the Cobaw Granite.

The highest alkali content in amphiboles is shown by hornblende close to the granite. Its structural formula is,

$Na_{.6}K_{.07}(Ca_{1.84}Mg_{.16})(Mg_{2.08}Fe_{2.40}Mn_{.05}Cr_{.01}Ti_{.11}Al^{vi}_{.38})(Si_{6.64}Al^{iv}_{1.36})O_{22}(OH)_2$

The lowest amount of alkalies in hornblende is in samples about 100m from the granite contact and a typical structural formula is,

$Na_{.33}K_{.02}(Ca_{1.84}Mg_{.16})(Mg_{2.45}Fe_{2.29}Mn_{.03}Ti_{.04}Al^{vi}_{.38})(Si_{6.64}Al^{iv}_{1.36})O_{22}(OH)_2$

In rocks near the granite alkalies, iron, titanium, manganese, and aluminium increase whereas magnesium and silicon decrease as the granitic contact is approached. Trends for alkalies, iron, titanium, manganese and magnesium follow bulk chemical changes (c.f. Liou et al, 1974) and aluminium and silicon are dependent on temperature.

Substitutions of $Na^{A}Al^{iv}$ for Si^{iv} (edenitic) and $Al^{vi}Al^{iv}$ for $Mg^{vi}Si^{iv}$ (tschermakitic) in these amphiboles lead to pargasitic composition (Fig. 17B).

18. Partition of major elements between

A pyroxene, plagioclase and amphibole

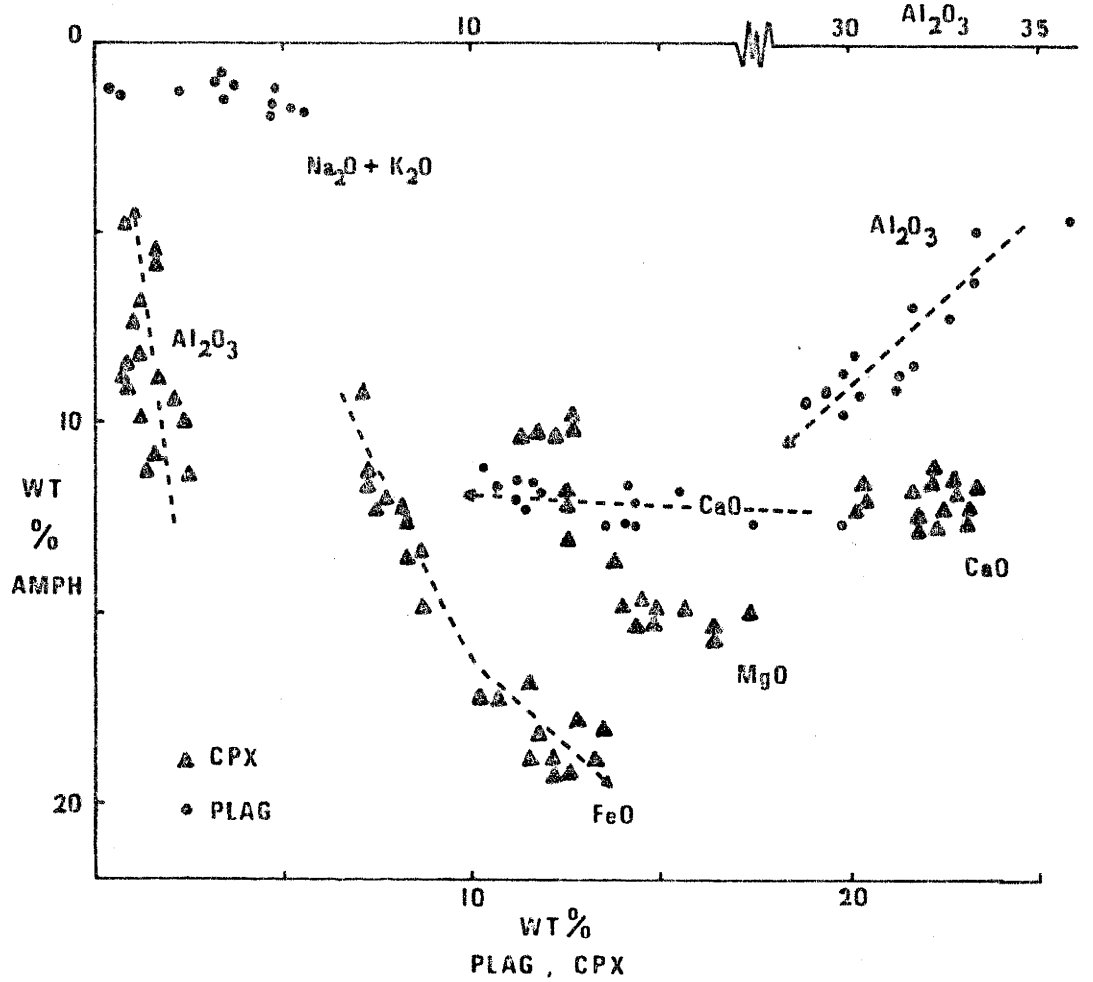

B Mg:Fe content of amphiboles, Mt. William

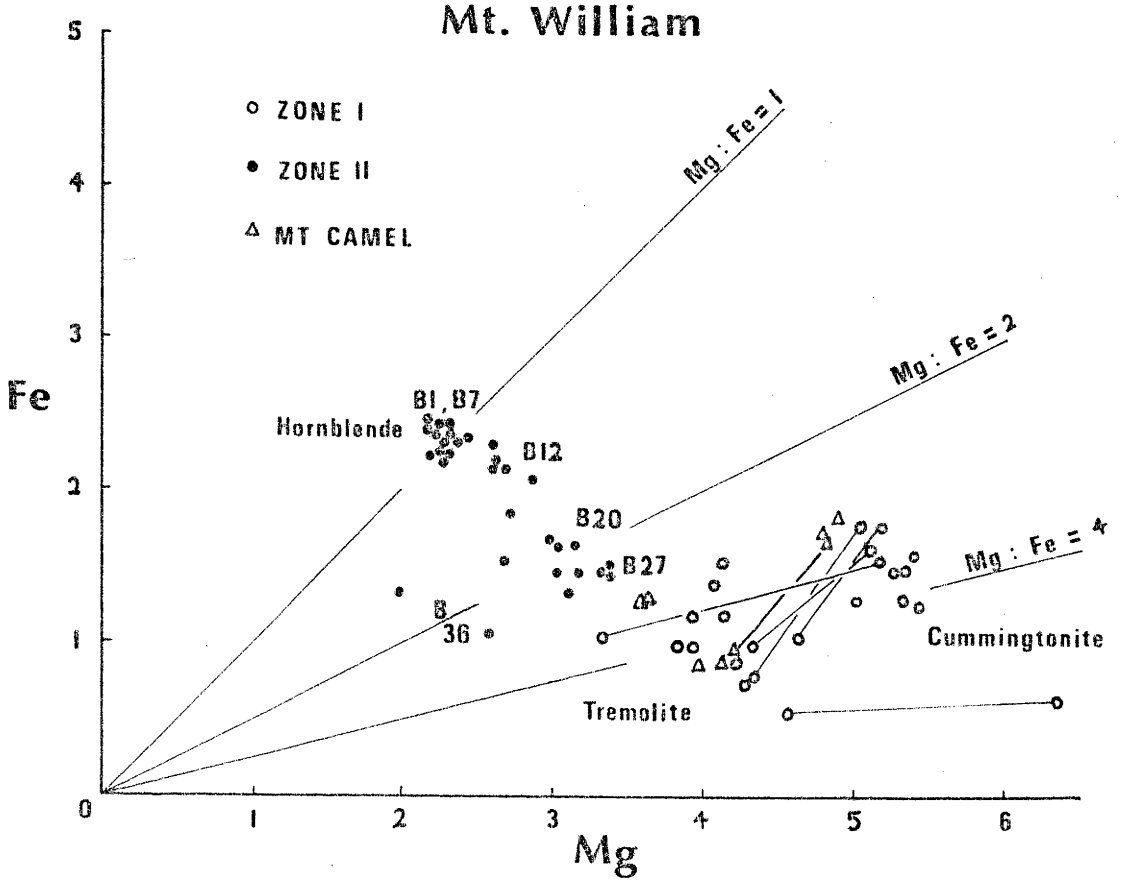

The partitioning of major elements between clinopyroxene, plagioclase and amphibole (Fig. 18A), shows the contribution that pyroxene and plagioclase make towards the composition of hornblende. Examination of analyses of clinopyroxene and amphiboles (Appendix 2) reveals that the silica content of pyroxenes remain constant throughout fractionation whereas amphiboles formed from them are lower in SiO_2. Clearly this is directly related to the temperature of contact metamorphism, higher temperatures resulting in less SiO_2 in hornblende. Consequently the Al^{iv} content of hornblende should increase as the granitic contact is approached (c.f. Harry, 1950; Binns, 1965). If the amount of Al^{iv} is an indicator of temperature then the alkali content of hornblendes in metadolerite at Mount William increases with increasing temperature (Fig. 17B).

It is also obvious that total aluminium in amphiboles increases with progressive metamorphism because plagioclase, the main contributor of Al, decreases in Al_2O_3 as hornblende increases in this component (Fig. 18A). Pyroxenes release an insignificant amount of aluminium to hornblende.

Calcium from pyroxene is used to form hornblende and excess amounts added to plagioclase, thereby enriching the feldspar in anorthite molecule. The surplus calcium from pyroxene goes into plagioclase to replace loss of alkalies which are scavenged by hornblende.

The MgO and FeO content of rocks determines the amount of these constituents in amphiboles (Fig. 17A), however the increase of iron and decrease of magnesium in clinopyroxene during fractionation, mimicked by hornblende, is evidence of compositional control of amphibole by pyroxene chemistry.

Major element fractionation between amphiboles (Fig. 19) is studied by adopting the method of Klein (1969), and plotting Ca/Ca+Na against

19. Major element fractionation in amphiboles (Klein, 1969)

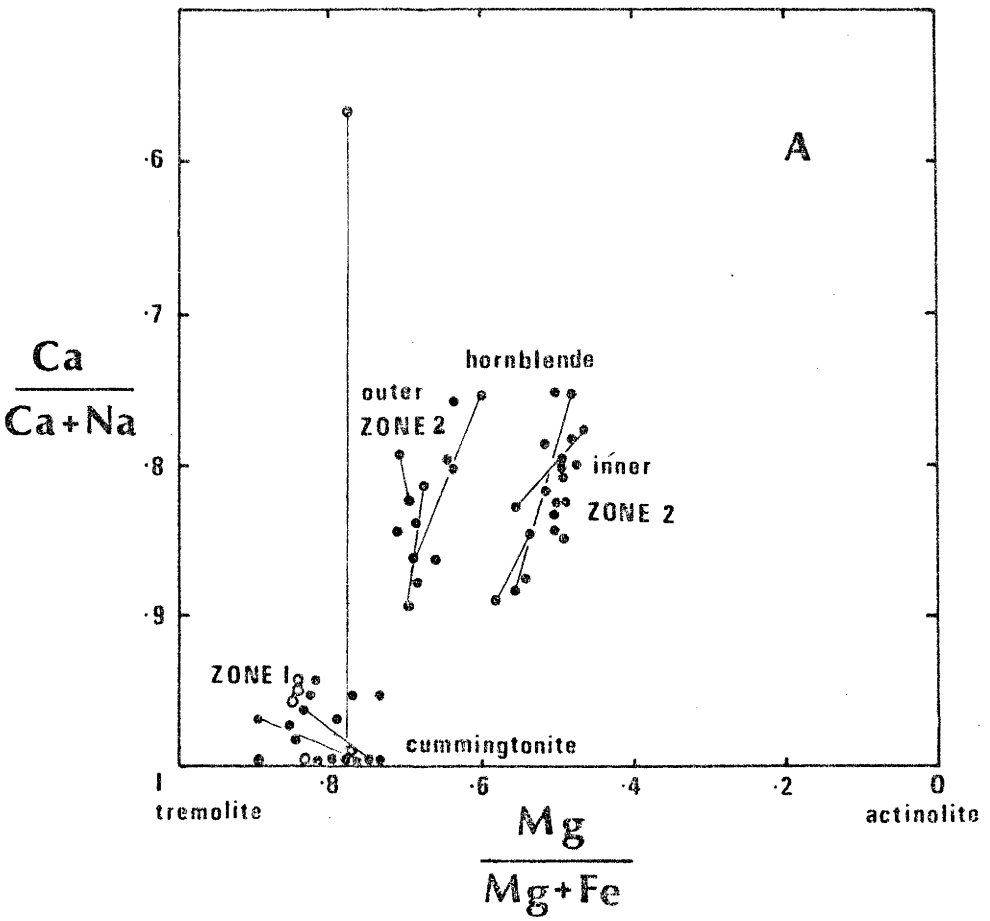

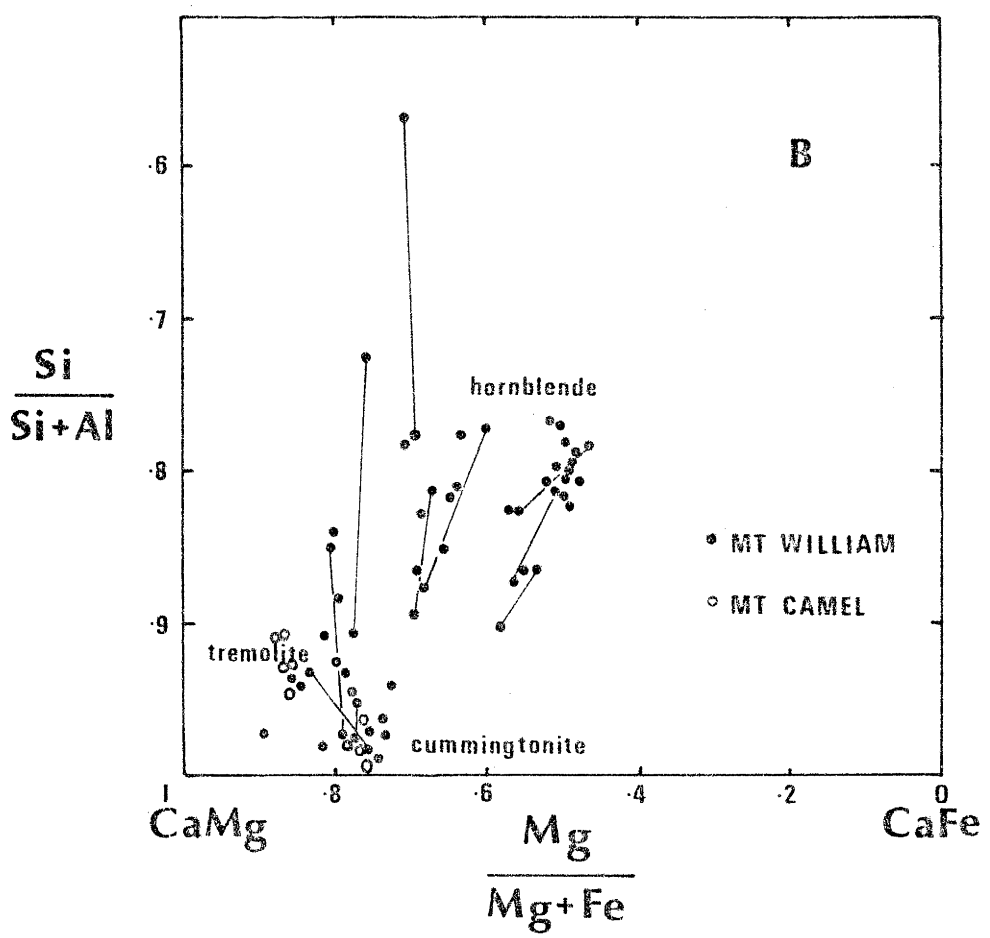

Mg/Mg+Fe and Si/Si+Al versus Mg/Mg+Fe. The ratio Ca/Ca+Na expresses the relation between calcium in the M4-sites and sodium, which may substitute for it when any of these sites are vacant. The inter-relation between the two main elements which occupy the octahedral sites is revealed by the ratio Mg/Mg+Fe. Substitutions of aluminium for silicon are shown in the ratio Si/Si+Al. Precise information regarding elemental partitioning in amphiboles cannot be obtained using electron probe analyses because ferric iron is unmeasured.

Amphiboles in metadolerite (Zone 2 - Mount William) are divided into two groups (Fig. 19). The apparent discontinuity in hornblende compositions between the inner and outer parts of Zone 2 is explained by the relation Mg/Mg+Fe of amphibole being dependent on that of its host rock.

The wide range in element fractionation in amphiboles in the two groups as well as within the same specimen reflects increasing substitutions of Na for Ca and Al for Si at higher temperature.

Minor amounts of Na substitute for Ca, and Al for Si in actinolite from Mount William (Zone 1) and Mount Camel. Cummingtonite does not contain sodium and negligible amounts of Al substitute for Si.

Variation in the composition of hornblende across Zone 2 is illustrated in Figure 20. From the chemical changes in amphibole it is possible to subdivide Zone 2 into at least two and possibly three parts or subzones. Subzone 2A contains hornblendes which decrease in Si and Mg, and increase in Al^{iv}, Al^{vi}, Ti, Fe, Mn, Ca, Na, and K with progressive metamorphism. Amphiboles in this part of the aureole formed in the highest grade of contact metamorphism at Mount William, and their compositions are affected more by temperature than bulk chemistry. Hornblendes in subzone 2B decrease in Al^{iv}, Al^{vi}, Ti, Mg, Na, K, and increase in Si, Fe, and Ca,

20. VARIATION IN HORNBLENDE COMPOSITION

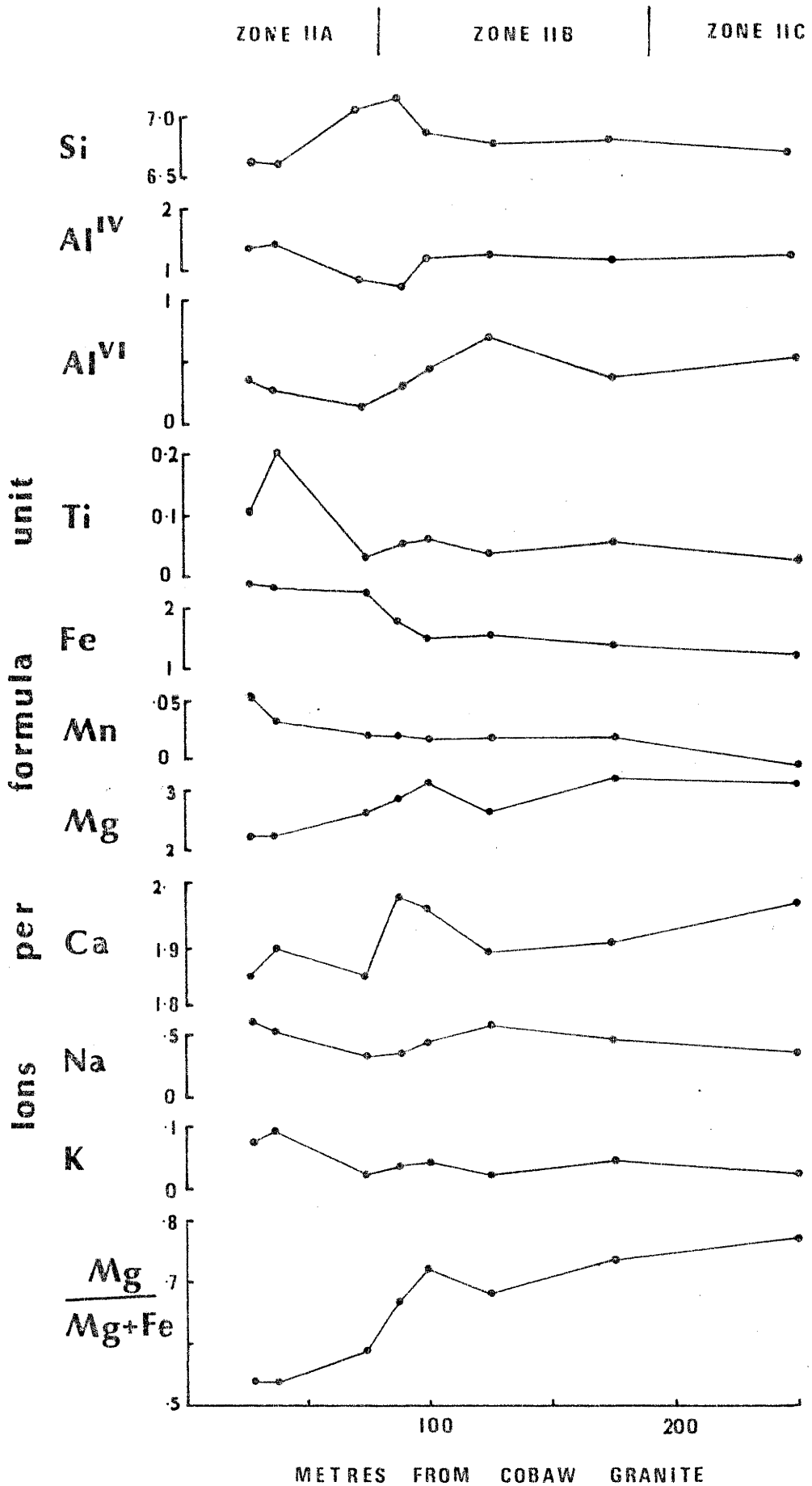

whereas Mn is relatively constant across the subzone. These trends are different from those in subzone 2A and result from increasing control of bulk chemistry on the amphibole composition. Subzone 2C is not a distinct subdivision on the basis of amphibole composition and it is established with the aid of plagioclase (see later). In this subzone Al^{iv}, Al^{vi}, and Ca decrease, Si, Ti, Fe, Mn, Na, and K increase and Mg is constant as the granite is approached.

The different chemical variations in hornblende composition are attributed to the combined effects of bulk chemistry and temperature. Through subzones 2C and 2B bulk chemistry and temperature affect the composition of hornblende whereas in subzone 2A temperature is the more important controlling influence.

Plagioclase

Electron probe analyses of plagioclase are listed in Appendix 2. The main emphasis concerning plagioclase is to determine its compositional variation across the metadolerite at Mount William and to find the elemental contribution from feldspar to hornblende during contact metamorphism.

The most calcic plagioclase of the metadolerite (An_{93-97}) occurs near the base of the sill (in the outer part of Zone 2), and because of its high anorthite content must be regarded as being metamorphic. The tendency for plagioclase to become more calcic during progressive metamorphism (Compton, 1958; Engel, Engel & Havens, 1964; Binns, 1965; Loomis, 1966; Liou et al, 1974) means that the primary feldspar probably had a composition of An_{80-85}.

From contact metamorphic studies earlier in this thesis it was determined that Zone 2 at Mount William represents the hornblende-hornfels facies of contact metamorphism. The effect of metamorphism on plagioclase composition in metadolerite at Mount William is illustrated in Figure 21. Bulk chemical variations of Ca, Na and K are related in the ratio Ca/Na+K and plotted as a function of distance from the Cobaw Granite. As the granite is approached the ratio $Ca/Na+K_{rock}$ decreases markedly, illustrating the increase of sodium and potassium in late fractionated phases of the sill. Two trends are evident when the pair of ratios $Ca/Na+K_{plag}$ and $Ca/Na+K_{rock}$ are combined.

The upper trend shows close correlation with that for bulk chemical changes ($Ca/Na+K_{rock}$), and therefore reflects compositional changes in primary plagioclase. This agrees with petrographic observations that feldspars become increasingly albitic toward the top of the sill (Appendix 1).

The lower trend increases slightly towards the Cobaw Granite, plagioclase becomes more calcic with progressive metamorphism agreeing with petrographic and geochemical observations. Also evident is that plagioclase near the Cobaw Granite undergoes greater compositional change than the feldspar farther away. This feature is contained in the reactions constructed when discussing contact metamorphism. The composition of feldspar converted from igneous to metamorphic in Zone 2C (the outer part of Zone 2) changes from An_{86} to An_{98}, whereas near the granite (Zone 2A) it is from An_{24} to An_{54}. Igneous plagioclase compositions were determined (after assuming isochemical metamorphism) by equalising reactants and products in the reaction from pyroxene, plagioclase, ilmenite and water to hornblende, plagioclase and sphene.

Zone 2 is subdivided into three parts on the relative compositional changes of plagioclase. Nearest the granite, rocks of Zone 2A consist of metamorphic feldspar only, because the highest grade of metamorphism completely recrystallised and reconstituted the feldspar. Between 80 metres and 180 metres from the Cobaw Granite in Zone 2B, partial recrystallisation of feldspar took place resulting in coexisting relict igneous and metamorphic plagioclases. Beyond 180 metres in Zone 2C little altered relict igneous plagioclase is found. The metamorphic effects in the last zone being less severe than in the other two, as expected from temperature gradients around the granitic body (Jaeger, 1957, 1959).

In summary therefore, the composition of plagioclase becomes more calcic with progressive metamorphism, depending upon the temperature conditions, and relict igneous feldspar is not preserved in the highest grade of the hornblende-hornfels facies found in the contact aureole at Mount William.

21. Variation in plagioclase composition across the metadolerite

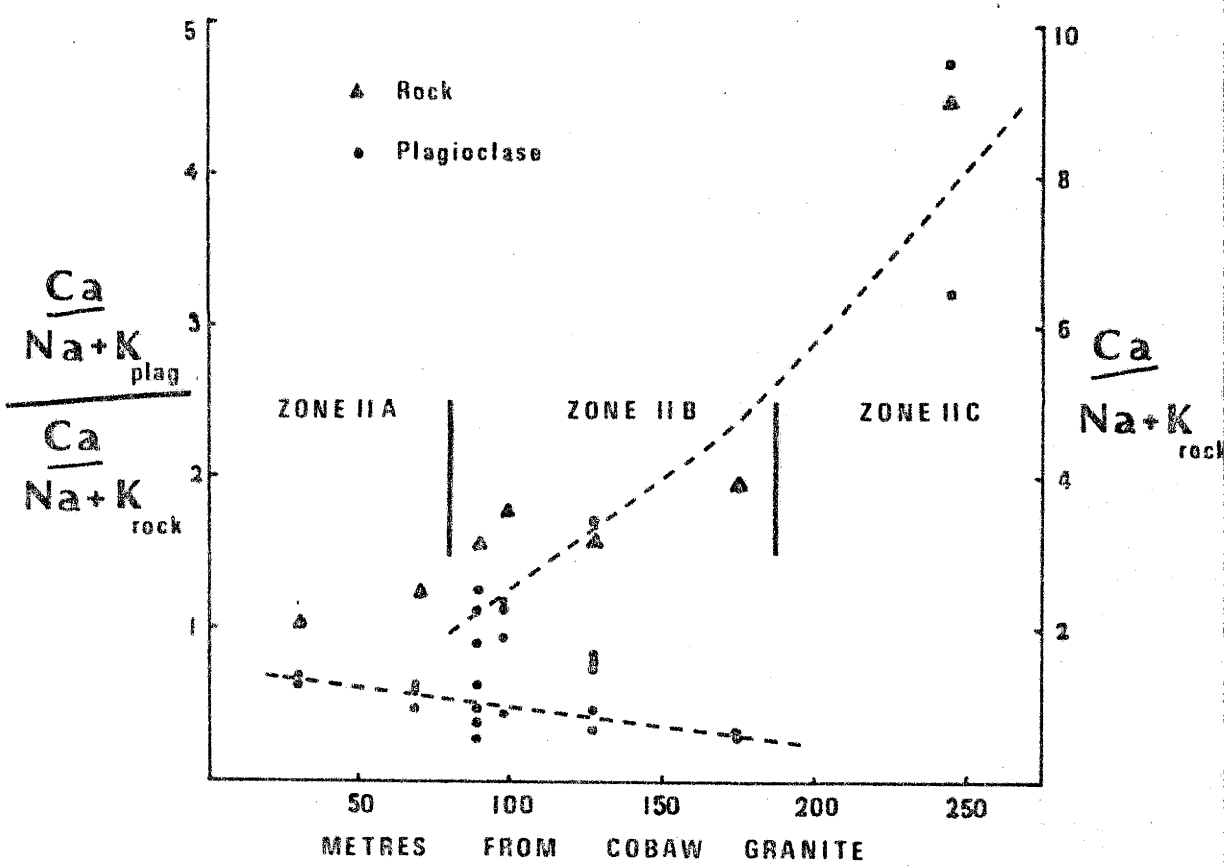

Clinopyroxene

The compositional change of clinopyroxene in metadolerite at Mount William is from augite toward hedenbergite, according to ionic proportions Ca-Mg-Fe (Fig. 22C). Through the metadolerite magnesium is depleted and iron enriched, agreeing with compositional change of magma with fractionation. The range of compositions is from $Ca_{34}Mg_{56}Fe_{10}$ to $Ca_{45}Mg_{37}Fe_{18}$ showing that calcium also increases with fractionation.

Clinopyroxenes in metadolerite show no evidence of zoning, however, growth of hornblende as rims around pyroxene cores would destroy compositional mantles near grain margins.

Compositional changes in pyroxenes from metadolerite at Mount William are dissimilar to pyroxenes from other tholeiitic intrusions, for example, from the Keweenawan lavas (Konda & Green, 1974), Beaver Bay Gabbro Complex (Konda, 1970), Duke Island Complex and other intrusions (Irvine, 1967). Clinopyroxenes from some diabasic rocks (Smith, 1970), have comparable compositions to those in the Mount William metadolerite. Alkaline magmas crystallise clinopyroxene usually with markedly different compositions (Gibb, 1973) to those in metadolerite at Mount William.

Experimental studies by Lindsley & Munoz (1969) showed that during cooling of tholeiitic magmas both orthopyroxene and clinopyroxene crystallise. Orthopyroxene is noticeably absent from the intrusion at Mount William and olivine and pigeonite are found near the base of the sill. The absence of Ca-poor pyroxene throughout primary crystallisation history is likely to take place in a critically under-saturated magma (Lindsley & Munoz, 1969). The trend line for calcium-rich pyroxenes will therefore lie between the typical tholeiitic clinopyroxene trend and the diopside-hedenbergite join, probably at an approximately constant calcium content (Lindsley & Munoz, 1969).

22.Composition of relict Clinopyroxene - metadolerite, Mt. William

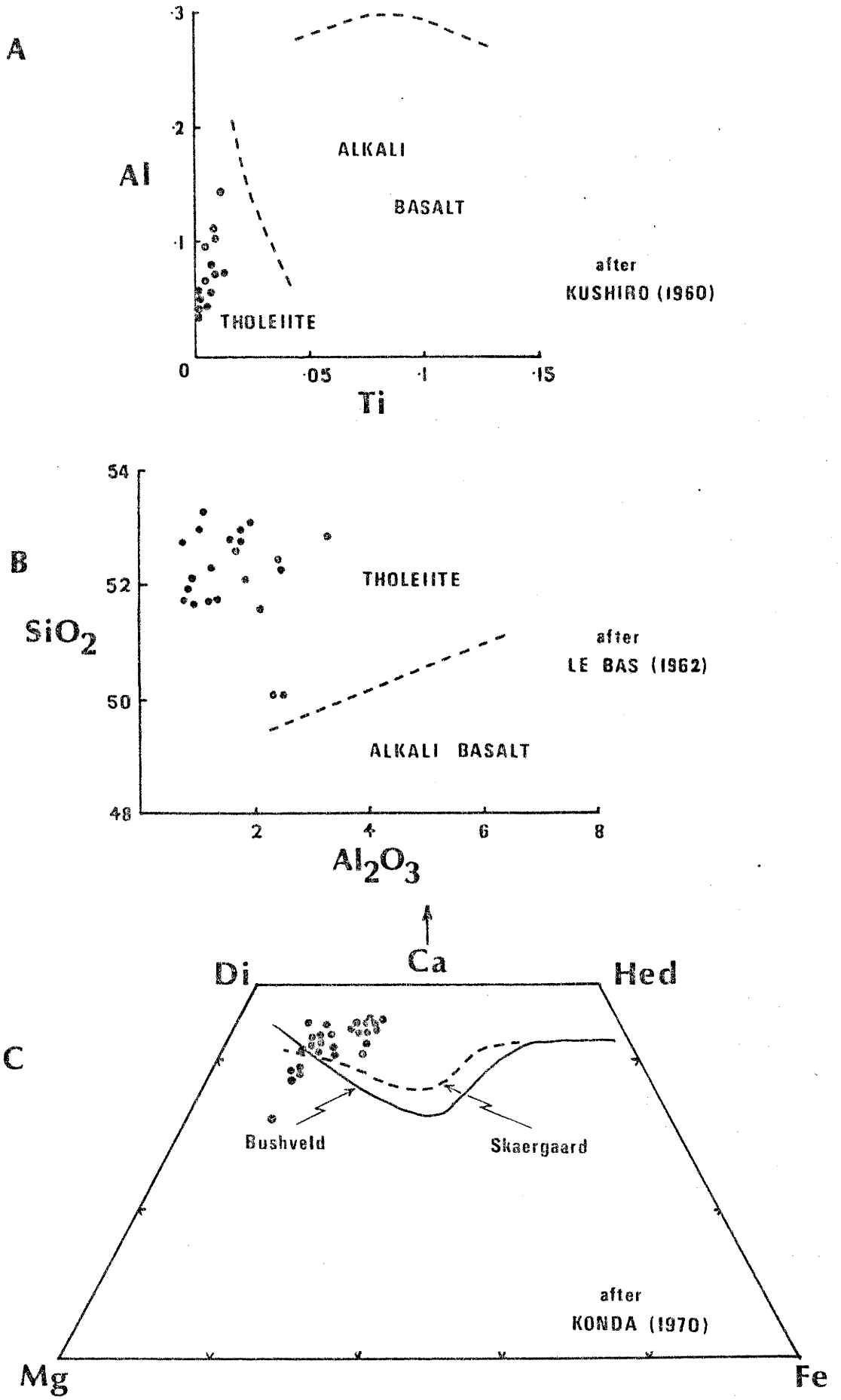

An undersaturated magma is not the parent liquid of the dolerite sill at Mount William because of the CIPW normative compositions of the rocks, and as magnesium-rich olivine, Ti- and Al-rich pyroxenes, nepheline and other undersaturated minerals are absent.

Barberi et al (1971), determined that some alkaline basic magmas crystallised pyroxenes showing similar compositional trends to pyroxenes of tholeiitic magmas and concluded that the fugacity of oxygen (fO_2) controls the compositional trend of pyroxene. The fO_2 of a cooling magma-water system is mainly controlled by dissociation of water (Hamilton & Anderson, 1967) and consequently is dependent on water content and magma temperature. The oxygen fugacity is also recognised as a factor of primary importance in magmatic differentiation and the main control of iron enrichment in a differentiating rock sequence (Osborn & Roeder, 1960). However, Hamilton & Anderson (1967), declared that variations of water pressure and therefore oxygen fugacity will have less effect on the crystallisation of tholeiitic magma than on alkaline basic magma.

The content of water in the magma and hence the oxygen fugacity contributed to the iron enrichment trend of clinopyroxene in the metadolerite at Mount William. The high activity of calcium in the magma played a major role, yielding lime-rich pyroxene and preventing crystallisation of orthopyroxene. Orthopyroxene and olivine crystallised initially and separated from the liquid leaving a lime-rich magma, which on intrusion precipitated clinopyroxene, plagioclase and minor amounts of olivine and pigeonite.

Hashimoto (1972) and Vallance (1973, 1974) used pyroxene compositions to diagnose the pristine characters of altered mafic rocks. They employed the techniques devised by Kushiro (1960) and Le Bas (1962). A similar approach is used here by plotting Ti against Al (Fig. 22A) and SiO_2 versus

Al_2O_3 (Fig. 22B). However, this method has been criticised by Gibb (1973), because the Al and Ti contents of the clinopyroxene are essentially a reflection of the low silica activity (Verhoogen, 1962; Brown, 1967) and the conditions under which the pyroxene crystallised (Barberi, 1971). In Figures 22A and 22B, clinopyroxenes from metadolerite at Mount William lie in tholeiitic fields confirming previous evidence of tholeiite parental magma for the dolerite. The diagrams also suggest that their use is justified in this case.

There is a systematic variation of titanium and aluminium in clinopyroxenes across the metadolerite. Comparison of Ti and Al with the Mg/Mg+Fe ratio for pyroxenes (Appendix 2) indicates that Ti increases and Al decreases with fractionation. These trends compare favourably with published analyses of clinopyroxenes (Evans & Moore, 1968; Smith & Carmichael, 1969; Smith & Lindsley, 1971). Trends for Ti and Al are explained by fractional crystallisation; when olivine, plagioclase and pyroxene were being precipitated the activity of Ti in the liquid would have increased markedly thus accounting for the rise in titanium. Continual crystallisation of plagioclase decreases the aluminium content of the liquid, consequently late formed pyroxenes have less Al.

SUMMARY

1. The compositions of amphiboles are affected by bulk chemistry and temperature, hornblendes from Zone 2 at Mount William are directly dependent on the compositions of plagioclase and clinopyroxene from which the amphibole formed.

2. Actinolite and cummingtonite in rocks from Mount William and Mount Camel are compositionally similar and cannot be used to discriminate rocks from these locations.

3. Zone 2 is subdivided into three parts on the basis of amphibole and plagioclase compositions attributed to increasing grade of contact metamorphism.

4. Actinolite and hornblende form a continuous compositional series and an immiscibility gap does not exist.

5. The compositional range of clinopyroxenes in metadolerite at Mount William is from $Di_{34}En_{56}Fs_{10}$ to $Di_{45}En_{37}Fs_{18}$ and the trend is similar to pyroxenes in other tholeiitic dolerite intrusions.

DISCUSSION

Actinolite-cummingtonite hornfels developed as a result of contact metamorphism of magnesium-rich rocks from the Heathcote Greenstone. These rocks, compositionally similar to olivine pyroxenite, are derived from completely altered parental rocks of Alpine-type ultramafic affinity. Whether the original rocks formed by (submarine) extrusion or 'cold' intrusion remains unsolved because of poor contact relations and absence of convincing primary textural features. Interpretations of features similar to amygdales, chilled margins, brecciated flow tops and tuffaceous texture leads to the dubious conclusion that the greenstones are flows rather than 'cold' intrusions. The overall composite nature of the unit, observed in the field, indicates successive layers rather than a single episode of intrusion or a massive flow.

Extrusion of melts of ultramafic composition are a controversial problem in geology (Hess, 1955; Cawthorn & Strong, 1974; Green, 1975; Nesbitt & Sun, 1976). Extreme alteration of greenstone in the Mount William-Heathcote-Colbinabbin Belt means that a precise petrogenesis of these rocks cannot be determined. Partial melting of the mantle, differentiation, and rapid rise to the surface in an area with high geothermal gradient is interpreted as a possible petrogenetic model for parent rocks of actinolite-cummingtonite hornfelses of the Heathcote Greenstone.

Though rocks of the Mount William Group and Knowsley East Formation are Cambrian on account of their fossil assemblage, an age has not been determined for the Heathcote Greenstone. If the greenstones are much older than Cambrian then the origin of these rocks may be more readily explained because of the thin crust and favourable geotectonic environments during the early history of the earth (Anhaeusser, 1976).

Deuteric alteration and surface weathering probably affected the volcanic rocks prior to sedimentation in the Upper Cambrian. Continuous deposition of marine sediments occurred during the Ordovician and Silurian in a gradually subsiding trough, making a sedimentary pile at least 10km thick. Burial metamorphism affected the rocks, facilitating element migration and mineral reconstitution. Progressive alteration of the rocks together with regional metamorphism up to the lower part of the greenschist facies changed most original minerals and textures.

After low-grade regional metamorphism, dolerite intruded as sills up to 1000m thick and as small lenses and dykes. Emplacement of large sills, for example at Mount William, caused contact metamorphism of altered volcanics enabling additional mineralogical and geochemical changes to take place. The width of the aureole about the dolerite at Mount William was probably several hundred metres (Jaeger, 1957, 1959). Smaller intrusions, for example in the Mount Camel area, with narrow contact aureoles would have had less effect on the country rocks.

Emplacement of the Cobaw and Crosbie Granites during the Devonian caused contact metamorphism of greenstone adjacent to these plutons. In some places, as at Mount William, the rocks were isochemically metamorphosed whereas in other areas, for example at Mount Camel, metasomatic processes affected the rocks.

The complex history of alteration of original magnesium-rich rocks and final contact metamorphism resulted in development of actinolite-cummingtonite hornfelses.

Metadolerite at Mount William, consisting of relict igneous minerals, hornblende and sphene was less affected and shows less alteration than magnesium-rich rocks. Good preservation of primary minerals and textures in

the metadolerite strongly indicates that it was not altered by burial and low-grade regional metamorphism, being only contact metamorphosed by the Cobaw Granite. Preservation of igneous geochemical trends and the lack of degradation features typical of burial and regional metamorphism (c.f. Jolly & Smith, 1972; Smith, 1970; Heimlich & Uthe, 1976), indicate that dolerite was emplaced after these alteration processes and before intrusion of the Cobaw Granite.

After intrusion of a hydrous dolerite at a temperature of about 1300°C (Wager, 1960), magnesium-rich clinopyroxene, plagioclase, olivine and ?orthopyroxene crystallised. The presence of small amounts of olivine and ?orthopyroxene suggests removal of these minerals from a melt in a magma chamber prior to emplacement. Pyrrhotite enriched in nickel, chalcopyrite and minor magnetite were also precipitated in the early stages of cooling.

Later, with preferential crystal settling of clinopyroxene and plagioclase in layers, the melt gradually became depleted in magnesium and enriched in iron. Sulphides became progressively depleted in nickel and ilmenite started to crystallise as the titanium content of the liquid increased. Pyrrhotite cores with pyrite rims indicate that the fugacity of sulphur rose steadily as the liquid cooled.

Fractional crystallisation of the melt caused an increase in its water content resulting in reaction between crystallising clinopyroxene and water with formation of hornblende. After this micropegmatite phase crystallised the liquid became enriched in iron and depleted in magnesium. Apatite started to crystallise because of the high activity of phosphorous in the liquid.

Clinopyroxene changes in composition from $Ca_{34}Mg_{56}Fe_{10}$ to $Ca_{45}Mg_{37}Fe_{18}$ and plagioclase from An_{80-85} to An_{25-30} with fractionation. The geochemical

23. THOLEIITIC FRACTIONATION TRENDS

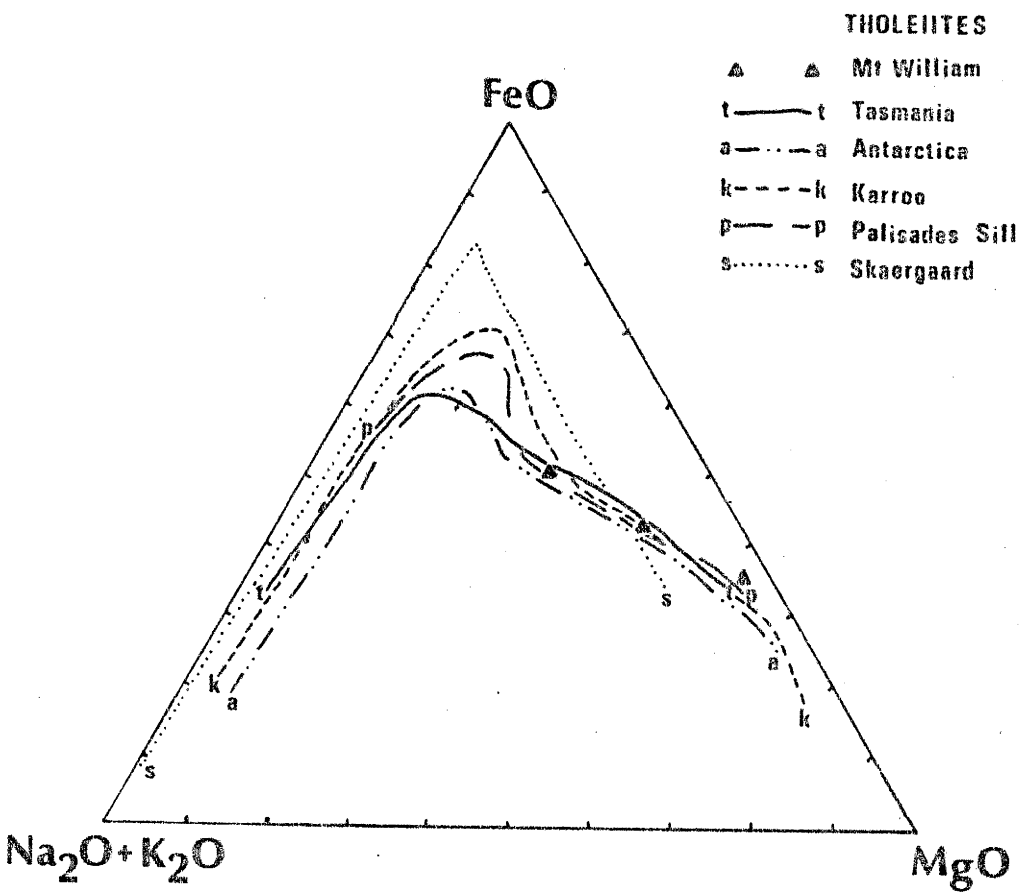

and mineralogical trends found in metadolerite at Mount William, and illustrated by an AFM diagram (Fig. 23) conform to usual fractionation sequences of tholeiitic magma (Wager & Mitchell, 1951; McDougall, 1962; Wager & Brown, 1967; Walker, 1969). However, the metadolerite at Mount William is not extremely fractionated unlike other tholeiitic intrusions where strong enrichment of alkalies is typical. Enrichment of iron and alkalies and depletion of magnesium in metadolerite at Mount William are attributed to injection of an olivine tholeiitic liquid from which most crystals of olivine and orthopyroxene were removed, low initial concentrations of alkalies, and the hydrous nature of the melt.

Greenstone country rocks from which actinolite-cummingtonite hornfelses developed belong to the quartz-albite-chlorite subfacies of the greenschist facies of regional metamorphism (Turner & Verhoogen, 1960). The metamorphic facies of rocks from Mount William and Mount Camel are illustrated in Figure 24. Variation of calcium in Mount Camel rocks reflect Ca-metasomatism in that area. Actinolite-cummingtonite-rich rocks belong to the albite-epidote hornfels facies of contact metamorphism (Turner & Verhoogen, 1960), and a temperature of at least 400°C is implied (Winkler, 1965).

Metadolerite from Mount William is subdivided into three parts, subzone 2A is the highest grade region of the contact aureole being nearest the Cobaw Granite. A temperature for metamorphism of less than 600°C is indicated (Winkler, 1965), because the rocks belong to the hornblende-hornfels facies and do not reach up to the pyroxene-hornfels facies. Rocks in this part of the aureole contain strongly recrystallised plagioclase, brown hornblende, sphene and minor relict clinopyroxene. Subzone 2B, is also within the hornblende-hornfels facies (Fig. 19) and comprises both recrystallised and relict igneous plagioclase, brown-green hornblende, sphene

24. METAMORPHIC FACIES

(After Turner & Verhoogen, 1960)

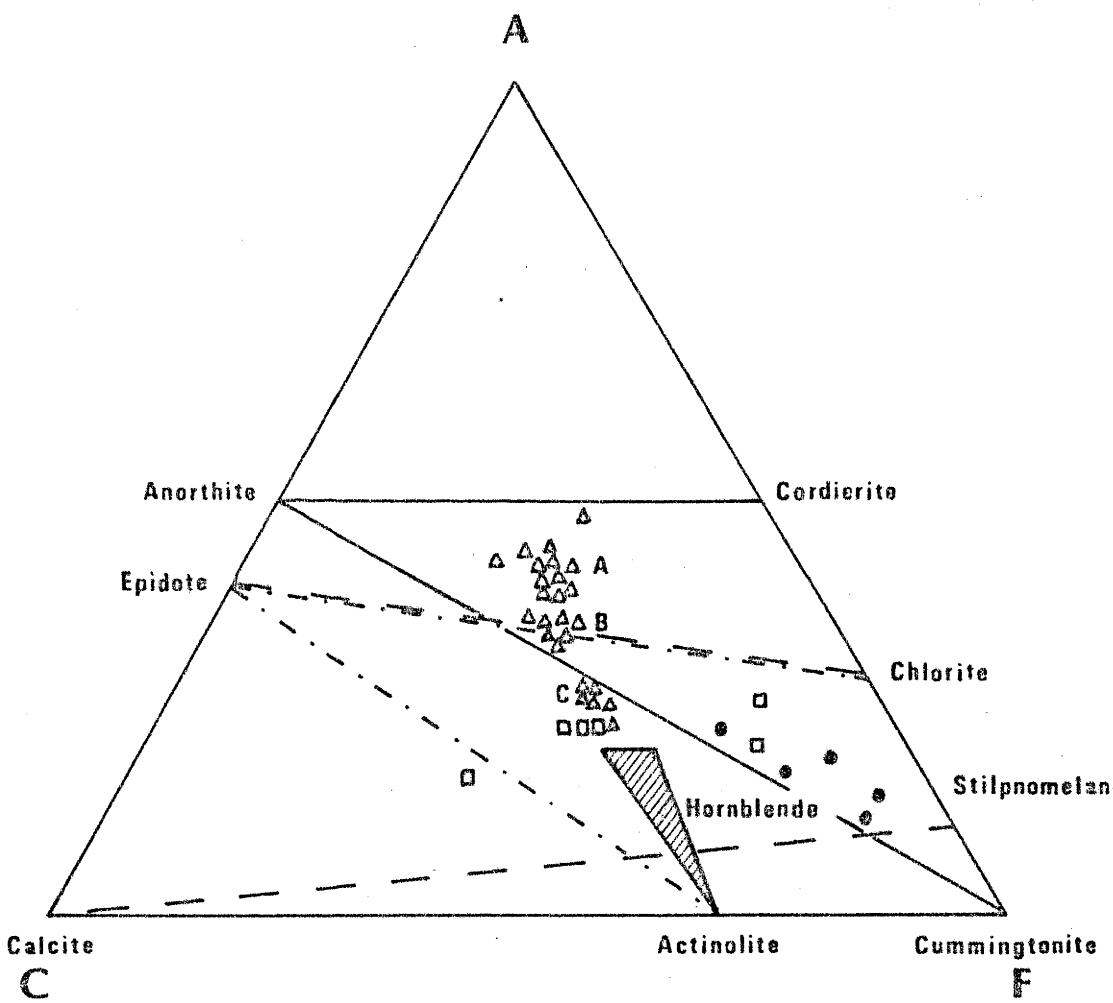

——— Hornblende – hornfels facies

– . – . Albite – epidote – hornfels facies

— — Greenschist facies

△ Mount William – Zone II(A, B, C)

● Mount William – Zone I

□ Mount Camel

and cores of relict clinopyroxene. The outermost part of Zone 2, subzone 2C, belongs to the albite-epidote hornfels facies (Fig. 24) and contains relict igneous plagioclase, bluish green hornblende rims around clinopyroxene and minor amounts of sphene.

With progressive metamorphism compositional changes are observed in amphiboles from Zones 1 and 2 (Table 2). Actinolite increases in SiO_2, MgO, CaO, and Cr_2O_3 and decreases in Al_2O_3, FeO, and MnO as the Cobaw Granite is approached. The trends for silicon and manganese parallel bulk chemical changes whereas the other components reflect variations in composition due to an increase in temperature.

Cummingtonite increases in SiO_2, FeO and MgO, and Al_2O_3, MnO, CaO and Cr_2O_3 decrease with an increase in temperature. In this case silicon, iron, manganese and calcium follow bulk chemistry and the other elemental oxides indicate compositional changes dependent on temperature.

Silicon, aluminium, magnesium and manganese share similar trends in actinolite and cummingtonite. Silicon and manganese in actinolite and cummingtonite are dependent upon bulk chemistry. The increase in SiO_2 means that more Si is contained in Z-sites, consequently there is less Al^{iv} in samples near the granite. Not only Al^{iv}, but also the total aluminium content is lower in rocks from the inner parts of Zone 1, an effect which is surely temperature dependent.

Magnesium increases in actinolite and cummingtonite against a bulk chemical trend of decreasing MgO. It is therefore accepted more readily into Y-sites at higher temperature in both amphiboles. Mg and Fe are used to fill the Y-sites in actinolite, so that the relative abundance of magnesium and iron, as well as temperature control the Mg/Fe ratio. Availability of magnesium in altered ultramafics and increasing acceptance of Mg with

progressive metamorphism means that the iron content of actinolite decreases as the granite is approached. In cummingtonite magnesium is used to fill X- and Y-sites and Fe is minor, so that there is less competition between magnesium and iron and the Fe content increases with progressive metamorphism, following bulk chemistry.

Calcium is used to fill the X-sites in actinolite so that its increase with a rise in temperature does not follow bulk chemistry and reflects greater acceptance of Ca into actinolite with progressive metamorphism. On the other hand, as calcium is only a minor constituent of cummingtonite its concentration is governed by bulk chemistry and not temperature.

Actinolite and cummingtonite formed in the altered ultramafic rocks at Mount William and Mount Camel in response to thermal metamorphism and because of favourable bulk chemical compositions. The chemistry of these amphiboles depends on temperature and composition of the host rock.

The close relation between *mg* values of rocks and amphiboles (Fig. 17A), division of amphiboles into two groups revealed by major element fractionation (Fig. 19), and subdivision of Zone 2 into three parts using compositional trends of hornblendes (Fig. 20) all reinforce the belief that the aureole at Mount William is zoned with respect to amphibole compositions. In particular, subzone 2A contains hornblendes compositionally different from those in the other subzones, a feature attributed to the highest grade of contact metamorphism in rocks at Mount William. The chemistry of amphiboles in this zone is essentially controlled by temperature whereas hornblendes in subzones 2B and 2C are influenced by temperature and bulk chemistry.

Similarities and differences between samples from Mount William and Mount Camel are discussed to determine features which may be used to

discriminate axe stones. Table 7 summarises petrographic and geochemical features of greenstone from the two areas.

TABLE 7

SIMILAR		DIFFERENT	
Mt. William - Mt. Camel		Mt. William	Mt. Camel
General appearance	Hard, contain spheroids.	green-black	brown-green, epidote-carbonate veins
Petrography	actinolite, cummingtonite, albite spheroids quartz spheroids carbonate spheroids iron oxide, acicular, decussate texture	strongly recrystallised, sheared	weakly recrystallised, tuffaceous texture, pseudomorphs after ?Cpx, diopside
Geochemistry	SiO_2, FeO, MnO, K_2O, Rb, Sr, Pb, Zr, Nb, Ni, Cu, Zn.	TiO_2 <0.1wt%	TiO_2 >0.1wt%
		Al_2O_3<4.0	Al_2O_3>4.0
		Fe_2O_3>2.5	Fe_2O_3<2.5
		MgO >19.0	MgO <19.0
		CaO <6.0	CaO >6.0
		Na_2O <0.3	Na_2O >0.3
		P_2O_5 <0.02	P_2O_5 >0.02
		Y >3.0	Y <3.0
		low Ti/Zr	high Ti/Zr
		distinct Ti-Zr-Y and Ti-Zr plots	

As actinolite-cummingtonite hornfelses are hard and tough they were selected by Aboriginal man for axe stones. Most samples contain spheroids

of quartz, albite and carbonate which formed by alteration of primary minerals. Slight differences between stone from Mount William and Mount Camel are colour, texture and mineral assemblages (Table 7). The range of colour of the rocks is from green to black at Mount William and from green to brown at Mount Camel. Rocks at Mount Camel are generally less strongly recrystallised than at Mount William and contain amphibole pseudomorphs after ?pyroxene. Diopside is commonly found in actinolite-cummingtonite hornfels at Mount Camel and is absent at Mount William. Epidote and carbonate veins are common features in rocks near Mount Camel and rare at Mount William.

Actinolite-cummingtonite hornfels from Mount William and Mount Camel are geochemically similar, containing approximately equal amounts of SiO_2, FeO, MnO, and K_2O. Values for TiO_2, Al_2O_3, Fe_2O_3, MgO, CaO, Na_2O, and P_2O_5 are significantly different and from the limited number of analyses permit discrimination between hornfelses from the two areas (Table 7). Actinolite-cummingtonite hornfels at Mount William contain more Fe_2O_3 and MgO and less TiO_2, Al_2O_3, CaO, Na_2O, and P_2O_5 than their counterparts at Mount Camel. Greater concentration of aluminium, calcium and sodium at Mount Camel reflect element migration during alteration of the greenstones whereas titanium and phosphorous probably represent primary bulk chemical differences.

There is an overlap in trace element contents in actinolite-cummingtonite hornfels from both locations, however, in most samples yttrium is slightly higher in rocks from Mount William than Mount Camel. This contrasts with the opposite result found by Watchman & Freeman (1977), in a more detailed trace element study of axe stone from the two areas. Trace element contents therefore result in uncertain discrimination of sources for axe stones, even though good separation is found in some cases. This is attributed to variation in chemistry of the rocks across the outcrops at both locations.

25. Discrimination between greenstone from Mt. William and Mt. Camel

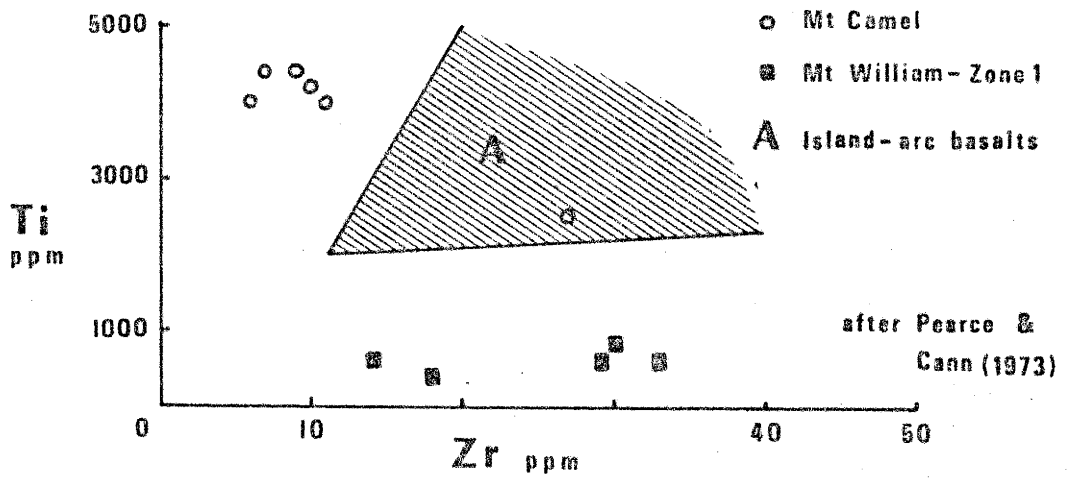

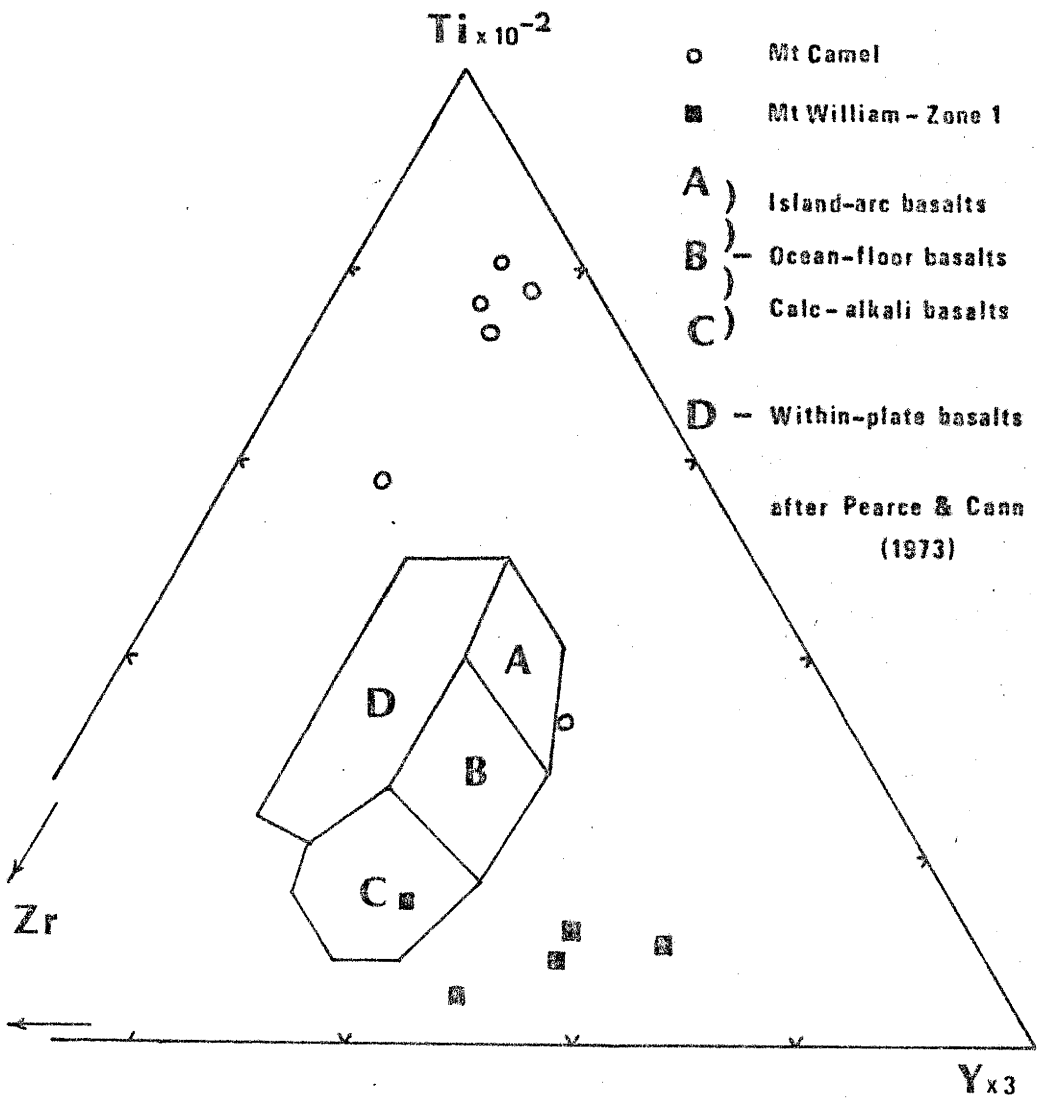

The wide range in trace element contents in hornfelses from both areas is accounted for by variable alteration and primary chemical inhomogeneity. Relative immobility of Ti, Zr and Y (Pearce & Cann, 1973) are used to discriminate between greenstone from Mount William and Mount Camel (Fig. 25). Concentration of these elements in greenstones from Victoria do not correlate with the different groups of basalts defined by Pearce & Cann (1973).

CONCLUSIONS

1. Parent rocks from which actinolite-cummingtonite hornfelses developed were Alpine-type ultramafic extrusives.

2. The metadolerite at Mount William retains mineralogical and geochemical features consistent with classical tholeiitic fractionation trends. Dehydration, recrystallisation and development of hornblende being the only noticeable changes caused by contact metamorphism.

3. Actinolite-cummingtonite hornfelses at Mount William and Mount Camel are distinguished by considering petrographic and geochemical features.

4. The contact aureole in greenstone at Mount William is zoned with respect to amphibole and plagioclase compositions.

5. Compositional changes of hornblende, actinolite and cummingtonite are affected by bulk chemistry and temperature. The role of bulk chemistry diminishes at high temperature.

REFERENCES

ANHAEUSSER, C.R., 1976. Geological and geochemical investigations of the Rooderkrans Ultramafic Complex and surrounding Archaean volcanic rocks, Krugersdorp District.

Econ. Geol. Research Unit, Univ. Witwatersrand No. 103.

APARICIO, A., & BELLIDO, F., 1976. Geochemical features of the metamorphism in the Sistema Central (Spain).

Chem. Geol., 17(4), 281-294.

BARBERI, F., BIZOUARD, H., and VARET, J., 1971. Nature of the clinopyroxene and iron enrichment in alkalic and transitional basaltic magmas.

Contr. Miner. Petrol., 33, 93-107.

BENSON, W.N., 1926. The tectonic conditions accompanying the intrusion of basic and ultrabasic igneous rocks.

Nat. Acad. Sci. Mem., 19(1), 1-90.

BINNS, R.A., 1965. Hornblendes from some basic hornfelses in the New England Region, New South Wales.

Mineral. Mag., 34, 52-65.

BROOKS, C., & HART, S.R., 1974. On the significance of komatiite.

Geology, 2(2), 107-110.

BROWN, D.A., CAMPBELL, K.S.W., and CROOK, K.A.W., 1968. The Geological Evolution of Australia and New Zealand,

Oxford: Pergamon Press.

BROWN, G.M., 1967. Mineralogy of basaltic rocks.

In Hess, H.H., & Poldervaart, A. (eds), BASALTS 1, New York: Interscience, 103-162.

BUDDINGTON, A.F., 1959. Granite emplacement.
Bull. geol. Soc. Amer., 70, 671-748.

CAHILL, B.J., 1968. The use of amphiboles to illustrate trends in contact metamorphism.
IMA 5th Gen. Meet. Cambridge, 1966, 189-203.

CANN, J.R., 1969. Spilites from the Carlsberg Ridge, Indian Ocean.
J. Petrology, 10, 1-19.

CANN, J.R., 1970. Rb, Sr, Y, Zr and Nb in some ocean floor basaltic rocks.
Earth Planet. Sci. Letters, 10, 7-11.

CAWTHORN, R.G., & STRONG, D.F., 1974. The petrogenesis of komatiites and related rocks as evidence for a layered upper mantle.
Earth Planet. Sci. Letters, 23, 369-375.

CHAPPELL, B.W., & WHITE, A.J.R., 1974. Two contrasting granite types.
Pacific Geol., 8, 173-174.

CHERNYSHEVA, V.I., 1971. Greenstone-altered rocks of rift zones in median ridges of the Indian Ocean.
Int. Geol. Rev., 13, 903-913.

COMPTON, R.R., 1958. Significance of amphibole paragenesis in the Bidwell Bar region, California.
Am. Mineralogist, 43, 890-907.

CRAWFORD, A., 1975. Geology and geochemistry of the Howqua Greenstone Belt.
unpubl. (B.Sc.) honours thesis, Univ. Melbourne.

CROOK, K.A.W., 1974. Kratonization of West Pacific-Type Geosynclines.
J. Geol., 82, 24-36.

CROOK, K.A.W., & FELTON, ANNE E., 1975. Tasman Geosyncline greenstone and ophiolites.

J. Geol. Soc. Aust., 22(1), 117-131.

DAWSON, J.B., 1967. Geochemistry and origin of kimberlites.

In Wyllie, P.J. (ed), ULTRAMAFIC AND RELATED ROCKS, New York: John Wiley, 269-278.

ENGEL, A.E.J., & ENGEL, C.G., 1961. Migration of elements during metamorphism in the northwest Adirondack Mountains, New York.

U.S. Geol. Surv. Professional Pap., 400(B), 465-470.

ENGEL, A.E.J., ENGEL, C.G., and HAVENS, R.G., 1964. Mineralogy of amphibolite interlayers in the gneiss complex, northwest Adirondack Mountains, New York.

J. Geol., 72(2), 131-156.

ENGLAND, R.N., 1972. Progressive metamorphism of amphibolites from the Cloncurry and Petermann Ranges areas.

unpubl. M.Sc. thesis, A.N.U.

ERNST, W.G., 1968. AMPHIBOLES, New York: Springer Verlag.

EVANS, B.W., & MOORE, J.G., 1968. Mineralogy as a function of depth in the prehistoric Makoopuhi tholeiitic lava lake, Hawaii.

Contr. Mineral. Petrol., 17, 85-115.

FLOWER, M.F.J., 1973. Trace element distribution in lavas from Anjouan and Grande Comore, western Indian Ocean.

Chem. Geol., 12, 81-98.

FAURE, G., & HURLEY, P.M., 1963. The isotopic compositions of strontium in oceanic and continental basalts: application to the origin of

igneous rocks.

J. Petrology, 4, 31-50.

GIBB, F.G., 1973. The zoned clinopyroxenes of the Shiant Isles sill, Scotland.

J. Petrology, 14, 203-230.

GOLDSCHMIDT, V.M., 1954. GEOCHEMISTRY, Oxford: Clarendon Press.

GOLES, G.G., 1967. Trace elements in ultramafic rocks.

In Wyllie, P.J., (ed), ULTRAMAFIC AND RELATED ROCKS, New York: John Wiley, 352-362.

GREEN, A.H., 1972. Geology of Mount Camel Range.

unpubl. B.Sc. (hons) Thesis, Univ. Melbourne.

GREEN, D.H., 1964. The metamorphic aureole of the peridotite at the Lizard, Cornwall.

J. Geol., 72, 543-563.

GREEN, D.H., 1975. Genesis of Archaean peridotitic magmas and constraints on Archaean geothermal gradients and tectonics.

Geology, 3, 15-18.

GREEN, D.H., NICHOLLS, I.A., VILJOEN, M.J., and VILJOEN, R.P., 1975. Demonstration of the existence of peridotitic liquids in earliest Archaean magmatism.

Geology, 3, 11-14.

GREENLAND, L. & LOVERING, J.F., 1966. Fractionation of fluorine, chlorine, and other trace elements during differentiation of a tholeiitic magma.

Geochim. Cosmoch. Acta, 30, 963-982.

GREGORY, J.W., 1903. The Heathcotian - a pre-Ordovician series - and its distribution in Victoria.

Proc. R. Soc. Vict., 15, 148-175.

GULACAR, O.F., & DELALOYE, M., 1976. Geochemistry of nickel, cobalt and copper in alpine-type ultramafic rocks.

Chem. Geol., 17(4), 269-280.

GUNN, B.M., 1966. Modal and element variation in Antarctic tholeiites.

Geochim. Cosmoch. Acta, 30, 881-920.

HALLBERG, J.A., 1972. Geochemistry of Archaean volcanic belts in the Eastern Goldfields region of Western Australia.

J. Petrology, 13, 45-56.

HALLBERG, J.A., & WILLIAMS, 1972. Archaean mafic and ultramafic rock associations in the eastern Goldfields region, Western Australia.

Earth Planet. Sci. Letters, 15, 191-200.

HAMILTON, D.L., & ANDERSON, G.M., 1967. Effects of water and oxygen pressures on the crystallization of basaltic magmas.

In Hess, H.H., & Poldervaart, A. (eds), BASALTS 1, New York: Interscience, 445-482.

HAMLYN, P.R., 1971. Geology of the Colbinabbin Range Greenstone Axis.

unpubl. B.Sc. (hons) Thesis, Univ. Melbourne.

HART, R.A., 1970. Chemical exchange between sea water and deep-ocean basalts.

Earth Planet. Sci. Letters, 9, 269-279.

HASHIMOTO, M., 1972. Relict clinopyroxene of Palaeozoic greenstones of the Tamba and Mikabu terranes, southwest Japan.

J. Jap. Ass. Miner. Petrol. econ. Geol., 67, 323-331.

HEIMLICH, R.A., & UTHE, R.E., 1976. Mineralogic variations across a thick amphibolite, Bighorn Mountains, Wyoming, U.S.A.
Lithos, 9, 55-63.

HESS, H.H., 1955. Serpentinites, orogeny and epeirogeny.
Geol. Soc. Am. Spec. Paper, 62, 391-407.

HESS, H.H., 1960. Stillwater igneous complex, Montana, a quantitative mineralogical study.
Geol. Soc. Am. Mem., 80, 1-230.

HIETANEN, A., 1962. Metasomatic metamorphism in Western Clearwater County, Idaho.
U.S. Geol. Surv. Prof. Paper, 334-A.

HIETANEN, A., 1974. Amphibole pairs, epidote minerals, chlorite and plagioclase in metamorphic rocks, Northern Sierra Nevada, California.
Am. Mineralogist, 59, 22-40.

IRVINE, T.N., 1967. The Duke Island ultramafic complex, southeastern Alaska.
In Wyllie, P.J., (ed), ULTRAMAFIC AND RELATED ROCKS, New York: John Wiley, 84-96.

JAEGER, J.C., 1957. The temperature in the neighbourhood of a cooling intrusive sheet.
Am. J. Sci., 255, 306-318.

JAEGER, J.C., 1959. Temperatures outside a cooling intrusive sheet.
Am. J. Sci., 257, 44-54.

JOLLY, W.T., & SMITH, R.E., 1972. Degradation and metamorphic differentiation of the Keweenawan tholeiitic lavas of northern Michigan, U.S.A.
J. Petrology, 13(2), 273-309.

JOYCE, A.S., 1970. Chemical variation in a pelitic hornfels.
Chem. Geol., 6, 51-58.

KLEIN, C.Jr., 1969. Two amphibole assemblages in the system actinolite-hornblende-glaucophane.
Am. J. Sci., 265, 211-217.

KONDA, T., 1970. Pyroxenes from the Beaver Bay gabbro complex of Minnesota.
Contrib. Mineral. Petrol., 29, 338-344.

KONDA, T., & GREEN, J.C., 1974. Clinopyroxenes from the Keweenawan Lavas of Minnesota.
Amer. Mineralogist, 59, 1190-1197.

KUSHIRO, I., 1960. Si-Al relation in clinopyroxenes from igneous rocks.
Am. J. Sci., 258, 548-554.

LEAKE, B.E., 1965. The relationship between tetrahedral Al and the maximum possible octahedral aluminium in natural calciferous and sub-calciferous amphiboles.
Am. Mineralogist, 50, 843-851.

LEAKE, B.E., 1968. A catalogue of analysed calciferous and subcalciferous amphiboles together with their nomenclature and associated minerals.
Geol. Soc. Am. Spec. Paper, 98. 1-210.

LEAKE, B.E., 1971. On aluminous and edenitic hornblendes.
Min. Mag., 38, 389-407.

LE BAS, 1962. The role of aluminium in igneous clinopyroxenes with relation to their parentage.
Am. J. Sci., 260, 267-288.

LINDSLEY, D.H., & MUNOZ, J.L., 1969. Subsolidus relations along the join hedenbergite-ferrosilite.

Am. J. Sci., 267-A, 295-324.

LIOU, J.G., KUNIYOSHI, S., and ITO, K., 1974. Experimental studies of the phase relations between greenschist and amphibolite in the basaltic system.

Am. J. Sci., 274, 613-632.

LOOMIS, A.A., 1966. Contact metamorphic reactions and processes in the Mount Tallac roof remnant, Sierra Nevada, California.

J. Petrology, 7, 221-245.

McBRYDE, I., & WATCHMAN, A., 1976. The distribution of greenstone axes in southeastern Australia: a preliminary report.

Mankind, 10(3), 163-174.

McDOUGALL, I., 1962. Differentiation of the Tasmanian Dolerites: Red Hill Dolerite-Granophyre Association.

Bull. geol. Soc. Am., 73, 279-316.

McDOUGALL, I., & LOVERING, J.F., 1963. Fractionation of chromium, nickel, cobalt and copper in a differentiated dolerite-granophyre sequence at Red Hill, Tasmania.

J. Geol. Soc. Aust., 10, 325-338.

McINTIRE, W.L., 1963. Trace element partition coefficients - a review of theory and applications to geology.

Geochim. Cosmoch. Acta, 27, 1209-1264.

McIVER, J.R., & LENTHALL, D.H., 1973. Mafic and ultramafic extrusives of the Onverwacht Group in terms of the system XO-YO-R_2O_3-ZO_2.

Econ. Geol. Research Unit, Univ. Witwatersrand No. 80.

McLAUGHLIN, R.J.W., & TATTAM, C.M., 1976. Plutonic rocks.
In Douglas, J.G., & Ferguson, J.A., (eds), GEOLOGY OF VICTORIA. Geol. Soc. Aust. Spec. Publ. No. 5.

MELSON, C.W., & VAN ANDEL, T.H., 1966. Metamorphism in the Mid-Atlantic ridge, 22°N Lat.
Mar. Geol., 4, 165-186.

NALDRETT, A.J., & MASON, G.D., 1968. Contrasting Archaean ultramafic igneous bodies in Dundonald and Clergue Township, Ontario.
Can. J. Earth Sci., 5, 111-143.

NESBITT, R.W., 1971. Skeletal crystal forms in the ultramafic rocks of the Yilgarn Block, Western Australia: evidence for an Archaean ultramafic liquid.
Geol. Soc. Aust. Spec. Publ., 3,

NESBITT, R.W., & SUN, S., 1976. Geochemistry of Archaean spinifex-textured peridotites and magnesian and low-magnesian tholeiites.
Earth Planet. Sci. Letters, 31, 433-453.

NICHOLLS, I.A., 1965. Studies on the mineralogy, petrology and chemistry of the greenstone of the Heathcote district.
unpubl. M.Sc. Thesis, Univ. Melbourne.

NOCKOLDS, S.R., 1954. Average chemical composition of some igneous rocks.
Bull. geol. Soc. Am., 65, 1007-32.

NORRISH, K., & CHAPPELL, B., 1967. X-ray fluorescence spectrography.
In Zussman, J., (ed), PHYSICAL METHODS IN DETERMINATIVE MINERALOGY, 161-214.

NORRISH, K., & HUTTON, J.T., 1969. An accurate x-ray spectrographic method for the analysis of a wide range of geological samples.

Geochim. Cosmoch. Acta, 33, 431-453.

OKI, Y., 1961. Metamorphism in the northern Kiso Range, Nagano Prefecture, Japan.

Japan. J. Geol. Geograph., 32, 479-496.

OSBORNE, E.F., & ROEDER, P.L., 1960. Effect of oxygen pressure on crystallization in simplified basalt systems.

21st. Int. Geol. Congr., Copenhagen, Rept. XIII, 147-155.

OVERSBY, B., 1971. Palaeozoic plate tectonics in the southern Tasman geosyncline.

Nature, Phys. Sci., 234, 45-47.

PACKHAM, G.H., & LEITCH, E.S., 1974. The role of plate tectonic theory in the interpretation of the Tasman Orogenic Zone.

In Denmead, A.K., Tweedale, G.W., and Wilson, A.F. (eds), THE TASMAN GEOSYNCLINE.

PAPIKE, J.J., ROSS, M., and CLARK, J.R., 1969. Crystal-chemical characterization of clino-amphiboles based on five new structure refinements.

Mineral. Soc. Am. Spec. Paper, 2, 117-136.

PEARCE, J.A., 1974. Basalt geochemistry used to investigate past tectonic environments on Cyprus.

Tectonophysics, 25, 41-67.

PEARCE, J.A., & CANN, J.R., 1973. Tectonic setting of basic volcanic rocks determined using trace element analyses.

Earth Planet. Sci. Letters, 19, 290-300.

PHILPOTTS, J.A., SCHNETZLER, C.C., and HART, S.R., 1969. Submarine basalts: some K, Rb, Sr, Ba, rare-earth, H_2O, and CO_2 data bearing on their alteration, modification by plagioclase, and possible source materials.

Earth Planet. Sci. Letters, 7, 293-299.

PITCHER, W.S., & SINHA, R.C., 1958. The petrochemistry of the Ardara aureole.

Quart. J. Geol. Soc. London, 113, 393-408.

PYKE, D.R., NALDRETT, A.J., and ECKSTRAND, O.R., 1973. Archaean ultramafic flows in Munro Township, Ontario.

Bull. geol. Soc. Am., 84(3), 955-978.

READ, H.H., 1949. A contemplation of time in plutonism.

Quart. J. Geol. Soc. London, 105, 101-156.

REED, S.J.B., 1972. Dead time corrections for x-ray intensity measurements with a Si (Li) detector.

J. Phys. E. Sci. Instr., S, 994-996.

REED, S.J.B., & WARE, N.G., 1973. Quantitative electron microprobe analysis using a Lithium drifted detector.

X-ray Spectrometry, 2, 69-74.

RINGWOOD, A.E., 1955. The principles governing trace element distribution during magmatic crystallization: Part I. The influence of electro-negativity. Part II. The rule of Complex Formation.

Geochim. Cosmoch. Acta, 7, 189-202; 242-254.

RIVALENTI, G., 1974. Chemistry and differentiation of mafic dikes in an area near Tiskenasset, West Greenland.

Can. J. Earth Sci., 12, 721-730.

ROBIE, A.A., BETHKE, P.M., TOULMIN, M.S., and EDWARDS, J.L., 1966. X-ray crystallographic data, densities and molar volumes of minerals.
In Clark, S.P., (ed), HANDBOOK OF PHYSICAL CONSTANTS.
Geol. Soc. Am. Mem., 97, 27-73.

RUCKMICK, J.C., & NOBLE, J.A., 1959. Origin of the ultramafic complex at Union Bay, southeastern Alaska.
Bull. geol. Soc. Am., 70, 981-1018.

RUTLAND, R.W.R., 1976. Orogenic evolution of Australia.
Earth Sci. Rev., 12, 161-196.

SEN, S.K., 1970. Magnesium-iron compositional variance in hornblende pyroxene granulites.
Contr. Miner. Petrol., 29, 76-88.

SHAW, D.M., 1954. Trace elements in pelitic rocks, 1. Variations during metamorphism.
Bull. geol. Soc. Am., 65, 1151-1166.

SHAW, D.M., 1956. Geochemistry of pelitic rocks, 3. Major elements and general geochemistry.
Bull. geol. Soc. Am., 67, 919-934.

SHIDO, F., 1958. Plutonic and metamorphic rocks of the Makoso and Iritoro districts in the central Abukuma plateau.
J. Fac. Sci. Tokyo Univ., 2(11), 132-217.

SHIDO, F., & MIYASHIRO, A., 1959. Hornblendes of basic metamorphic rocks.
J. Fac. Sci. Tokyo Univ., 2, 12-1, 85-102.

SINGLETON, O.P., 1949. The geology and petrology of the Tooboorac area.
Proc. R. Soc. Vict., 61, 75-104.

SKEATS, E.W., 1908. On the evidence of the origin, age and alteration of the rocks near Heathcote, Victoria.

Proc. R. Soc. Vict., 21, 302-348.

SMITH, R.E., 1968. Redistribution of major elements in the alteration of some basic lavas during burial metamorphism.

J. Petrology, 9(2), 191-219.

SMITH, A.L., & CARMICHAEL, I.S.E., 1969. Quaternary trachybasalts from south-eastern California.

Am. Mineralogist, 54, 909-923.

SMITH, D., 1970. Mineralogy and petrology of the diabasic rocks in a differentiated olivine diabase sill complex, Sierra Ancha, Arizona.

Contr. Miner. Petrol., 28, 95-113.

SMITH, D., & LINDSLEY, D.H., 1971. Stable and metastable augite crystallization trends in a single basalt flow.

Am. Mineralogist, 56, 225-233.

SOLOMON, M., & GRIFFITHS, J.R., 1974. Aspects of the early history of the southern Tasman Orogenic Zone.

In Denmead, A.K., Tweedale, G.W., and Wilson, A.F., (eds), THE TASMAN GEOSYNCLINE - A SYMPOSIUM.

Geol. Soc. Aust. Qld. Div.

STEWART, A.J., 1966. The petrography, structure, and mode of emplacement of the Cobaw Granite, Victoria.

Proc. R. Soc. Vict., 79(2), 275-317.

STEWART, A.J., 1971. Potassium-argan dates from the Cobaw Granite, central Victoria.

Proc. R. Soc. Vict., 84(2), 213-215.

STINDL, H., 1971. Electron microprobe study of diabase-granite contact zones in composite dykes, Mount Desert Island, Maine.
unpubl. Ph.D. Thesis, Univ. Illinois.

STOUT, J.H., 1972. Phase petrology and mineral chemistry of coexisting amphiboles from Telemark, Norway.
J. Petrology, 13, 99-145.

STUEBER, A.M., & MURTHY, V.R., 1966. Strontium isotope and alkali element abundances in ultramafic rocks.
Geochim. Cosmoch. Acta, 30, 1243-1259.

THAYER, T.P., 1967. Chemical and structural relations of ultramafic and feldspathic rocks in Alpine intrusive complexes.
In Wyllie, P.J., (ed), ULTRAMAFIC AND RELATED ROCKS, New York: John Wiley, 222-239.

THOMAS, D.E., 1939. The structure of Victoria with respect to the Lower Palaeozoic rocks.
Min. Geol. J. Vict., 1, 59-64.

THOMAS, D.E., 1959. The geological structure of Victoria.
J. Proc. Roy. Soc. N.S.W., 92, 182-190.

THOMAS, D.E., 1960. Lancefield 1:63360 geological map.
Mines Dep. Vict.

THOMAS, D.E., & SINGLETON, O.P., 1956. The Cambrian stratigraphy of Victoria.
Int. Geol. Congr., 20(2), 149-163.

THOMAS, D.E., SPENCER-JONES, D., and TATTAM, C.M., 1976. Cambrian.
In Douglas, J.G., & Ferguson, J.A., (eds), GEOLOGY OF VICTORIA.
Geol. Soc. Aust. Spec. Publ. No. 5.

THOMPSON, G., 1973. Trace element distributions in fractionated oceanic rocks, 2. Gabbros and related rocks.
Chem. Geol., 12, 99-111.

TURNER, F.J., & VERHOOGEN, J., 1960. IGNEOUS AND METAMORPHIC PETROLOGY.
New York: McGraw-Hill.

VALLANCE, T.G., 1973. Pyroxenes and the basalt-spilite reaction.
In Amstutz, (ed), SPILITES AND SPILITIC ROCKS, Heidelberg: Springer Verlag.

VALLANCE, T.G., 1974. Spilitic degradation of a tholeiitic basalt.
J. Petrology, 15(1), 79-96.

VERBEEK, A.A., & SCHREINER, G.D.L., 1967. Variations in $^{39}K:^{41}K$ ratio and movement of potassium in a granite-amphibolite contact region.
Geochim. Cosmoch. Acta, 31, 2125-2133.

VERHOOGEN, J., 1962. Distribution of titanium between silicates and oxides in igneous rocks.
Am. J. Sci., 260, 211-220.

VILJOEN, M.J., & VILJOEN, R.P., 1969a. The geology and geochemistry of the Lower Ultramafic unit of the Onverwacht Group and a proposed new class of igneous rocks.
Spec. Publ. Geol. Soc. S. Afr., 2, 55-85.

VILJOEN, M.J., & VILJOEN, R.P., 1969b. Evidence for the existence of a mobile extrusive peridotitic magma from the Komati Formation of the Onverwacht Group.
Spec. Publ. Geol. Soc. S. Afr., 2, 87-112.

VILLAUME, J.F., & ROSE, A.W., 1976. The geochemistry of some Archaean ultramafic lavas.

Chem. Geol., 19, 43-60.

VOGT, J.H.L., 1923. The physical chemistry of the crystallization and magmatic differentiation of igneous rocks: Part VIII.

J. Geology, 31, 407-419.

WAGER, L.R., & MITCHELL, R.L., 1951. The distribution of trace elements during strong fractionation of basic magma - a further study of the Skaergaard intrusion, East Greenland.

Geochim. Cosmoch. Acta, 1, 129-208.

WAGER, L.R., 1960. The relationship between the fractionation stage of basalt magma and the temperature of the beginning of its crystallization.

WAGER, L.R., & BROWN, G.M., 1967. LAYERED IGNEOUS ROCKS,

San Francisco: Freeman.

WALKER, K.R., 1969. A mineralogical, petrological and geochemical investigation of the Palisades Sill, New Jersey.

Geol. Soc. Am. Mem., 115, 175-187.

WATCHMAN, A.L., & FREEMAN, R.S., 1977. Discrimination between sources of Aboriginal greenstone axes in southeastern Australia by trace element analysis.

(in preparation).

WILLIAMS, G.E., 1964. The geology of the Kinglake District, central Victoria.

Proc. R. Soc. Vict., 77, 273-327.

WILLIAMS, D.A.C., & HALLBERG, J.A., 1973. Archaean layered intrusions of the Eastern Goldfields region, Western Australia.
Contr. Miner. Petrol., 38, 45-70.

WILLIAMS, H., TURNER, F.J., and GILBERT, C.M., 1954. PETROGRAPHY: AN INTRODUCTION TO THE STUDY OF ROCKS IN THIN SECTIONS,
San Francisco: Freeman.

WILSON, H.D.B., ANDREW, P., MOXHAM, R.L., and RAMLAL, K., 1965. Archaean volcanism in the Canadian Shield.
Can. J. Earth Sci., 2, 161-175.

WINKLER, H.G.F., 1965. PETROGENESIS OF METAMORPHIC ROCKS,
New York: Springer Verlag.

WYLLIE, P.J., 1967. ULTRAMAFIC AND RELATED ROCKS,
New York: John Wiley.

APPENDIX

1. PETROGRAPHY.

2. PETROCHEMISTRY.

APPENDIX 1 - PETROGRAPHY

Petrological features of greenstones not only indicate metamorphic processes and changes, but also from these features, initial rock types can be inferred.

At Mount William, field relations, hand specimen examination, and petrographic studies, allow subdivision of the Heathcote Greenstone into Upper and Lower units(Fig.5). The Lower unit, 500m thick, is composed of ?metavolcanics and chert and the Upper unit is metadolerite almost 1000m thick.

The stratigraphy of the Heathcote Greenstone at Mount Camel is similar to that at Mount William, however the structure is complicated because of folding, faulting, discontinuous outcrop patterns and a lack of contacts. Metavolcanics, ash beds, tuff, agglomerate and dolerite form the greenstone belt in this area(Fig.4,6).

Lower Unit - Mount William (Zone 1)

The basal part of the unit is characterised by spheroids filled by quartz, albite and carbonate(Plate 4.1). Long thin actinolite needles penetrate into these areas and short blades of amphibole form a rim around the margins. The rocks are composed of interlocking amphibole needles forming a decussate structure (Plate 4.2). Minor magnetite forms dust-like patches and small euhedral grains.

Amphibole needles are pale green to colourless and fall in the compositional range actinolite-cummingtonite (Appendix 2). Elongate cummingtonite is associated with small needles and prisms of actinolite within and adjacent to spheroids (Plate 5). Pseudomorphs and relict textural features are rare and give little evidence as to the nature of the original rocks.

PLATE 4

4.1 Photomicrograph of metavolcanic from the Lower Unit, Mount William (sample A13). Fibrous amphibole penetrates into the quartz filled ovoid area. The main mass of the rock is composed of amphibole needles and blades. 25x, x-nicols.

4.2 Randomly oriented needles and blades together with massive amphibole sheaves. Iron oxide grains are also common. (Sample A16, 25x magnification and x-nicols.)

There is a massive fine-grained amphibolite in the central parts of the unit. The texture is compact and decussate; it is the interlocking bundles of amphibole needles that give the rock its extreme toughness. Actinolite and cummingtonite are present with minor amounts of iron oxide and quartz. Extensive recrystallisation destroyed primary textures and minerals, making parent rock interpretations difficult.

The upper parts of the unit are characterised by irregular patches of altered fine-grained greenstone consisting of chlorite, actinolite and iron oxides. Actinolite needles are short and stubby, less acicular than those found in the central parts of the unit.

Field relations and variations in texture suggest that the Lower unit is composite, consisting of several small lenses and layers.

A thin lens of recrystallised and albitised chert marks the uppermost limit of the unit. It consists of cryptocrystalline feldspar and quartz, randomly oriented rosettes of ?tremolite and abundant granular iron oxides.

Upper Unit - Mount William (Zone 2)

The Upper unit is metadolerite because some original mineralogical and textural features are preserved, allowing subdivision into basal, layered, central, micropegmatite, upper and roof-marginal zones.

Basal Zone

The base of the dolerite sill has not been found because of soil and scree cover. Specimens A9-A11 and B30-B37 are located near the bottom of the intrusion. The primary mineral assemblage is augite, plagioclase, olivine, magnetite and sulphides.

Altered olivine is subordinate to plagioclase and clinopyroxene in the lower parts. Relict olivine is bound by rims of serpentine and pale coloured amphibole. Olivine is replaced by serpentine which forms clusters

PLATE 5

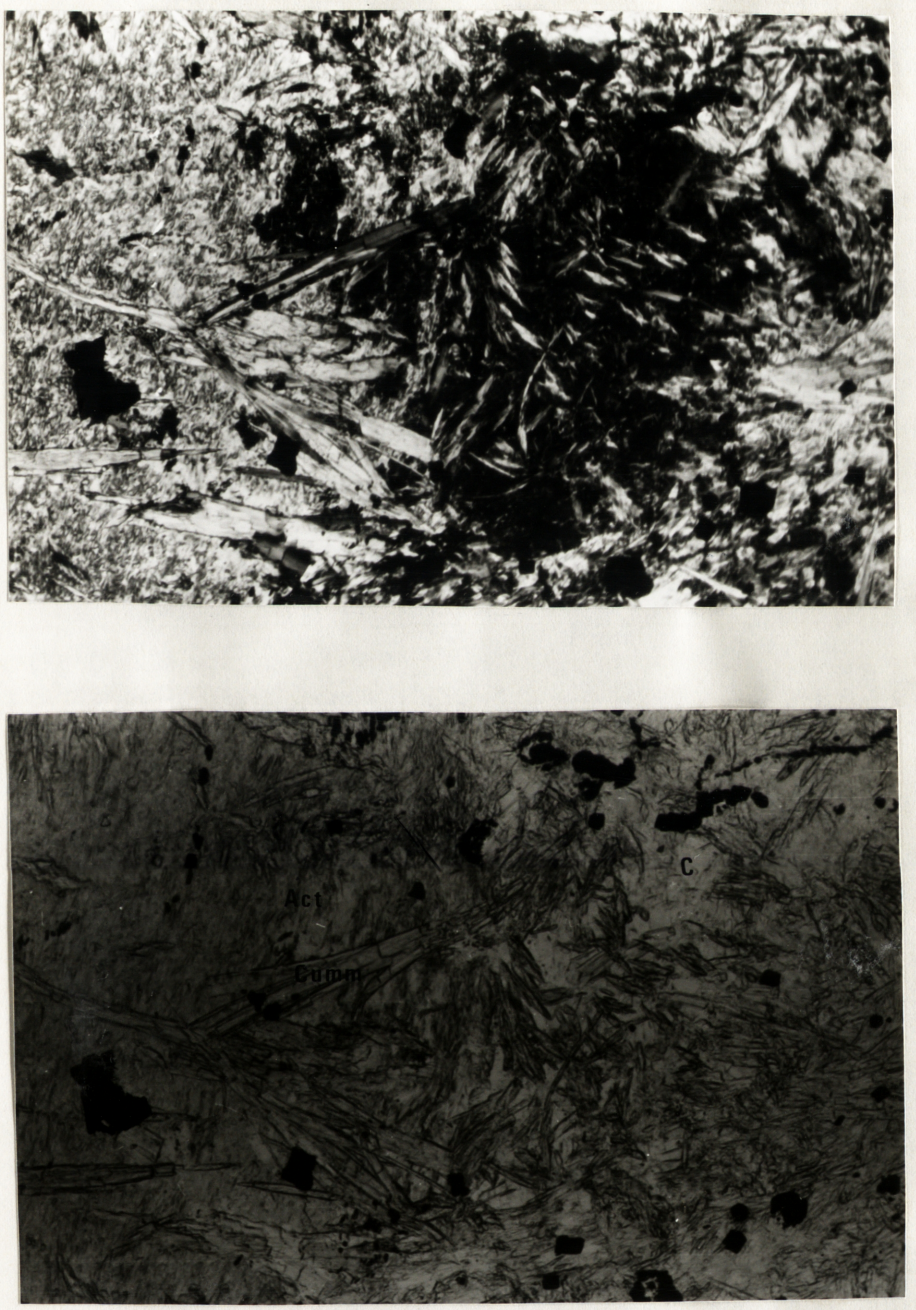

5.1, 2. Cummingtonite (Cumm) developed in association with actinolite (Act) and carbonate (C). Minor euhedral iron oxide grains. Sample A16, x-nicols (above), plane polarised light (below), 100x.

of grey ragged blades, commonly associated with granular iron oxides. There is no evidence that orthopyroxene was a primary mineral in these rocks.

Plagioclase is common, usually recrystallised and occurring mainly as groundmass to mafic minerals. In some places relict sub-ophitic texture is discernible. Recrystallisation of plagioclase presumably during contact metamorphism, resulted in mosaics of small anhedral grains intergrown with thin stubby amphibole needles and dusty opaques. The composition of feldspar is An_{97-98}. The high anorthite component of this feldspar suggests that it is not primary, its calcium content increasing during metamorphism.

Augite($Ca_{34}Mg_{56}Fe_{10}$) is the most abundant mineral in the basal rocks. It occurs as microphenocrysts up to 2mm in diameter and commonly shows simple twinning. Few grains are euhedral and most are rimmed by amphibole. The pleochroic colour of pyroxene ranges from pale green-brown to pink. Relict sub-ophitic texture is preserved and reaction coronas between plagioclase and augite contain actinolitic hornblende. Rare exsolution textures of augite and pigeonite are usually replaced by amphibole. Before replacement, pigeonite formed broad lamellae parallel with the (001) plane in augite. Microprobe analyses confirm that the parallel growths are replaced by amphibole (B15, Appendix 2).

The main metamorphic effects are recrystallisation of plagioclase, reaction between clinopyroxene and feldspar at grain boundaries to form amphiboles, and uralitisation of clinopyroxene. Composite grains of augite and pigeonite are almost completely replaced whereas only rims of individual augite are altered. Small thin amphibole needles penetrate recrystallised plagioclase and the texture of the rocks is essentially blastophitic.

Magnetite occurs in several different forms depending upon whether it is of primary or secondary origin. Relict primary magnetite is

PLATE 6

6.1 Weathered surface showing layering in metadolerite at Mount William.

6.2 Relict igneous layering within metadolerite at Mount William.

developed as small euhedral tabular and skeletal grains. Dust-like clusters and segregations of secondary magnetite are more common, having formed from reaction between olivine, clinopyroxene and plagioclase. Any excess iron which could not be accepted into the newly formed amphibole structure separated as dust-like inclusions and segregations.

Pyrrhotite, chalcopyrite and pentlandite are common sulphide minerals developed interstitially to the silicates. Flame-like exsolutions of pentlandite out of pyrrhotite suggest that basal parts of the sill are enriched in nickel.

Layered Zone

This part of the sill is characterised by relict igneous layering. Two types of layers are observed, both relatively simple though poorly defined.

Graded layering is common when progressively less clinopyroxene occurs upwards through each layer. The other type is produced by alternating bands, successively enriched and depleted in clinopyroxene (Plate 6.2). The thickness of each layer ranges from 1cm to 4cm and is generally thicker in the upper parts of the zone. The layers are most evident on weathered surfaces (Plate 6.1) and more difficult to see in thin sections (A6-A9, B15-B30).

The original mineralogy of the Layered Zone comprises augite, plagioclase and titanomagnetite. Metamorphic minerals are hornblende and epidote with minor sphene. Augite ($Ca_{41}Mg_{46}Fe_{13}$ to $Ca_{47}Mg_{40}Fe_{13}$) forms subhedral microphenocrysts up to 2mm in diameter. Relict exsolution lamellae of pigeonite and augite are uncommon.

Hornblende forms blades and prisms within augite, margins around augite grain boundaries and along cooling cracks (Plates 8, 9, 10). It is pale green-brown and commonly contains platelets of iron oxide and small blebs of chalcopyrite.

Euhedral plagioclase laths (An_{67-72}) are subophitic to clinopyroxene. Most feldspar is relatively fresh and not recrystallised, although in some places, affected by deformation and recrystallisation, granular epidote is found.

A characteristic alteration feature of original opaque minerals is poikiloblastic texture. Preferential loss of titanium from primary ilmenite resulted in skeletal poikiloblasts of colourless sphene intimately intergrown with relict ilmenite. Titanium and iron were accepted into the hornblende structure from ilmenite until TiO_2 reached excessive amounts, when small platelets of sphene exsolved along crystallographically preferred directions in the amphibole.

Pyrrhotite and chalcopyrite occur as anhedral and interstitial grains as well as small blebs within silicates. Pentlandite is infrequent and pyrrhotite rimmed by pyrite is common in the upper parts of the Layered Zone.

Central Zone

The nature of the dolerite in this section of the sill is obscured by strong recrystallisation. Parts of the central zone are covered by soil and scree so that the only samples studied are those adjacent to the Cobaw Granite (B1-B14).

Original igneous layering is not observed and the texture of the rocks is granoblastic. Few primary minerals remain, augite ($Ca_{47}Mg_{36}Fe_{17}$ to $Ca_{49}Mg_{25}Fe_{26}$) occurs as small cores bounded by wide rims, blades and prisms of brown hornblende.

Bladed amphibole grains contain rods and platelets of sphene and chalcopyrite. Idioblastic hornblende grains showing prismatic cleavage are devoid of impurities.

Plagioclase (An_{49-57}) is strongly recrystallised, euhedral twinned laths are rare, and triple-point grain boundaries are common features of

PLATE 7

7.1 Micropegmatoid in metadolerite at Mount William.

7.2 Ophitic texture of dolerite retained by rocks in the Upper Unit, Mount William. (25x, plane polarised light).

the granular groundmass. Leucocratic areas are clear and free from inclusions, and small stubby hornblende rods occur along grain boundaries, rarely penetrating into feldspar.

Sphene is widely developed, interstitially to silicates and around iron oxide cores. Recrystallised chalcopyrite occurs as grains up to 1mm in diameter as well as rounded blebs in hornblende and along grain boundaries. Most pyrrhotite grains are bound by thin mantles of pyrite, implying an increase in partial pressure (or activity) of sulphur during fractionation (or metamorphism).

Micropegmatite Zone

A medium to coarse-grained micropegmatite, at least 50m thick, crops out stratigraphically above the central portion of the metadolerite. Contacts between micropegmatite and rocks above and below are covered by rubble and soil of a large slump structure.

The micropegmatite (A5), is composed of plagioclase, hornblende and magnetite (Plate 7.1). Plagioclase (An_{23-27}) forms long broad laths up to 4mm in length and are not compositionally zoned. Abundant rods of ?sodic-amphibole penetrate into the feldspar.

Bluish green hornblende blades up to 4mm in length are curved and bent around plagioclase. The grains of amphibole are composed of many small individual blades and show amphibole twins on (100).

Large skeletal magnetite grains, up to 2.5mm long, are developed in mafic-rich areas adjacent to small fields of chlorite.

Upper Zone

This zone is 100m thick and lies stratigraphically above the micropegmatite. The dolerite has an ophitic texture and contains the mineral assemblage pyroxene, plagioclase and iron oxide (A4-A3). In the lower parts near the micropegmatite, plates of clinopyroxene, up to 3.5mm

in diameter, are common whereas toward the roof of the sill they reach 1mm in length.

Large plates of augite enclose long thin plagioclase crystals (Plate 7.2). Primary augite has been largely replaced by uralite and a green amphibole is developed between plagioclase and pyroxene. The composition of original pyroxenes in this zone cannot be determined because of the extensive alteration.

Long slender plagioclase laths have compositions of An_{25-27}. Recrystallisation of feldspar is limited to small anhedral groundmass crystals.

Skeletal magnetite is minor, forming large grains up to 3mm in diameter. Pyrite and chalcopyrite are minor.

Roof-marginal Zone

Contact relations at the top of the sill are not readily observed because of a lack of exposures. Samples were only collected from two small rubbly outcrops and these provide evidence of a chilled margin (A2 and A1).

The chilled margin is brecciated and composed of two distinct rock types, a very fine-grained almost glassy rock and a slightly more coarse-grained basalt. Both types are much finer grained than all other rocks in the sill.

Plagioclase (An_{25}) and iron oxide are primary minerals associated with small equant grains of ragged amphibole which pseudomorph pyroxene. Initial pyroxene composition is undetermined because it is completely replaced by amphibole.

Mount Camel

The rocks studied at Mount Camel come from a narrow band of greenstone, stratigraphically equivalent to the Lower unit at Mount William. The main rock type is amphibolite which consists of actinolite and

cummingtonite needles arranged in a decussate texture, small plates of diopside with ragged terminations, and amphibole pseudomorphs after ?pyroxene.

Lavas, metamorphosed to amphibolite, contain spheroids filled by quartz and strongly resemble similar features found in rocks at Mount William. Recrystallised ash and tuff beds show well developed tuffaceous texture. The rocks are strongly recrystallised and contain interlocking acicular amphiboles, minor quartz, albite, carbonate and iron oxides. Carbonate and epidote veins are abundant in some places, indicating mobility of calcium.

Cobaw Granite

The granitic phase of the Cobaw Granite (G2) lies in close proximity to the greenstones at Mount William. It is coarse-grained and consists of perthite, quartz, and biotite with minor plagioclase.

Large anhedral grains of perthite dominate the mineralogy. Small quartz grains are interspersed between feldspar and graphic intergrowths are absent. Long thin apatite needles and tabular zircons are found within quartz and feldspar. Small stubby blades and flakes of green-brown biotite contain short fine acicular rutile, small subrounded zircon and pleochroic haloes.

North of Mount William a narrow microgranodiorite dyke cuts across metadolerite and amphibolite. The microporphyritic acidic rock contains phenocrysts, up to 1mm in diameter, of andesine, orthoclase and quartz, with minor biotite. The granular groundmass is made up of anhedral quartz and feldspar. Andesine is commonly concentrically zoned whereas orthoclase is unzoned and untwinned. Quartz grains are anhedral, slightly resorbed, and contain needles and rods of fluor-apatite and biotite intergrowths. Flakes of red-brown biotite have ragged terminations and contain inclusions of iron oxide and small tabular zircon crystals.

Crosbie Granite

The Crosbie Granite in outcrop is a medium to coarse-grained leucocratic granite. It contains large orthoclase crystals up to 2cm in diameter graphically intergrown with quartz. Minor amounts of biotite form long thin blades.

Lack of fresh rock exposures are characteristic of this pluton.

PLATE 8

8.1 Clinopyroxene (Px) core bounded by blades of hornblende (H) surrounded by a groundmass of recrystallised plagioclase (Pl). Sample B1, 25x magnification x-nicols.

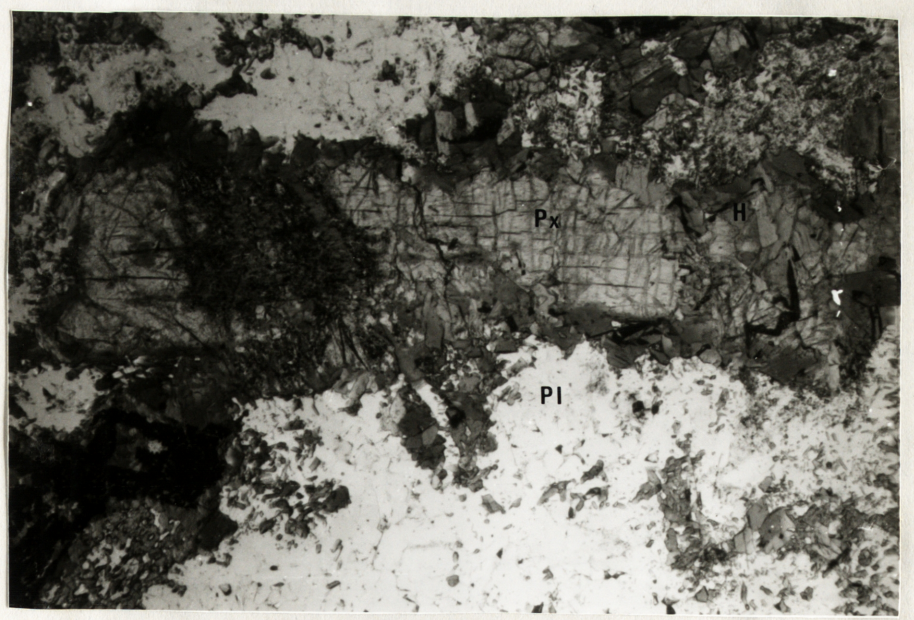

8.2 Same as above under plane polarised light.

PLATE 9

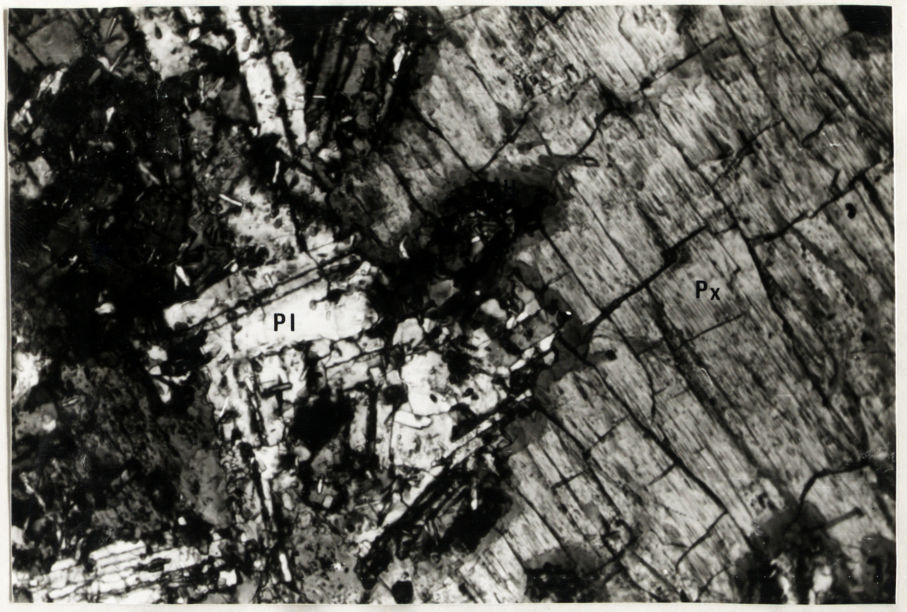

9.1 Photomicrograph showing the contact relations and reaction between plagioclase (Pl) and pyroxene (Px) with a rim of hornblende (H) developed. Plagioclase retains primary textural features and contains growths of amphibole rods. Sample B26, 100x, x-nicols.

9.2 Same as above using plane polarised light.

PLATE 10

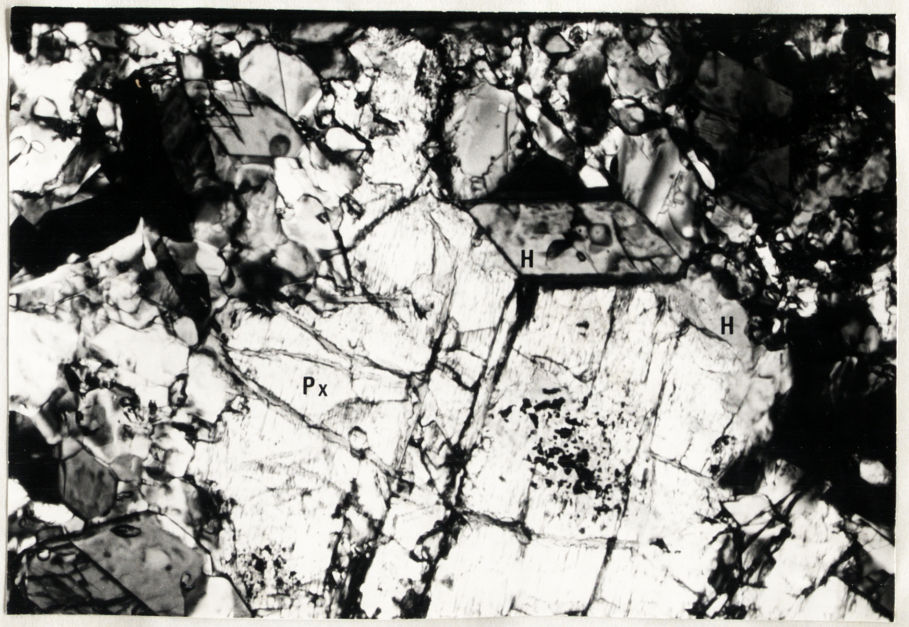

10.1 Characteristic metamorphic alteration features of clinopyroxene. Hornblende (H) is developed along cracks, around the margins and as prisms and blades by reaction between plagioclase (pl) and pyroxene (px). Sample B2, 100x, plane-polarised light.

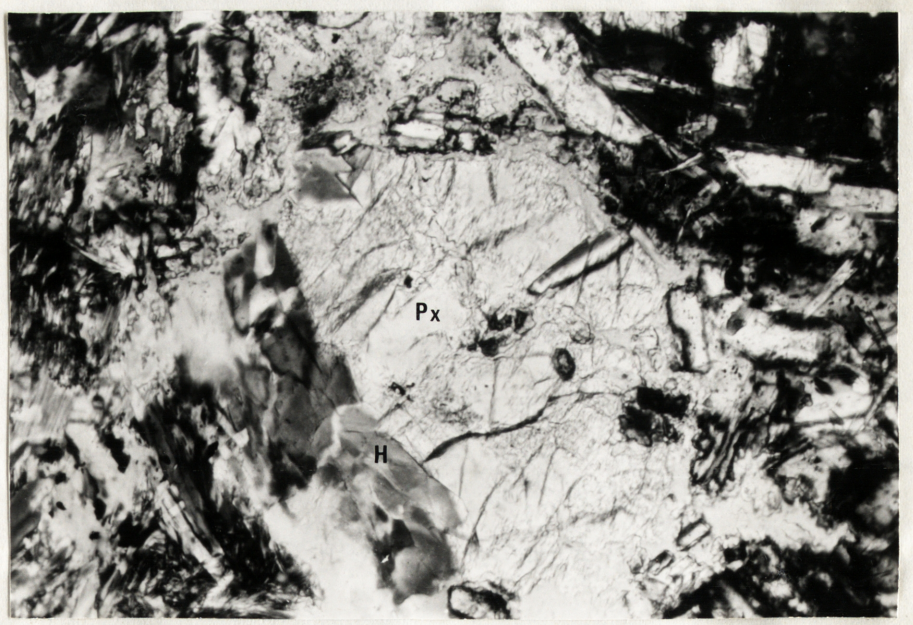

10.2 Rods and blades of hornblende (dark) in recrystallised plagioclase (light). Sample B18, 100x, plane-polarised light.

APPENDIX 2 - PETROCHEMISTRY

Analytical Methods

Major element analyses were obtained by using a combination of x-ray fluorescence (XRF) spectrometry and wet chemical methods (Norrish & Hutton, 1969). Sodium was determined by flame photometry and FeO by titration of an ingested sample solution using potassium dichromate. The amount of water lost at 200°C (H_2O-) was measured prior to heating the rock powder at 1000°C to determine H_2O+ and CO_2. Duplicate measurements were made for FeO and single determinations for water and carbon dioxide.

For XRF methods three fusion discs were prepared for each sample. Mixtures of lithium tetraborate (1.5 gms), sodium nitrate (0.02 gms) and sample powder (0.68 gms) were fused and when liquid pressed into glass discs.

Duplicate sodium analyses were obtained by ingesting rock powders in hydrofluoric and sulphuric acids and determining the amount of sodium in the resultant solution.

Trace element analyses were determined by XRF spectrometry (Norrish & Chappell, 1967) on pressed powder pellets. Rb, Sr, Y and Pb were measured with a molybdenum target x-ray tube using a scintillation counter, LiF_{200} analysing crystal and coarse collimator. Zr, Nb, Ni, Cu and Zn were determined under similar conditions but with a tungsten target x-ray tube.

Mass absorption coefficients were measured for each sample and corrections made for interelement effects, instrument drift and detector dead time. Duplicate analyses were recorded for each sample and then averaged.

Mineral analyses were made using the electron microprobe of the Research School of Earth Sciences, A.N.U., Canberra. An Ortec detector and main amplifier and a Northern Scientific NS710 multichannel analyser

were used. The operating conditions were a channel width of 20eV, accelerating current of 15kV, probe current of 3nA and a counting time of 100 seconds. Corrections were made for background, overlap, matrix and dead time according to Reed (1972) and Reed & Ware (1973).

Pyroxene, plagioclase and amphibole were analysed in samples B1, B7, B12, B15, B20, B27, B31, B36, A12, A14, A16 at Mount William and D and E at Mount Camel. Several spot analyses were recorded for each grain and at least three grains analysed in each polished thin section.

In the following tables a dash signifies that the content of the element is below the detection limit. For microprobe analyses total iron is given as FeO.

Reference Numbers

A.N.U. No.	Thesis No.	A.N.U. No.	Thesis No.
	Mount William	38300	B20
38265	A1	1	B21
6	A2	2	B22
7	A3	38303	B23
8	A4	4	B24
9	A5	5	B25
38270	A6	6	B26
1	A7	7	B27
2	A8	8	B28
3	A9	9	B29
4	A10	38310	B30
5	A11	1	B31
6	A12	2	B32
7	A13	3	B33
8	A14	4	B34
9	A15	5	B35
38280	A16	6	B36
1	B1	7	B37
2	B2		Mount Camel
3	B3	8	A
4	B4	9	B
5	B5	38320	C
6	B6	1	D
7	B7	2	E
8	B8	3	F
9	B9		
38290	B10		
1	B11		
2	B12		
3	B13		
4	B14		
5	B15		
6	B16		
7	B17		
8	B18		
9	B19		

BULK CHEMICAL ANALYSES

Mount William

A1-A11 - Upper unit

A12-A16 - Lower unit

B1-B37 - Upper unit.

Wt%	A1	A2	A3	A4	A5	A6	A7	A8
SiO_2	48.76	47.03	45.61	49.66	47.73	47.57	47.30	47.30
TiO_2	1.93	1.23	1.73	1.30	.91	.57	.58	.58
Al_2O_3	13.20	14.19	14.83	14.59	14.73	17.13	10.94	9.44
Fe_2O_3	2.03	2.38	2.95	2.07	0.00	.32	2.29	2.59
FeO	14.37	10.40	10.86	9.77	10.73	7.23	7.38	7.20
MnO	.27	.94	.67	.51	.20	.16	.19	.19
MgO	6.38	8.81	7.23	5.99	8.52	8.39	13.38	14.07
CaO	7.18	9.59	10.81	9.20	12.69	14.88	14.63	15.06
Na_2O	2.96	3.25	3.06	4.11	4.59	1.74	.89	.83
K_2O	.11	.05	.12	.15	.27	.11	.09	.08
P_2O_5	.18	.13	.18	.16	.10	.07	.06	.06
S	.03	.02	.33	.08	.08	.06	.04	.08
H_2O+	1.40	1.42	1.47	1.31	1.24	1.15	1.76	1.66
H_2O-	.12	.05	.07	.06	.12	.08	.08	.06
CO_2	.09	.07	.07	.28	.05	.13	.18	.21
Sub Total	99.01	99.56	99.99	99.21	101.96	99.59	99.79	99.41
O = S	.02	.01	.16	.04	.04	.03	.02	.04
TOTAL	98.99	99.55	99.83	99.17	101.92	99.56	99.77	99.37
Parts per million								
Rb	6	0	3	3	10	2	1	2
Sr	226	47	66	106	54	149	124	74
Y	36	23	35	28	1	15	12	11
Pb	3	4	3	3	4	3	2	4
Zr	112	67	102	80	114	36	29	25
Nb	6	3	4	4	3	1	2	1
Ni	46	106	56	45	15	83	233	282
Cu	122	108	160	114	8	205	128	190
Zn	146	110	120	79	67	59	66	63
Norm								
or	.65	.30	.71	.89	1.60	.65	.53	.47
ab	25.05	27.10	22.97	34.78	11.01	14.72	7.53	7.02
an	22.41	23.98	26.37	20.92	18.79	38.61	25.59	21.80
di	10.07	18.65	21.46	19.59	35.83	28.27	37.33	41.97
hy (ne*)	30.22	.22*	1.59*	2.37	15.08*	.19	11.22	10.25
ol	1.93	21.65	16.62	13.05	16.12	13.96	10.92	10.80
mt	2.94	3.45	4.28	3.00	-	.46	3.32	3.76
il	3.67	2.34	3.29	2.47	1.73	1.08	1.10	1.10
ap	.43	.31	.43	.38	.24	.17	.14	.14
other	1.67	1.58	2.85	1.80	1.56	1.47	2.09	2.08
Molecular %								
or	1.35	.58	1.42	1.57	5.1	1.2	1.58	1.60
ab	52.07	52.75	45.89	61.46	35.1	27.27	22.38	23.97
an	46.58	46.67	52.69	36.97	59.8	71.53	76.04	74.43
di	23.85	46.02	54.1	55.95	53.45	66.64	62.77	66.6
hy (ne*)	71.58	.54*	4.0*	6.77	22.5*	.45	18.87	16.26
ol	4.57	53.43	41.9	37.27	24.05	32.91	18.36	17.14
Ca	25.6	30.4	35.5	35.3	36.9	43.9	34.9	34.7
Mg	37.5	46.0	39.0	37.8	40.7	40.8	52.5	53.4
Fe	36.8	23.6	25.5	26.9	22.4	15.3	12.6	11.9
$\frac{Mg}{Mg+Fe}$	.505	.661	.605	.584	.646	.728	.806	.818

Wt%	A9	A10	A11	A12	A13	A14	A15	A16
SiO_2	47.92	48.62	48.18	54.47	53.44	55.84	55.21	51.20
TiO_2	.58	.82	.76	.03	.04	.03	.03	.01
Al_2O_3	11.33	15.72	18.18	3.26	2.99	3.08	2.44	1.29
Fe_2O_3	1.04	2.81	0.00	5.20	7.40	3.04	2.65	6.13
FeO	7.71	6.31	8.14	7.25	6.28	8.73	10.29	4.85
MnO	.18	.18	.16	.18	.21	.17	.20	.24
MgO	13.04	8.07	7.13	22.85	19.20	23.75	22.20	24.12
CaO	14.89	14.01	13.39	3.92	7.63	2.29	4.04	5.80
Na_2O	1.06	1.73	2.34	.19	.27	.20	.17	.22
K_2O	.08	.12	.13	.07	.03	.02	.02	.01
P_2O_5	.08	.09	.10	.01	.02	.01	.01	.01
S	.04	.05	.03	-	.01	-	-	-
H_2O+	1.84	1.16	1.31	2.39	2.16	2.42	2.55	3.67
H_2O-	.11	.12	.11	.05	.05	.07	.01	.08
CO_2	.07	.14	.12	.05	.10	.04	.07	1.65
Sub Total	99.97	99.95	100.08	99.92	99.82	99.69	99.90	99.28
O = S	.02	.03	.01	-	-	-	-	-
TOTAL	99.95	99.92	100.07	99.92	99.82	99.69	99.90	99.28
Parts per million								
Rb	1	2	4	5	2	2	9	1
Sr	83	162	122	348	304	52	448	72
Y	11	12	19	7	7	6	5	6
Pb	1	1	3	5	3	5	5	5
Zr	24	29	47	29	30	14	33	18
Nb	1	1	2	-	1	-	-	1
Ni	258	147	138	522	409	272	277	398
Cu	149	163	95	2	3	45	2	4
Zn	66	60	91	114	82	93	86	82
Norm								
or	.47	.71	.77	.41	.18	.12	.12	.06
ab	8.97	14.64	19.80	1.61	2.28	1.69	1.44	1.86
an	25.92	34.77	38.72	7.84	6.86	7.45	5.84	2.50
di	38.14	27.49	22.21	9.13	24.32	3.06	11.31	20.55
hy	8.24	14.89	.36	61.90	42.13	71.48	66.91	54.73
ol (q*)	13.32	.08	14.95	8.92*	10.89*	8.87*	7.73*	5.24*
mt	1.51	4.07	-	7.54	10.73	4.41	3.84	8.89
il	1.10	1.56	1.44	.06	.08	.06	.06	.02
ap	.19	.21	.24	.02	.05	.02	.02	.02
other	2.09	1.51	1.60	2.49	2.32	2.53	2.63	5.40
Molecular %								
or	1.33	1.42	1.3	4.16	1.93	1.30	1.62	1.36
ab	25.37	29.21	33.39	16.33	24.46	18.25	19.46	42.08
an	73.30	69.37	65.31	79.51	73.60	80.45	78.92	56.56
di (q*)	63.88	64.74	59.19	11.16*	14.08*	10.66*	8.99*	6.51*
hy	13.80	35.07	.96	11.42	31.45	3.66	13.15	25.52
ol	22.31	.19	39.85	77.44	54.47	85.70	77.82	67.97
Ca	35.6	44.0	43.2	8.3	17.4	4.8	8.4	11.8
Mg	51.2	41.8	37.9	80.5	72.3	82.1	76.2	81.0
Fe	13.2	14.2	18.9	11.1	10.3	13.1	15.4	7.1
$\frac{Mg}{Mg+Fe}$	.795	.746	.667	.879	.876	.862	.832	.919

Wt%	B1	B2	B3	B4	B5	B6	B7	B8
SiO_2	49.66	49.27	49.70	49.80	49.43	50.91	49.17	49.11
TiO_2	1.15	1.13	1.09	1.05	1.05	1.05	1.06	1.01
Al_2O_3	16.61	16.70	16.74	17.17	16.93	17.46	17.02	18.15
Fe_2O_3	1.8	2.37	2.15	2.56	2.36	1.70	2.29	1.81
FeO	8.58	8.42	8.62	8.14	8.58	6.85	8.10	7.94
MnO	.19	.19	.18	.18	.19	.17	.19	.18
MgO	5.50	5.49	5.40	5.29	5.80	5.43	5.86	5.57
CaO	11.59	11.30	11.30	11.07	11.24	12.55	11.90	12.26
Na_2O	3.15	3.29	3.38	3.41	3.21	3.06	2.96	2.68
K_2O	.17	.17	.19	.23	.22	.17	.18	.14
P_2O_5	.09	.10	.09	.10	.09	.10	.09	.08
S	.01	.02	.06	.03	.05	.01	.02	.01
H_2O+	1.04	1.00	1.06	1.03	.89	.90	1.06	1.03
H_2O-	.06	.06	.07	.06	.03	.06	.08	.06
CO_2	-	.03	-	-	.10	.03	.01	-
Sub Total	99.6	99.54	100.03	100.12	100.17	100.44	99.99	100.03
O = S	-	.01	.03	.01	.02	-	.01	-
TOTAL	99.6	99.53	100.00	100.11	100.15	100.44	99.98	100.03
Parts per million								
Rb	3	3	3	3	2	2	3	3
Sr	125	166	167	209	161	111	163	143
Y	20	21	21	21	20	20	23	20
Pb	-	-	1	1	1	1	1	-
Zr	57	57	56	57	52	51	61	54
Nb	4	3	3	4	3	4	2	4
Ni	33	36	39	36	42	40	42	41
Cu	20	101	209	122	75	20	143	42
Zn	66	75	81	78	76	49	73	64
Norm								
or	1.00	1.00	1.12	1.36	1.30	1.00	1.06	.83
ab	26.65	27.84	28.60	28.85	27.16	25.89	25.05	22.68
an	30.68	30.30	29.94	30.86	31.14	33.40	32.62	37.08
di	21.65	20.68	21.07	19.27	19.79	23.09	21.21	19.11
hy	7.33	5.42	4.60	6.12	5.74	9.76	6.73	9.83
ol	6.17	7.38	8.10	6.60	8.35	1.62	6.61	4.68
mt	2.61	3.44	3.12	3.71	3.42	2.46	3.32	2.62
il	2.18	2.15	2.07	1.99	1.99	1.99	2.01	1.92
ap	.21	.24	.21	.24	.21	.24	.21	.19
other	1.11	1.11	1.19	1.12	1.07	1.00	1.17	2.00
Molecular %								
or	1.71	1.69	1.88	2.23	2.18	1.66	1.81	1.37
ab	45.57	47.08	47.93	47.23	45.57	42.95	42.66	37.42
an	52.46	51.24	50.18	50.52	52.25	55.41	55.55	61.18
di	61.49	61.77	62.39	60.24	58.42	66.98	61.38	56.83
hy	20.82	16.19	13.62	19.13	16.94	28.31	19.48	29.23
ol	17.52	22.04	23.98	20.63	24.65	4.7	19.13	19.92
Ca	43.2	42.8	42.9	43.1	41.6	47.5	43.5	45.2
Mg	33.8	34.3	33.7	34.1	35.5	33.8	35.3	33.8
Fe	23.0	22.9	23.4	22.8	22.9	18.7	21.2	20.9
$\frac{Mg}{Mg+Fe}$	.595	.599	.590	.599	.608	.645	.624	.617

Wt%	B9	B10	B11	B12	B13	B14	B15	B16
SiO_2	49.34	49.09	49.18	49.08	48.95	48.69	49.10	48.83
TiO_2	1.01	.95	.91	.89	.87	.82	.79	.76
Al_2O_3	18.02	17.90	17.52	16.65	16.97	16.13	16.86	17.33
Fe_2O_3	2.13	2.18	1.83	1.82	1.96	2.06	1.52	1.80
FeO	7.68	7.71	7.87	8.23	7.99	8.08	7.93	6.86
MnO	.17	.17	.17	.18	.17	.18	.17	.16
MgO	5.00	5.71	5.91	6.67	6.64	7.85	7.37	7.85
CaO	12.14	12.23	12.40	12.71	12.79	12.35	12.97	12.25
Na_2O	2.87	2.55	2.43	2.26	2.27	2.15	1.96	2.54
K_2O	.17	.11	.19	.11	.14	.13	.10	.14
P_2O_5	.08	.08	.08	.08	.08	.07	.08	.08
S	.04	.03	.07	.05	.07	.04	.03	.03
H_2O+	1.03	1.09	1.16	1.16	1.07	1.30	1.23	1.25
H_2O-	.06	.06	.06	.06	.08	.07	.02	.05
CO_2	.01	.03	.10	.09	.20	.16	.06	.07
Sub Total	99.75	99.89	99.89	100.04	100.24	100.08	100.19	100.00
O = S	.02	.01	.03	.02	.03	.02	.01	.01
TOTAL	99.73	99.88	99.86	100.02	100.21	100.06	100.18	99.99
Parts per million								
Rb	1	2	2	2	2	-	2	2
Sr	200	165	153	156	147	163	156	155
Y	19	19	18	18	18	17	16	16
Pb	1	1	2	1	1	-	1	1
Zr	50	51	48	48	46	42	45	45
Nb	3	3	2	2	3	2	3	2
Ni	39	47	54	66	64	87	82	92
Cu	73	146	87	175	158	182	195	86
Zn	68	72	66	72	74	71	65	57
Norm								
or	1.00	.65	1.12	.65	.83	.77	.59	.83
ab	24.29	21.58	20.56	19.12	19.21	18.19	16.58	21.49
an	35.78	37.07	36.34	34.96	35.70	33.98	36.91	35.47
di	19.71	18.94	20.26	22.60	22.29	21.86	21.98	20.08
hy	9.64	13.30	13.16	13.66	12.27	13.64	16.11	7.31
ol	3.00	1.99	2.57	3.17	3.86	5.36	2.79	9.18
mt	3.09	3.16	2.65	2.64	2.84	2.99	2.20	2.61
il	1.92	1.80	1.54	1.69	1.65	1.56	1.50	1.44
ap	.19	.19	.19	.19	.19	.17	.19	.19
other	1.14	1.21	1.39	1.36	1.52	1.57	1.34	1.40
Molecular %								
or	1.64	1.1	1.9	1.37	1.4	1.46	1.09	1.44
ab	39.78	36.5	35.4	37.42	34.4	34.36	30.66	37.18
an	58.58	62.5	62.5	61.18	63.9	64.19	68.25	61.36
di	60.92	55.3	56.3	56.83	57.9	53.49	53.76	54.90
hy	29.80	38.8	36.6	29.23	31.9	33.38	39.41	19.99
ol	9.27	5.8	7.1	13.92	10.0	13.12	6.82	25.10
Ca	46.8	44.9	44.6	42.9	43.4	39.7	42.1	40.7
Mg	31.8	34.7	35.1	37.1	37.1	41.6	39.4	42.9
Fe	21.3	20.4	20.3	19.9	19.5	18.7	18.5	16.4
$\frac{Mg}{Mg+Fe}$	.599	.630	.633	.651	.656	.690	.681	.724

Wt%	B17	B18	B19	B20	B21	B22	B23	B24
SiO_2	49.64	49.04	48.87	49.03	48.88	48.68	48.75	48.60
TiO_2	.74	.73	.74	.79	.80	.67	.72	.65
Al_2O_3	15.73	18.04	16.65	15.76	14.40	14.21	14.96	15.59
Fe_2O_3	1.92	1.63	2.02	1.57	2.06	2.02	1.74	1.58
FeO	6.94	5.97	5.99	6.85	7.83	7.01	7.14	6.51
MnO	.16	.14	.15	.18	.18	.16	.16	.15
MgO	8.55	7.03	8.19	8.70	9.20	9.71	8.90	9.03
CaO	12.48	13.17	13.65	12.37	12.31	14.26	14.11	14.79
Na_2O	2.40	2.49	2.31	2.27	2.14	1.35	1.89	1.57
K_2O	.15	.13	.10	.08	.09	.09	.08	.19
P_2O_5	.08	.07	.07	.07	.06	.06	.06	.06
S	.04	.01	.03	.02	.03	.05	.06	.05
H_2O+	1.25	1.09	1.09	1.29	1.45	1.26	1.21	1.14
H_2O-	.04	.02	.03	.04	.10	.04	.02	.05
CO_2	.11	.04	.07	.07	.11	.65	.16	.16
Sub Total	100.23	99.60	99.96	100.09	99.64	100.22	99.97	100.12
O = S	.02	-	.01	.01	.01	.02	.03	.02
TOTAL	100.21	99.60	99.95	100.08	99.63	100.20	99.94	100.10
Parts per million								
Rb	1	2	2	2	2	1	-	3
Sr	166	179	156	127	109	144	141	162
Y	17	18	18	16	16	12	15	12
Pb	2	5	3	-	-	3	1	6
Zr	46	54	47	41	38	32	34	30
Nb	2	1	1	1	2	1	1	2
Ni	96	94	94	105	115	150	122	144
Cu	181	91	123	66	92	220	211	188
Zn	56	49	50	55	68	62	58	57
Norm								
or	.89	.77	.59	.47	.53	.53	.47	1.12
ab	20.31	21.07	19.55	19.21	18.11	11.42	15.99	13.28
an	31.70	37.66	34.77	32.58	29.42	32.45	32.10	34.93
di	24.01	22.03	26.17	22.91	25.32	30.56	30.35	30.70
hy	11.20	6.39	5.37	12.45	13.58	16.51	8.51	8.48
ol	6.31	6.61	7.80	6.12	6.34	2.41	7.07	6.54
mt	2.78	2.36	2.93	2.28	2.99	2.93	2.52	2.29
il	1.41	1.39	1.41	1.50	1.52	1.27	1.37	1.23
ap	.19	.17	.17	.17	.14	.14	.14	.14
other	1.44	1.16	1.22	1.42	1.69	2.00	1.45	1.40
Molecular %								
or	1.68	1.29	1.07	1.19	1.10	1.19	.97	2.27
ab	38.39	35.42	35.60	34.93	37.69	25.72	32.92	26.92
an	59.91	63.31	63.32	63.87	61.22	73.08	66.09	70.80
di	57.82	62.90	66.52	57.31	55.96	61.76	66.07	67.14
hy	26.97	18.24	13.65	34.64	30.01	33.76	18.53	18.55
ol	15.19	18.87	19.82	8.04	14.01	4.87	15.39	14.30
Ca	39.5	45.4	43.4	39.1	37.2	40.4	41.6	43.1
Mg	44.7	39.9	42.9	45.3	45.8	45.3	43.3	43.3
Fe	15.8	14.8	13.6	15.6	16.9	14.3	15.1	13.7
$\frac{Mg}{Mg+Fe}$	.739	.730	.759	.744	.730	.760	.741	.760

Wt%	B25	B26	B27	B28	B29	B30	B31	B32
SiO_2	48.48	47.95	49.01	48.77	48.04	48.60	48.05	48.03
TiO_2	.67	.65	.69	.70	.60	.59	.56	.60
Al_2O_3	14.63	19.58	14.16	13.92	11.28	10.72	10.48	9.26
Fe_2O_3	1.61	1.32	2.00	2.00	1.30	2.21	2.49	2.09
FeO	6.98	5.11	6.86	7.22	8.07	7.32	7.15	8.03
MnO	.16	.13	.17	.17	.18	.17	.19	.19
MgO	10.02	6.01	10.20	9.86	12.91	13.35	13.56	14.01
CaO	14.08	15.06	13.50	14.28	14.32	14.79	14.58	14.60
Na_2O	1.73	2.19	1.90	1.55	1.03	.89	.82	.80
K_2O	.13	.26	.08	.11	.09	.09	.07	.08
P_2O_5	.05	.05	.06	.06	.05	.05	.04	.05
S	.03	.04	.02	.04	.03	.06	.05	.08
H_2O+	1.29	1.01	1.31	1.21	1.62	1.44	1.57	1.70
H_2O-	.03	.68	.05	.04	.04	.08	.06	.06
CO_2	.11	.15	.06	.15	.13	.02	.08	.19
Sub Total	100.00	100.17	100.07	100.07	99.69	100.38	99.75	99.77
O = S	.01	.02	.01	.02	.01	.03	.02	.04
TOTAL	99.99	100.15	100.06	100.05	99.68	100.35	99.73	99.73
Parts per million								
Rb	1	4	-	1	1	2	2	1
Sr	129	111	92	135	89	81	79	55
Y	14	13	15	14	16	13	11	13
Pb	-	1	-	1	-	1	-	2
Zr	30	34	32	31	26	25	22	26
Nb	2	2	1	2	1	1	1	1
Ni	152	135	145	155	241	253	257	264
Cu	198	90	137	240	177	221	207	235
Zn	57	46	58	59	61	61	83	73
Norm								
or	.77	1.54	.47	.53	.53	.53	.41	.47
ab	14.64	17.04	16.08	8.72	8.72	7.53	6.94	6.77
an	31.77	42.83	29.87	25.89	25.89	24.99	24.71	21.44
di	30.44	25.55	29.54	36.09	36.09	38.50	37.89	40.66
hy (*=ne)	7.44	.81*	10.58	12.20	12.20	15.18	15.94	14.75
ol	9.76	7.29	7.74	11.30	11.30	7.61	7.33	9.37
mt	2.33	1.91	2.90	1.88	1.88	3.20	3.61	3.03
il	1.27	1.23	1.31	1.14	1.14	1.12	1.06	1.14
ap	.12	.12	.14	.12	.12	.12	.09	.12
other	1.46	1.88	1.44	1.82	1.82	1.60	1.76	2.03
Molecular %								
or	1.63	2.51	.90	1.50	1.51	1.60	1.28	1.64
ab	31.04	27.74	36.77	24.82	24.82	22.79	21.65	23.61
an	67.35	69.73	62.36	73.68	73.68	75.69	77.07	74.76
di	63.89	75.94	55.24	60.56	60.56	62.83	61.95	62.78
hy (*=ne)	15.62	2.41*	30.02	20.47	20.47	24.75	26.06	22.78
ol	20.49	21.67	14.76	18.96	18.96	12.42	11.99	14.47
Ca	39.5	52.7	38.3	39.9	34.6	35.2	34.7	33.6
Mg	46.4	34.6	47.7	45.6	51.4	52.3	53.1	53.1
Fe	14.1	12.8	14.0	14.5	14.0	12.5	12.2	13.3
$\frac{Mg}{Mg+Fe}$	.767	.731	.773	.759	.786	.807	.813	.800

Wt%	B33	B34	B35	B36	B37
SiO_2	47.91	47.99	51.25	47.86	47.81
TiO_2	.52	.56	1.83	.53	.52
Al_2O_3	11.19	10.62	12.77	10.15	11.00
Fe_2O_3	2.25	1.54	6.90	2.06	2.09
FeO	6.94	7.92	7.30	7.33	7.14
MnO	.17	.19	.38	.17	.18
MgO	13.42	13.59	4.85	14.23	13.59
CaO	15.13	14.68	7.86	14.62	14.45
Na_2O	.90	.89	.86	.87	.87
K_2O	.07	.08	.12	.06	.08
P_2O_5	.04	.04	.21	.04	.05
S	.03	.04	.02	.04	.03
H_2O+	1.58	1.69	1.59	1.84	1.78
H_2O-	.07	.09	.10	.06	.04
CO_2	.06	.15	.48	.12	.11
Sub Total	100.28	100.07	96.52	99.98	99.74
O = S	.01	.02	.01	.02	.01
TOTAL	100.27	100.05	96.51	99.96	99.73
Parts per million					
Rb	-	1	3	1	1
Sr	103	92	98	77	90
Y	11	12	42	11	12
Pb	2	7		3	3
Zr	22	23	24	21	24
Nb	1	2	2	1	1
Ni	267	266	269	281	265
Cu	192	202	233	184	132
Zn	59	80	128	61	76
Norm					
or	.41	.47	.71	.35	.47
ab	7.62	7.53	7.28	7.36	7.36
an	26.29	24.75	30.63	23.61	25.87
di	38.81	38.43	5.64	38.94	36.42
hy	10.56	11.82	14.70	12.24	13.95
ol (q*)	10.52	11.71	21.38*	11.32	9.58
mt	3.26	2.23	10.00	2.99	3.03
il	.99	1.06	3.48	1.01	.99
ap	.09	.09	.50	.09	.12
other	1.74	1.97	2.21	2.06	1.96
Molecular %					
or	1.19	1.44	1.84	1.01	1.39
ab	22.21	22.99	18.85	34.64	21.84
an	76.61	75.56	79.31	64.34	76.76
di	64.81	62.03	13.52	61.71	60.75
hy	17.64	19.08	35.23	22.10	23.27
ol (q*)	17.56	18.9	51.25*	16.17	15.98
Ca	35.8	34.3	37.3	33.8	34.4
Mg	52.4	52.4	37.8	54.1	53.3
Fe	11.8	13.3	24.9	12.1	12.2
$\frac{Mg}{Mg+Fe}$	.817	.797	.603	.817	.814

WT%	COBAW GRANITE	MICROGRANODIORITE MT. WILLIAM
SiO_2	73.44	68.70
TiO_2	0.24	0.63
Al_2O_3	13.72	14.37
Fe_2O_3	0.09	0.47
FeO	2.07	3.91
MnO	0.03	0.06
MgO	0.26	1.18
CaO	1.31	2.36
Na_2O	3.06	2.84
K_2O	4.63	3.43
P_2O_5	0.13	0.21
S	-	.02
H_2O+	0.47	.89
H_2O-	0.05	.08
CO_2	0.11	.17
TOTAL	99.62	99.31
PPM		
Rb	153	
Sr	121	
Y	79	
Pb	42	
Zr	192	
Nb	11	
Ni	5	
Cu	6	
Zn	74	

BULK CHEMICAL ANALYSES

Mount Camel

Wt%	A	B	C	D	E	F
SiO_2	53.94	50.08	56.28	50.12	51.29	50.78
TiO_2	.21	.12	.21	.22	.19	.20
Al_2O_3	6.76	5.83	8.00	9.28	8.51	8.99
Fe_2O_3	2.30	2.17	2.78	2.14	2.35	1.74
FeO	7.47	5.47	8.82	6.61	6.06	6.83
MnO	.23	.24	.19	.18	.19	.17
MgO	19.16	11.06	15.83	14.37	13.32	13.83
CaO	6.61	22.05	5.16	14.54	15.29	14.99
Na_2O	.70	.35	.38	.59	.54	.51
K_2O	.05	.26	.04	.07	.09	.05
P_2O_5	.03	.07	.04	.03	.03	.04
S	.01	.01	-	.01	-	.01
H_2O+	2.33	1.09	2.15	1.77	2.07	1.82
H_2O-	.07	.07	.08	.05	.04	.07
CO_2	.03	1.07	.22	.09	.16	.08
Sub Total	99.90	99.93	100.18	100.07	100.13	100.10
O = S	-	-	-	-	-	-
TOTAL	99.90	99.93	100.18	100.07	100.13	100.10
Parts per million						
Rb	2	1	3	2	1	2
Sr	25	277	30	46	52	25
Y	2	6	2	1	1	7
Pb	3	3	3	3	3	3
Zr	7	27	9	11	6	10
Nb	-	-	-	-	-	-
Ni	423	479	312	491	856	395
Cu	4	3	2	3	3	6
Zn	92	109	89	91	76	92
Norm						
or	.30	1.54	.24	.41	.53	.30
ab	5.92	2.96	3.22	4.99	4.57	4.32
an	15.16	13.57	20.00	22.47	20.53	22.09
di	13.89	75.40	4.28	39.52	44.00	41.65
hy (wo +)	53.01	.46+	51.28	26.53	21.41	25.60
ol (q *)	5.39*	.24*	14.20*	.24	2.98*	1.18*
mt	3.33	3.15	4.03	3.10	3.41	2.52
il	.40	.23	.40	.42	.36	.38
ap	.07	.17	.09	.07	.07	.09
other	2.44	2.24	2.45	1.92	2.27	1.98
Molecular %						
or	1.40	8.52	1.00	1.47	2.07	1.12
ab	27.69	16.38	13.70	17.90	17.83	16.17
an	70.90	75.09	85.26	80.62	80.11	82.71
di	19.21	99.68	6.13	59.64	64.33	60.85
hy	73.31	-	73.48	40.03	31.30	37.40
ol (q *)	7.45*	.32*	20.35*	.36	4.36*	1.72
Ca	15.2	49.8	13.8	33.9	36.7	35.1
Mg	72.5	41.3	69.4	55.1	52.8	53.4
Fe	12.3	8.9	16.8	11.0	10.5	11.5
$\frac{Mg}{Mg+Fe}$	.855	.823	.805	.834	.834	.823

AVERAGE ANALYSES OF VICTORIAN GREENSTONE (1-6, 8) AND THE AVERAGE OF 250 RIDGE THOLEIITES (7), FROM CRAWFORD (1975, Table 10).

1. Fine-grained metadolerite, Howqua.

2. Holocrystalline metadolerite, Howqua.

3. Metabasalt, Howqua.

4. Metadolerite, Dookie.

5. Meta-andesite, Heathcote.

6. Metadolerite, Heathcote.

7. Ridge tholeiites.

8. Basaltic komatiite, Howqua.

Wt%	1	2	3	4	5	6	7	8
SiO_2	47.65	47.96	47.72	48.11	62.85	46.80	49.41	50.07
TiO_2	.96	.65	1.80	1.10	.26	1.07	1.33	.06
Al_2O_3	14.69	13.87	13.21	14.29	13.83	13.80	15.63	3.40
Fe_2O_3	2.86	2.58	3.59	2.11	1.93	3.27	2.24	4.25
FeO	8.65	8.19	10.80	8.92	4.18	9.06	7.28	9.22
MnO	.18	.20	.19	.23	.11	.20	.17	.08
MgO	8.71	8.67	6.76	7.85	5.78	7.30	8.03	16.70
CaO	12.82	12.98	9.45	10.64	4.34	11.29	11.57	10.35
Na_2O	1.94	1.55	2.89	3.00	3.54	2.20	2.50	.41
K_2O	.21	.17	.17	.22	1.39	.17	.18	.08
P_2O_5	.10	.07	.20	.14	.12	.10	.14	.08
S								
H_2O+ H_2O- CO_2	2.35	3.12	3.21	-	2.00	-	-	5.45
Sub Total	101.12	100.01	99.99	96.61	100.33	95.26	98.48	100.14
O = S	-	-	-	-	-	-	-	-
TOTAL	101.12	100.01	99.99	96.61	100.33	95.26	98.48	100.14
Parts per million								
Rb	6	6	6	9	11	5	3	3
Sr	165	183	120	146	120	145	145	17
Y	25	13	48	27	-	25	31	3
Pb	-	-	-	-	-	-	-	-
Zr	45	23	126	51	44	61	108	12
Nb	-	-	-	-	-	-	-	-
Ni	107	91	53	86	63	97	144	499
Cu	-	-	-	-	-	-	-	-
Zn	-	-	-	-	-	-	-	-
Norm								
or	1.24	1.00	1.00	1.30	8.21	1.00	1.06	.47
ab	16.42	13.12	24.45	25.39	29.95	18.62	21.15	3.47
an	30.75	30.39	22.57	24.88	17.75	27.28	30.89	7.20
di	26.16	27.26	19.05	22.05	2.42	22.95	20.70	34.93
hy	9.38	18.50	17.74	5.41	19.09	15.47	15.82	38.34
ol (q*)	8.62	1.49	2.90	12.12	17.35*	2.93	2.75	3.82*
mt	4.15	3.74	5.21	3.06	2.80	4.74	3.25	6.16
il	1.82	1.23	3.42	2.09	.49	2.03	2.53	.11
ap	.24	.17	.47	.33	.28	.24	.33	.19
other	2.35	3.12	3.21	-	2.00	-	-	5.45
Molecular %								
or	2.56	2.25	2.08	2.52	14.68	2.13	1.99	4.22
ab	33.92	29.48	50.92	49.23	53.57	39.70	39.83	31.15
an	63.52	68.28	47.00	48.24	31.75	58.17	58.17	64.63
di	59.23	57.69	47.99	55.71	6.23	55.50	52.71	45.31
hy	21.25	39.15	44.69	13.67	49.12	37.41	40.29	49.73
ol (q*)	19.55	3.15	7.31	30.62	44.65*	7.09	7.00	4.96*
Ca	38.4	39.1	33.4	35.4	25.6	37.9	38.6	23.2
Mg	42.9	43.1	39.3	43.2	56.5	40.3	44.1	61.9
Fe	18.6	17.8	27.3	21.4	17.8	21.8	17.4	14.9
$\frac{Mg}{Mg+Fe}$	.698	.708	.590	.669	.760	.649	.717	.806

MINERAL ANALYSES

Amphiboles

WT%	B1	B1	B1	B1	B1	B1	B1	B1
SiO_2	45.35	45.57	44.96	45.01	45.27	44.59	45.04	44.69
TiO_2	.70	.66	.48	.99	.72	.91	.83	.62
Al_2O_3	9.49	9.73	9.17	10.04	9.23	9.56	8.85	10.57
FeO	18.00	18.16	18.91	19.47	19.07	18.91	18.85	17.85
MnO	.24	.24	.29	.40	.35	.20	.23	.15
MgO	10.36	10.27	10.23	10.18	10.48	10.17	10.51	9.71
CaO	12.37	12.36	11.99	11.67	11.77	12.02	11.84	12.08
Na_2O	1.27	1.37	1.68	2.11	1.63	1.41	1.50	1.24
K_2O	.46	.45	.34	.39	.32	.41	.26	.44
Cr_2O_3	-	-	-	.10	.12	-	-	-
TOTAL	98.24	98.80	98.05	100.36	98.96	98.17	97.91	97.34
	NUMBER OF IONS ON BASIS OF 23(O)							
Si	6.77	6.77	6.77	6.64	6.75	6.70	6.78	6.72
Al^{iv}	1.23	1.23	1.23	1.36	1.25	1.30	1.23	1.28
Al^{vi}	.34	.47	.39	.38	.37	.39	.23	.59
Ti	.08	.07	.05	.11	.08	.10	.09	.07
Fe	2.25	2.26	2.38	2.40	2.38	2.38	2.37	2.24
Mn	.03	.03	.04	.05	.05	.03	.03	.02
Mg	2.31	2.27	2.30	2.24	2.33	2.28	2.36	2.18
Ca	1.98	1.97	1.93	1.84	1.88	1.93	1.91	1.95
Na	.37	.39	.49	.60	.47	.41	.44	.36
K	.09	.08	.07	.07	.06	.08	.05	.08
Cr	-	-	-	.01	.01	-	-	-
TOTAL	15.54	15.55	15.65	15.71	15.62	15.59	15.50	15.49
$\frac{Mg}{Mg+Fe}$	.570	.565	.554	.546	.558	.552	.561	.555
Ca	29.2	29.2	28.2	27.5	27.6	28.4	27.7	29.5
Mg	40.3	40.0	39.8	39.6	40.4	39.6	40.6	39.1
Fe	30.5	30.8	32.0	32.9	32.0	32.1	31.7	31.4

WT%	B7	B7	B7	B7	B7	B7	B7
SiO_2	46.96	44.07	44.3	44.73	43.97	44.08	45.31
TiO_2	.48	1.65	.62	.43	1.87	1.76	1.21
Al_2O_3	8.31	9.58	11.33	9.12	9.92	9.99	8.68
FeO	17.11	19.24	17.06	18.2	19.21	19.74	18.85
MnO	.38	.24	.13	.24	.40	.17	.23
MgO	12.01	9.75	10.14	10.70	10.0	9.74	10.48
CaO	11.51	11.63	11.79	11.24	11.82	11.65	11.89
Na_2O	1.32	1.61	1.45	1.68	1.82	1.86	1.41
K_2O	.20	.39	.33	.34	.43	.41	.29
Cr_2O_3	-	.11	-	-	-	.11	-
TOTAL	98.29	98.27	97.15	96.68	99.44	99.51	98.37
			NUMBER OF IONS ON BASIS OF 23(O)				
Si	6.94	6.64	6.65	6.79	6.56	6.57	6.78
Al^{iv}	1.06	1.36	1.35	1.21	1.44	1.43	1.22
Al^{vi}	.39	.22	.65	.42	.30	.33	.31
Ti	.05	.19	.07	.05	.21	.19	.14
Fe	2.12	2.42	2.14	2.31	2.39	2.46	2.36
Mn	.05	.03	.02	.03	.05	.02	.03
Mg	2.65	2.19	2.27	2.42	2.22	2.17	2.34
Ca	1.82	1.88	1.89	1.83	1.89	1.86	1.91
Na	.38	.47	.42	.49	.52	.54	.41
K	.04	.08	.06	.07	.09	.07	.06
Cr	-	.01	-	-	-	.18	-
TOTAL	15.49	15.59	15.52	15.62	15.67	15.82	15.55
$\frac{Mg}{Mg+Fe}$	.618	.538	.578	.574	.544	.532	.560
Ca	26.4	27.9	28.9	26.8	28.1	27.8	27.8
Mg	45.4	38.7	41.0	42.0	39.1	38.4	40.4
Fe	28.2	33.3	30.0	31.2	32.8	33.8	31.7

WT%	B12	B12	B12	B20	B20	B20	B20
SiO_2	48.53	50.22	49.52	49.7	50.67	47.75	47.82
TiO_2	.42	.49	.56	.52	.48	.60	.50
Al_2O_3	6.98	4.68	6.45	7.33	4.88	9.31	8.34
FeO	18.76	16.74	18.11	13.52	12.02	12.14	12.09
MnO	.24	.24	.26	.16	.16	.14	.14
MgO	11.99	13.10	12.15	14.79	15.49	14.00	14.68
CaO	11.75	12.09	11.88	12.75	12.80	12.67	12.64
Na_2O	1.19	.83	.94	1.10	.83	1.59	1.35
K_2O	.12	.11	.13	.12	-	.18	.10
Cr_2O_3	-	-	-	-	-	.13	-
TOTAL	99.08	98.5	98.01	98.10	97.34	98.52	97.67
	NUMBER OF IONS ON BASIS OF 23(O)						
Si	7.09	7.36	7.19	7.08	7.35	6.89	6.95
Al^{iv}	.91	.64	.81	.92	.65	1.11	1.05
Al^{vi}	.18	.17	.29	.32	.19	.47	.38
Ti	.04	.05	.06	.05	.05	.07	.06
Fe	2.29	2.05	2.20	1.61	1.46	1.47	1.47
Mn	.03	.03	.04	.02	.02	.02	.02
Mg	2.61	2.86	2.63	3.14	3.35	3.01	3.18
Ca	1.84	1.90	1.85	1.94	1.99	1.96	1.97
Na	.33	.24	.26	.31	.24	.45	.38
K	.02	.02	.02	.02	-	.03	.02
Cr	-	-	-	-	-	.02	-
TOTAL	15.44	15.31	15.34	15.41	15.29	15.48	15.48
$\frac{Mg}{Mg+Fe}$	.595	.642	.607	.715	.748	.726	.737
Ca	26.1	26.5	26.4	27.2	27.2	28.5	27.8
Mg	43.9	47.2	44.6	52.0	54.4	51.9	53.2
Fe	29.9	26.3	28.9	20.7	18.4	19.6	19.0

WT%	B27	B27	B27	B27	B27	B27
SiO_2	49.26	46.91	46.26	50.50	47.71	45.17
TiO_2	.28	.62	.53	.37	.44	.83
Al_2O_3	5.73	8.94	9.52	5.98	11.49	11.47
FeO	12.34	13.34	13.55	12.47	12.88	14.93
MnO	.20	.14	-	-	.16	.15
MgO	15.30	13.89	13.66	15.61	12.72	12.59
CaO	11.62	12.13	12.23	12.24	12.32	12.25
Na_2O	.88	1.71	1.69	1.08	2.15	2.25
K_2O	.06	.16	.15	.09	.12	.24
Cr_2O_3	.15	.16	-	.15	-	.13
TOTAL	95.82	98.00	97.60	98.48	97.25	96.84
	NUMBER OF IONS ON BASIS OF 23(0)					
Si	7.27	6.85	6.79	7.25	6.79	6.55
Al^{iv}	.73	1.15	1.21	.75	1.21	1.45
Al^{vi}	.26	.39	.34	.26	.72	.50
Ti	.03	.07	.06	.04	.04	.09
Fe	1.52	1.63	1.66	1.49	1.53	1.81
Mn	.03	.02	-	-	.02	.02
Mg	3.37	3.02	2.99	3.34	2.69	2.72
Ca	1.84	1.89	1.92	1.88	1.88	1.90
Na	.25	.48	.48	.30	.60	.63
K	.01	.03	.03	.02	.02	.05
Cr	.02	.02	-	.02	-	.02
TOTAL	15.33	15.56	15.58	15.36	15.51	15.72
$\frac{Mg}{Mg+Fe}$	.740	.705	.698	.742	.694	.660
Ca	25.4	27.2	27.5	26.1	28.9	28.1
Mg	55.2	51.3	50.6	54.9	49.3	47.5
Fe	19.4	21.5	21.9	19.1	21.8	24.5

WT%	B15	B15	B15	B31	B36	B36	B36
SiO_2	49.70	54.27	49.36	47.01	46.87	39.01	47.31
TiO_2	.50	.12	.45	.59	.32	.70	.63
Al_2O_3	7.00	2.73	7.06	9.51	10.96	25.38	11.47
FeO	14.73	13.54	15.61	11.84	11.11	9.18	11.37
MnO	.12	.19	.15	.14	-	-	-
MgO	13.60	15.74	13.18	14.75	14.82	12.11	14.79
CaO	12.79	12.86	12.78	12.22	12.79	10.40	12.73
Na_2O	1.18	.41	1.04	1.65	1.32	1.22	1.47
K_2O	.23	-	.18	.20	.07	.13	.08
Cr_2O_3	.16	.14	.18	.12	.22	.17	.16
TOTAL	100.01	99.22	99.57	98.04	98.48	98.29	98.12
	NUMBER OF IONS ON BASIS OF 23(O)						
Si	7.13	7.67	7.11	6.82	6.73	5.53	6.69
Al^{iv}	.87	.33	.89	1.18	1.27	2.47	1.31
Al^{vi}	.32	.13	.31	.44	.58	1.77	.59
Ti	.05	.01	.04	.06	.04	.08	.07
Fe	1.77	1.60	1.88	1.44	1.33	1.09	1.34
Mn	.02	.03	.02	.02	-	-	-
Mg	2.90	3.31	2.83	3.19	3.17	2.56	3.12
Ca	1.97	1.94	1.98	1.90	1.97	1.58	1.93
Na	.33	.12	.30	.46	.37	.33	.41
K	.03	-	.04	.04	.01	.02	.02
Cr	.02	.02	.02	.01	.03	.02	.02
TOTAL	15.40	15.14	15.40	15.55	15.49	15.45	15.50
$\frac{Mg}{Mg+Fe}$	.679	.728	.659	.741	.754	.752	.749
Ca	27.9	26.5	27.9	27.1	28.3	28.1	28.1
Mg	48.9	53.5	47.5	54.0	54.1	54.1	53.8
Fe	23.1	20.0	24.5	18.9	17.6	17.8	18.1

WT%	A12	A12	A12	A12	A12	A12
SiO_2	55.45	56.54	55.77	57.44	54.78	54.4
TiO_2	-	-	-	-	-	-
Al_2O_3	2.94	.46	1.78	3.08	3.08	4.61
FeO	6.6	14.95	15.39	8.94	6.33	8.47
MnO	-	.25	.19	.11	-	-
MgO	21.00	24.72	24.12	22.89	20.64	20.76
CaO	11.19	.54	.60	6.98	11.83	7.91
Na_2O	.15	-	-	.21	.19	.26
K_2O	-	-	-	-	-	-
Cr_2O_3	.82	.11	.24	.34	.62	.51
TOTAL	98.15	97.58	98.1	96.94	97.47	96.93
	NUMBER OF IONS ON BASIS OF 23(0)					
Si	7.69	7.92	7.79	7.77	7.65	7.62
Al^{iv}	.31	.08	.21	.23	.35	.38
Al^{vi}	.16	-	.08	.26	.16	.38
Ti	-	-	-	-	-	-
Fe	.77	1.75	1.80	1.01	.74	.99
Mn	-	.03	.03	.02	-	-
Mg	4.34	5.16	5.02	4.62	4.30	4.33
Ca	1.66	.08	.09	1.01	1.77	1.19
Na	.03	-	-	.05	.05	.07
K	-	-	-	-	-	-
Cr	.08	.01	.03	.03	.07	.06
TOTAL	15.05	15.04	15.05	14.99	15.09	15.01
$\frac{Mg}{Mg+Fe}$	.880	.791	.782	.855	.883	.849
Ca	22.1	1.0	1.2	13.6	23.4	16.4
Mg	68.5	78.4	77.3	73.8	67.5	71.0
Fe	9.4	20.6	21.5	12.5	8.9	12.6

WT%	A12	A12	A12	A12	A12	A12
SiO_2	55.91	55.20	54.33	54.23	54.71	56.61
TiO_2	-	-	-	-	-	-
Al_2O_3	1.17	1.26	2.42	3.23	3.41	.71
FeO	12.83	11.64	9.79	9.68	7.36	14.19
MnO	.16	-	-	-	-	-
MgO	19.66	19.16	18.58	19.63	20.36	24.53
CaO	8.64	9.67	11.54	9.68	11.03	1.62
Na_2O	.22	-	.32	.18	.25	-
K_2O	-	-	-	.08	-	-
Cr_2O_3	.21	.12	.22	.11	.85	.19
TOTAL	98.79	97.04	97.19	96.82	97.98	97.85
	NUMBER OF IONS ON BASIS OF 23(0)					
Si	7.85	7.87	7.73	7.69	7.63	7.90
Al^{iv}	.15	.13	.27	.31	.37	.10
Al^{vi}	.05	.08	.13	.23	.19	.01
Ti	-	-	-	-	-	-
Fe	1.51	1.39	1.16	1.15	.86	1.66
Mn	.02	-	-	-	-	-
Mg	4.12	4.07	3.94	4.15	4.23	5.10
Ca	1.30	1.48	1.76	1.47	1.65	.24
Na	.06	-	.09	.05	.07	-
K	-	-	-	.01	-	-
Cr	.02	.01	.02	.01	.09	.02
TOTAL	15.07	15.02	15.10	15.07	15.08	15.03
$\frac{Mg}{Mg+Fe}$	.779	.791	.814	.823	.864	.799
Ca	17.2	19.4	23.5	19.8	22.1	3.1
Mg	64.5	63.7	62.3	66.0	67.3	77.4
Fe	18.3	16.8	14.3	14.2	10.6	19.5

WT%	A14	A14	A14	A14	A14	A14	A14
SiO_2	56.48	56.92	56.66	60.01	54.71	55.48	54.71
TiO_2	-	-	-	-	-	-	-
Al_2O_3	2.5	1.08	1.76	.95	3.52	6.15	3.41
FeO	12.92	13.56	12.53	10.77	11.94	11.06	7.36
MnO	-	-	-	-	-	.11	-
MgO	25.56	26.13	25.66	27.23	25.39	24.58	20.36
CaO	.4	.51	.36	1.03	.32	.59	11.03
Na_2O	.17	-	-	-	-	-	.25
K_2O	-	-	-	-	-	-	-
Cr_2O_3	-	-	-	-	.16	.19	.85
TOTAL	98.02	98.2	96.96	96.96	96.04	98.16	97.98
	NUMBER OF IONS ON BASIS OF 23(O)						
Si	7.79	7.86	7.87	8.01	7.67	7.57	7.63
Al^{iv}	.21	.14	.13	-	.33	.43	.37
Al^{vi}	.18	.04	.16	.14	.26	.55	.20
Ti	-	-	-	-	-	-	-
Fe	1.49	1.57	1.46	1.20	1.40	1.26	.86
Mn	-	-	-	-	-	.03	-
Mg	5.25	5.38	5.31	5.41	5.31	5.00	4.23
Ca	.06	.08	.05	.14	.05	.09	1.65
Na	.05	-	-	-	-	-	.07
K	-	-	-	-	-	-	-
Cr	-	-	-	-	.02	.02	.09
TOTAL	15.03	15.05	14.98	14.92	15.03	14.95	15.08
$\frac{Mg}{Mg+Fe}$	.774	.977	.699	.853	.830	.836	.864
Ca	0.8	0.8	0.8	1.9	0.6	1.2	22.1
Mg	81.3	80.8	81.9	83.7	82.5	82.6	67.3
Fe	17.9	18.3	17.4	14.4	16.9	16.2	10.6

WT%	A16	A16	A16	A16	A16	A16
SiO_2	53.08	49.94	53.44	45.71	56.27	50.13
TiO_2	-	-	-	-	-	-
Al_2O_3	3.18	4.4	1.32	14.74	8.81	7.52
FeO	5.16	12.33	4.48	8.46	8.81	7.84
MnO	-	.38	-	.33	.36	.34
MgO	29.78	23.53	20.98	15.12	19.74	17.96
CaO	-	2.26	11.76	8.5	10.27	9.12
Na_2O	-	-	.22	-	-	-
K_2O	-	-	-	-	-	-
Cr_2O_3	.20	.37	.32	-	.12	.10
TOTAL	91.41	93.2	92.51	92.85	104.39	93.02
	NUMBER OF IONS ON BASIS OF 23(0)					
Si	7.60	7.35	7.81	6.72	7.34	7.34
Al^{iv}	.40	.65	.19	1.28	.66	.66
Al^{vi}	.13	.12	.04	1.27	.69	.64
Ti	-	-	-	-	-	-
Fe	.62	1.52	.55	1.04	.96	.96
Mn	-	.05	-	.04	.04	.04
Mg	6.35	5.16	4.57	3.31	3.84	3.92
Ca	-	.36	1.84	1.34	1.44	1.43
Na	-	-	.06	-	-	-
K	-	-	-	-	-	-
Cr	.02	.04	.04	-	.01	.01
TOTAL	15.12	15.24	15.09	15.00	14.98	15.00
$\frac{Mg}{Mg+Fe}$	.930	.814	.915	.805	.837	.841
Ca	0.0	4.5	23.7	21.5	20.9	20.6
Mg	93.0	77.8	69.8	63.1	66.2	66.8
Fe	6.9	17.8	6.5	15.3	12.9	12.6

WT%	D	D	D	D	D	D	E	E
SiO_2	54.39	55.22	56.44	56.40	54.67	56.47	60.69	60.66
TiO_2	.27	.24	-	-	.22	-	-	-
Al_2O_3	3.84	3.68	.94	.34	3.59	1.10	1.54	1.61
FeO	7.49	7.88	14.07	15.89	8.46	14.85	11.99	12.02
MnO	-	.14	.19	.14	-	-	-	-
MgO	19.87	20.40	22.83	23.10	20.03	23.01	18.78	18.68
CaO	11.69	11.24	3.49	1.30	10.38	3.04	14.38	14.32
Na_2O	.24	.24	-	-	-	-	-	-
K_2O	-	-	-	-	-	-	-	-
Cr_2O_3	.71	.54	.14	-	.54	.17	.14	.11
TOTAL	98.50	99.57	98.11	97.17	97.89	98.64	107.51	107.40
	NUMBER OF IONS ON BASIS OF 23(O)							
Si	7.56	7.59	7.90	7.98	7.63	7.87	7.86	7.86
Al^{iv}	.44	.41	.10	.02	.37	.13	.14	.14
Al^{vi}	.19	.18	.06	.04	.22	.05	.09	.11
Ti	.03	.02	-	-	.02	-	-	-
Fe	.87	.91	1.65	1.88	.99	1.73	1.30	1.30
Mn	-	.02	.02	.02	-	-	-	-
Mg	4.11	4.18	4.76	4.87	4.17	4.78	3.62	3.61
Ca	1.74	1.66	.52	.19	1.55	.45	1.99	1.99
Na	.07	.07	-	-	-	-	-	-
K	-	-	-	-	-	-	-	-
Cr	.08	.06	.02	-	.06	.02	.01	.01
TOTAL	15.09	15.09	15.02	14.99	15.02	15.03	15.02	15.01
$\frac{Mg}{Mg+Fe}$	.859	.856	.788	.769	.845	.781	.782	.781
Ca	23.5	22.2	6.8	2.5	21.0	5.9	26.7	26.6
Mg	65.7	66.6	73.5	74.9	66.8	73.4	57.4	57.3
Fe	10.8	11.2	19.7	22.5	12.2	20.7	16.0	16.1

PLAGIOCLASE

Mount William

B1, B7, B12, B15, B20, B27, B31, B36

Mount Camel

E

WT%	B1	B1	B1	B7	B7	B7
SiO_2	52.04	53.32	53.57	52.62	52.49	54.39
TiO_2	-	-	-	-	-	-
Al_2O_3	38.92	31.23	31.32	29.96	30.63	29.35
FeO	-	.40	.30	-	.18	-
MnO	-	-	-	-	-	-
MgO	.27	.21	.21	.34	.31	.22
CaO	11.39	11.17	11.11	11.97	11.61	10.25
Na_2O	5.07	4.49	4.47	4.86	4.60	5.63
K_2O	.15	.24	.21	.12	.18	.16
Cr_2O_3	.13	-	-	.13	-	-
TOTAL	97.97	101.06	101.20	102.82	101.55	101.85
			NUMBER OF IONS ON BASIS OF 8(O)			
Si	2.41	2.38	2.39	2.39	2.38	2.45
Al^{iv}	.59	.62	.61	.61	.62	.55
Al^{vi}	.99	1.02	1.03	.99	1.01	1.01
Ti	-	-	-	-	-	-
Fe	-	.02	.01	-	.01	-
Mn	-	-	-	-	-	-
Mg	.02	.01	.01	.02	.02	.01
Ca	.56	.54	.53	.58	.56	.50
Na	.46	.39	.39	.43	.40	.49
K	.01	.02	.01	.01	.01	.01
Cr	.01	-	-	.01	-	-
TOTAL	5.04	4.99	4.99	5.03	5.01	5.02
Ca	55.8	58.1	58.2	58.3	58.6	50.7
Na	43.4	40.6	40.8	41.1	40.4	48.5
K	0.8	1.3	1.1	0.6	1.0	0.8

WT%	B12	B12	B12	B12	B12	B12	B12
SiO_2	56.08	52.28	49.98	53.24	47.23	48.82	52.12
TiO_2	-	-	-	-	-	-	-
Al_2O_3	27.79	32.21	33.36	29.66	35.88	34.41	30.35
FeO	.13	.29	-	-	.21	.30	-
MnO	-	-	-	-	-	-	-
MgO	.25	.38	.17	.26	.25	.22	.28
CaO	9.27	13.86	15.16	11.36	14.10	16.49	12.28
Na_2O	6.32	4.03	3.10	5.27	2.18	2.33	4.76
K_2O	.15	.14	.07	.20	.15	.08	.11
Cr_2O_3	-	.13	-	-	-	-	.10
TOTAL	103.29	103.31	101.84	103.98	97.23	102.64	103.57
			NUMBER OF IONS ON BASIS OF 8(O)				
Si	2.52	2.31	2.24	2.41	2.15	2.18	2.36
Al^{iv}	.48	.69	.76	.59	.85	.82	.64
Al^{vi}	.99	.99	1.00	.99	1.08	.99	.98
Ti	-	-	-	-	-	-	-
Fe	.01	.01	-	-	.01	.01	-
Mn	-	-	-	-	-	-	-
Mg	.02	.02	.01	.02	.02	.01	.02
Ca	.45	.66	.73	.55	.69	.79	.60
Na	.55	.35	.27	.46	.19	.20	.42
K	.01	.01	.01	.01	.01	.01	.01
Cr	-	.01	-	-	-	-	.01
TOTAL	5.02	5.03	5.02	5.04	4.99	5.02	5.03
Ca	45.3	65.9	73.4	54.7	78.1	79.9	59.3
Na	53.9	33.3	26.2	44.3	21.1	19.7	40.1
K	0.8	0.8	0.4	1.0	0.9	0.4	0.6

WT%	B20	B20	B20	B20	B20	B20
SiO_2	51.77	51.54	49.91	51.55	55.50	46.73
TiO_2	-	-	-	-	-	-
Al_2O_3	32.61	30.50	31.77	31.34	28.35	34.27
FeO	.13	.81	.25	-	-	-
MnO	-	-	-	-	-	-
MgO	.34	1.34	.48	.23	.28	.24
CaO	14.31	13.54	14.19	12.06	9.93	16.93
Na_2O	3.65	3.38	3.33	4.70	5.85	1.77
K_2O	.11	-	.07	.12	.09	.07
Cr_2O_3	-	-	-	-	-	-
TOTAL	102.92	101.11	102.29	101.71	102.95	102.22
	NUMBER OF IONS ON BASIS OF 8(O)					
Si	2.29	2.32	2.28	2.34	2.50	2.15
Al^{iv}	.71	.68	.72	.66	.50	.85
Al^{vi}	.99	.94	.99	1.01	1.00	1.00
Ti	-	-	-	-	-	-
Fe	.01	.03	.01	-	-	-
Mn	-	-	-	-	-	-
Mg	.02	.09	.03	.02	.02	.02
Ca	.68	.65	.69	.59	.48	.83
Na	.31	.30	.30	.41	.51	.16
K	.01	-	.01	.01	.01	.01
Cr	-	-	-	-	-	-
TOTAL	5.02	5.01	5.02	5.03	5.01	5.01
Ca	68.8	69.7	70.7	59.3	49.2	84.2
Na	30.6	30.3	28.9	40.2	50.4	15.4
K	0.6	0.0	0.4	0.6	0.4	0.4

WT%	B27	B27	B31	B36	B36
SiO_2	53.34	54.01	44.00	42.93	40.33
TiO_2	-	-	-	-	-
Al_2O_3	30.83	29.35	35.24	36.72	38.12
FeO	-	-	.21	-	1.62
MnO	-	-	-	-	-
MgO	.28	.20	.78	.26	2.15
CaO	10.62	10.91	18.93	19.80	17.39
Na_2O	4.76	5.43	.73	.22	.27
K_2O	.18	.11	.11	.07	.12
Cr_2O_3	-	-	-	-	-
TOTAL	100.52	102.42	101.52	102.06	99.98
	NUMBER OF IONS ON BASIS OF 8(O)				
Si	2.40	2.44	2.04	1.99	1.88
Al^{iv}	.60	.56	-	.01	.12
Al^{vi}	1.03	1.00	1.92	2.00	1.89
Ti	-	-	-	-	-
Fe	-	-	.01	-	.06
Mn	-	-	-	-	-
Mg	.02	.01	.05	.02	.15
Ca	.51	.53	.94	.98	.87
Na	.42	.48	.07	.02	.02
K	.01	.01	.01	.01	.01
Cr	-	-	-	-	-
TOTAL	4.99	5.02	5.04	5.02	5.09
Ca	55.6	53.2	93.1	97.6	96.7
Na	43.4	46.2	6.3	2.0	2.7
K	1.1	0.6	0.6	0.4	0.7

WT%	B15	B15	B15	B15	E
SiO_2	46.98	47.80	53.72	49.16	55.69
TiO_2	-	-	-	-	-
Al_2O_3	32.62	33.35	31.53	35.02	26.52
FeO	.74	-	-	-	1.21
MnO	-	-	-	-	-
MgO	.81	.30	.28	.27	1.90
CaO	16.40	15.88	12.95	16.99	10.69
Na_2O	2.16	2.57	4.67	2.35	5.28
K_2O	.12	.10	.12	.07	.15
Cr_2O_3	.16	-	.15	.14	.31
TOTAL	99.99	100.00	103.41	104.00	101.75
	NUMBER OF IONS ON BASIS OF 8(O)				
Si	2.17	2.19	2.36	2.17	2.49
Al^{iv}	.83	.81	.64	-	.51
Al^{vi}	.94	.99	.99	1.82	.88
Ti	-	-	-	-	-
Fe	.03	-	-	-	.05
Mn	-	-	-	-	-
Mg	.06	.02	.02	.02	.13
Ca	.81	.78	.61	.80	.51
Na	.19	.23	.39	.20	.46
K	.01	.01	.01	.01	.01
Cr	.01	-	.01	.01	.01
TOTAL	5.04	5.03	5.03	5.02	5.04
Ca	53.3	77.5	61.1	80.3	53.3
Na	45.9	21.9	38.4	19.3	45.9
K	0.8	0.6	0.6	0.4	0.8

CLINOPYROXENE

Mount William

B1, B7, B12, B15, B20, B27, B31, B36

Mount Camel

E

WT%	B1	B1	B1	B1	B1	B1	B1
SiO_2	51.51	51.64	50.48	50.41	51.92	51.68	51.91
TiO_2	.19	.13	.27	.31	.12	-	-
Al_2O_3	2.12	.93	2.42	2.35	.88	.83	.68
FeO	13.53	12.46	13.36	13.42	12.40	13.00	12.98
MnO	.23	.39	.36	.32	.34	.37	.36
MgO	11.81	11.50	11.55	11.55	11.41	11.23	11.20
CaO	20.05	22.81	20.20	20.12	23.09	22.81	22.65
Na_2O	.30	-	.52	.50	-	.20	-
K_2O	.08	-	.09	-	-	-	-
Cr_2O_3	.17	.14	.26	-	.16	.21	.20
TOTAL	101.92	101.08	99.51	98.98	100.31	100.32	99.31
			NUMBER OF IONS ON BASIS OF 6(O)				
Si	1.95	1.97	1.93	1.94	1.97	1.97	1.98
Al^{iv}	.05	.04	.07	.06	.03	.03	.02
Al^{vi}	.05	.01	.04	.04	.01	.01	.01
Ti	.01	.01	.01	.01	.01	-	-
Fe	.43	.40	.43	.43	.39	.41	.41
Mn	.01	.01	.01	.01	.01	.01	.01
Mg	.67	.65	.66	.66	.65	.64	.64
Ca	.82	.93	.83	.83	.94	.93	.93
Na	.02	-	.04	.04	-	.01	-
K	.01	-	.01	-	-	-	-
Cr	.01	.01	.01	-	.01	.01	.01
TOTAL	4.01	4.01	4.02	4.02	4.01	4.02	4.00
$\frac{Mg}{Mg+Fe}$	.668	.680	.665	.664	.679	.665	.665
Ca	40.7	44.9	41.4	41.2	45.5	45.0	44.9
Mg	39.6	37.4	39.0	39.0	37.0	36.6	36.6
Fe	19.7	17.6	19.6	19.7	17.5	18.4	18.4

WT%	B7	B7	B7	B12	B12	B12
SiO_2	51.71	51.69	52.03	52.27	52.73	52.76
TiO_2	.17	.22	.11	-	-	-
Al_2O_3	1.38	1.22	.90	1.26	.78	.79
FeO	12.14	10.88	10.65	11.60	11.50	11.95
MnO	.29	.42	.29	.28	.27	.23
MgO	12.12	12.31	12.60	12.47	12.45	12.45
CaO	21.84	22.97	22.88	22.24	23.08	22.30
Na_2O	.18	-	.28	-	.21	-
K_2O	-	-	-	-	-	-
Cr_2O_3	.16	.29	.26	.23	.23	.19
TOTAL	100.16	100.38	100.46	100.34	101.25	100.65
	NUMBER OF IONS ON BASIS OF 6(O)					
Si	1.96	1.96	1.96	1.97	1.97	1.98
Al^{iv}	.04	.04	.04	.03	.03	.02
Al^{vi}	.02	.01	.01	.02	.01	.02
Ti	.01	.01	.01	-	-	-
Fe	.38	.34	.34	.36	.36	.38
Mn	.01	.01	.01	.01	.01	.01
Mg	.69	.69	.71	.69	.69	.70
Ca	.89	.93	.93	.90	.93	.90
Na	.01	-	.01	-	.01	-
K	-	-	-	-	-	-
Cr	.01	.01	.01	.01	.01	.01
TOTAL	4.01	4.01	4.01	4.00	4.01	3.99
$\frac{Mg}{Mg+Fe}$	.697	.722	.731	.712	.713	.705
Ca	43.2	44.9	44.6	43.5	44.5	43.3
Mg	39.6	39.7	40.5	40.2	39.6	39.9
Fe	17.2	15.3	14.9	16.3	15.9	16.7

WT%	B15	B15	B15	B15	B15	B20	B20	B20
SiO_2	51.81	53.27	51.67	52.70	51.90	52.76	52.93	53.30
TiO_2	.43	.26	.36	.29	.39	.21	-	.11
Al_2O_3	2.37	1.78	2.74	1.80	2.59	1.79	1.05	1.14
FeO	8.92	8.35	9.02	8.00	8.95	8.38	7.56	7.80
MnO	-	-	-	-	.12	.18	.28	.13
MgO	16.12	16.78	15.80	16.55	16.02	14.59	14.42	14.42
CaO	20.16	20.64	19.98	20.12	19.59	21.92	23.57	23.41
Na_2O	-	-	.19	-	.20	.35	-	-
K_2O	-	-	-	-	-	-	-	-
Cr_2O_3	.20	.17	.23	.54	.24	.34	-	.35
TOTAL	100.10	101.25	99.29	99.19	100.00	100.52	99.81	100.66
	NUMBER OF IONS ON BASIS OF 6(O)							
Si	1.92	1.94	1.92	1.95	1.92	1.95	1.97	1.97
Al^{iv}	.08	.06	.08	.05	.08	.05	.03	.03
Al^{vi}	.02	.09	.04	.03	.03	.03	.02	.02
Ti	.01	.01	.01	.01	.01	.01	-	.01
Fe	.28	.25	.28	.25	.28	.26	.24	.24
Mn	-	-	-	-	-	.01	.01	.01
Mg	.89	.91	.87	.91	.88	.80	.80	.80
Ca	.80	.81	.79	.80	.78	.87	.94	.93
Na	-	-	.01	-	.01	.03	-	-
K	-	-	-	-	-	-	-	-
Cr	.01	.01	.01	.02	.01	.01	-	.01
TOTAL	4.01	4.09	4.02	3.99	4.01	4.01	4.01	3.99
$\frac{Mg}{Mg+Fe}$	.806	.821	.800	.826	.805	.800	.815	.809
Ca	37.9	38.0	38.1	37.9	37.4	42.2	44.7	44.3
Mg	50.0	50.9	49.6	51.4	50.4	46.3	45.1	45.0
Fe	12.1	11.1	12.4	10.8	12.2	11.6	10.3	10.6

WT%	B20	B20	B27	B27	B27	B27
SiO_2	52.76	53.06	52.92	52.55	52.1	52.36
TiO_2	.21	.20	.32	.24	-	.11
Al_2O_3	1.79	1.91	1.77	1.73	1.83	2.46
FeO	8.38	7.18	8.20	8.44	8.99	8.33
MnO	.18	.15	.29	.13	.25	.26
MgO	14.59	14.49	14.75	16.49	13.98	16.60
CaO	21.92	23.49	21.75	20.15	22.10	22.89
Na_2O	.35	.18	-	-	.33	-
K_2O	-	-	-	-	-	-
Cr_2O_3	.34	.27	-	.27	.29	.19
TOTAL	100.52	100.93	97.95	99.16	99.87	103.10
	NUMBER OF IONS ON BASIS OF 6(O)					
Si	1.95	1.95	1.96	1.94	1.95	1.89
Al^{iv}	.05	.05	.04	.06	.05	.11
Al^{vi}	.03	.04	.04	.02	.03	-
Ti	.01	.01	.01	.01	-	-
Fe	.26	.22	.25	.26	.28	.25
Mn	.01	.01	.01	.01	.01	.01
Mg	.80	.79	.82	.91	.78	.90
Ca	.87	.93	.86	.80	.89	.89
Na	.03	.01	-	-	.01	-
K	-	-	-	-	-	-
Cr	.01	.01	-	.01	.01	.01
TOTAL	4.01	4.01	3.99	4.01	4.01	4.05
$\frac{Mg}{Mg+Fe}$	.800	.822	.805	.818	.781	.821
Ca	42.2	44.7	41.9	37.8	42.8	40.7
Mg	46.3	45.5	46.8	50.9	44.7	48.7
Fe	11.6	9.8	11.3	11.3	12.5	10.6

WT%	B31	B31	B31	B31	B36	B36
SiO_2	52.87	52.26	52.42	51.93	52.81	52.70
TiO_2	.21	.19	.12	.22	.42	.49
Al_2O_3	1.36	2.23	1.59	2.29	1.62	3.23
FeO	6.89	7.50	7.79	7.97	7.25	7.41
MnO	.17	.22	.15	.12	-	-
MgO	14.78	14.57	14.45	14.36	15.70	17.40
CaO	23.46	22.14	22.98	22.19	21.88	17.24
Na_2O	-	.26	.18	.33	-	.17
K_2O	-	-	-	-	-	-
Cr_2O_3	.27	.62	.32	.59	.33	.46
TOTAL	101.76	101.62	99.65	98.87	100.10	99.08
	NUMBER OF IONS ON BASIS OF 6(O)					
Si	1.96	1.94	1.95	1.93	1.95	1.94
Al^{iv}	.04	.06	.05	.07	.05	.06
Al^{vi}	.02	.04	.02	.03	.02	.07
Ti	.01	.01	-	.01	.01	.01
Fe	.21	.23	.24	.25	.22	.23
Mn	.01	.01	.01	.01	-	-
Mg	.82	.81	.80	.80	.86	.95
Ca	.93	.88	.92	.88	.87	.68
Na	-	.02	.01	.02	-	.01
K	-	-	-	-	-	-
Cr	.01	.02	.01	.02	.01	.01
TOTAL	4.00	4.01	4.01	4.01	3.99	3.98
$\frac{Mg}{Mg+Fe}$	.832	.817	.810	.805	.832	.843
Ca	44.4	42.9	43.9	43.0	41.3	33.6
Mg	46.2	46.6	45.5	45.9	48.9	55.9
Fe	9.3	10.4	10.6	11.1	9.8	10.4

WT%	E	E	E	E	E	E	E
SiO_2	52.92	54.10	54.16	53.07	53.80	54.51	54.08
TiO_2	-	-	-	.25	-	-	-
Al_2O_3	1.11	.79	1.48	1.13	1.83	-	.54
FeO	8.27	9.58	9.47	10.29	9.14	6.68	9.01
MnO	-	.12	.15	-	-	-	.14
MgO	12.58	13.52	14.30	12.00	13.64	14.34	13.32
CaO	25.36	22.41	21.20	25.09	22.58	25.40	25.44
Na_2O	-	-	-	-	-	-	-
K_2O	-	-	-	-	-	-	-
Cr_2O_3	1.47	.60	.29	.32	.36	.49	.11
TOTAL	101.65	101.13	101.05	102.15	101.36	101.41	102.64
			NUMBER OF IONS ON BASIS OF 6(O)				
Si	1.96	2.00	1.99	1.96	1.98	2.00	1.98
Al^{iv}	.04	-	.01	.04	.02	-	.02
Al^{vi}	.01	.04	.06	.01	.06	-	-
Ti	-	-	-	.01	-	-	-
Fe	.26	.30	.29	.32	.28	.21	.28
Mn	-	.01	.01	-	-	-	.01
Mg	.69	.74	.78	.66	.75	.78	.73
Ca	1.00	.89	.83	.99	.89	1.00	1.00
Na	-	-	-	-	-	-	-
K	-	-	-	-	-	-	-
Cr	.04	.02	.01	.01	.01	.01	.01
TOTAL	4.00	3.98	3.98	4.00	3.98	4.00	4.01
$\frac{Mg}{Mg+Fe}$	.777	.764	.776	.729	.774	.831	.773
Ca	48.8	43.4	41.1	48.0	43.7	47.2	47.2
Mg	39.8	43.2	45.7	37.9	43.6	43.9	40.8
Fe	11.4	13.4	13.2	14.1	12.7	8.9	12.0

ILMENITE

B1, B12, B20, B27

SPHENE

B7

WT%	ILMENITE						SPHENE
	B1	B1	B1	B12	B20	B27	B7
SiO_2	-	1.17	1.03	8.29	-	3.07	35.69
TiO_2	53.95	52.14	51.95	44.44	52.59	48.37	25.80
Al_2O_3	-	.21	.32	1.29	-	1.46	10.31
FeO	45.82	43.43	45.57	37.15	45.51	43.62	.89
MnO	1.37	1.52	1.50	1.50	1.67	1.34	-
MgO	.24	.62	.53	.47	.53	2.06	.23
CaO	.17	.51	.53	2.29	.37	1.05	23.97
Na_2O	-	-	-	.20	-	.06	.61
K_2O	-	.09	.10	-	-	-	.09
Cr_2O_3	-	-	-	-	-	-	.11
TOTAL	101.56	99.69	101.52	95.64	100.67	101.04	97.70
	NUMBER OF IONS ON BASIS OF 4(O)						
Si	-	.04	.03	.27	-	.10	.92
Al	-	.01	.01	.05	-	.06	.31
Ti	1.34	1.30	1.29	1.10	1.31	1.18	.50
Fe	1.26	1.21	1.25	1.02	1.29	1.18	.02
Mn	.04	.04	.04	.04	.05	.04	-
Mg	.01	.03	.02	.02	.02	.10	.01
Ca	.01	.02	.02	.08	.01	.04	.66
Na	-	-	-	.01	-	-	.03
K	-	-	-	-	-	-	-
Cr	-	-	-	-	-	-	-
TOTAL	2.66	2.65	2.68	2.61	2.68	2.69	2.45